ALMA MATER STUDIORUM - UNIVERSITÀ DI BOLOGNA

SCUOLA DI INGEGNERIA E ARCHITETTURA

DIPARTIMENTO DI INGEGNERIA INDUSTRIALE

CORSO DI LAUREA MAGISTRALE IN INGEGNERIA ENERGETICA

TESI DI LAUREA MAGISTRALE

In

Metodi matematici e numerici per l'energetica M

APPLICATION OF PHASE CHANGE MATERIALS FOR HEAT STORAGE IN WATER TANKS

CANDIDATO:
Edoardo Lippa

RELATORE:
Prof. Domiziano Mostacci

CORRELATORI:
Prof. Matthias Rädle
Frederik Wunder
Sebastian Sonnick

Anno accademico 2018/19

Sessione III

Abstract

La tesi mira a studiare l'applicazione dei Phase Change Materials (PCM) in un serbatoio d'acqua per aumentare la capacità di accumulo termico negli impianti di riscaldamento degli edifici. La possibilità di utilizzare l'acqua come acqua calda sanitaria è stata esclusa dallo studio, per cui si è ipotizzato di utilizzarla solo per il riscaldamento o il raffreddamento a pavimento.

La prima parte della tesi è dedicata ad un'ampia introduzione su tutti i tipi di PCM, sulle loro particolari proprietà, sulle loro applicazioni e in particolare sul loro utilizzo per l'accumulo termico nei serbatoi d'acqua.

I PCM mostrano un'elevata entalpia di fusione con la capacità, in un volume relativamente piccolo, di immagazzinare o rilasciare grandi quantità di energia come calore latente durante la fusione e la solidificazione. Inoltre, i PCM in pratica richiedono che le loro temperature di transizione di fase superiore e inferiore siano all'interno dell'intervallo di temperatura operativa per una data applicazione e posseggano un'elevata conducibilità termica per un efficiente trasferimento di calore con un comportamento di scambio di fase congruente per evitare la separazione irreversibile dei loro costituenti.

Durante lo sviluppo dei PCM, sono stati studiati molti gruppi diversi di materiali, tra cui composti inorganici (sale e idrati salini), composti organici come paraffine, acidi grassi e persino materiali polimerici come il PEG.

La relazione tra la struttura fondamentale e le proprietà di immagazzinamento dell'energia di questi PCM è stata esaminata negli anni per determinare i meccanismi di accumulazione/emissione di calore con riferimento alle loro caratteristiche finali di immagazzinamento dell'energia.

Il lavoro svolto, oggetto dell’elaborato, ha previsto un'analisi delle diverse modalità di incapsulamento del PCM in contenitori di diverse forme e dimensioni. L'attenzione si è concentrata su una forma parallelepipeda da inserire in un serbatoio rettangolare o cubico.

La ricerca ha richiesto diverse esperienze in laboratorio. La prima esperienza che è stata effettuata ha riguardato la produzione effettiva di un PCM. Successivamente gli altri esperimenti hanno riguardato la misura di alcune

proprietà termiche del PCM, come i calori specifici (fase solida e liquida) e il calore latente. In particolare, per queste misurazioni sono stati utilizzati un calorimetro e il metodo T-history, di cui sono forniti anche i riferimenti bibliografici.

Una parte dello studio ha compreso anche l'uso di Matlab per eseguire una simulazione numerica di tipo annuale di un impianto di riscaldamento. Nel capitolo relativo a questa parte computazionale della ricerca, vengono spiegate le relazioni e i metodi utilizzati per calcolare gli scambi e le perdite di calore che si verificano durante il funzionamento dell'impianto. Si è ipotizzato di utilizzare energia elettrica da pannelli fotovoltaici per far funzionare la pompa di calore dell'impianto. Sono quindi stati utilizzati i dati, forniti dal dipartimento CeMOS, relativi alla radiazione solare in Germania a Mannheim. Per quanto riguarda la simulazione della richiesta di energia durante l'anno, sono stati utilizzati i dati di una piccola casa indipendente, anch’essi precedentemente raccolti dal dipartimento CeMOS.

L'ultima parte di questa ricerca ha riguardato la costruzione e la messa in funzione di un sistema sperimentale. È stato costruito un serbatoio d'acqua con 180 “PCMboxes” all'interno e le connessioni di ingresso e di uscita per il flusso d’acqua. Successivamente è stato costruito l'intero sistema di tubazioni, comprese le pompe idrauliche e la pompa di calore. Una volta costruito il sistema, sono state effettuate delle misurazioni per stimare la capacità di accumulo termico del serbatoio.

Alla fine della tesi è presente una conclusione dove vengono spiegate alcune idee su possibili lavori che possono essere svolti in futuro.

Per quanto riguarda la produzione di PCM, cercando possibilmente di evitare le paraffine, in quanto tossiche ed infiammabili, e cercando sempre di utilizzare PCM “salt hydrates” (inerti), si potrebbe tentare di produrne uno con una temperatura di cambiamento di fase di 34-36 °C; mantenere l'acqua a queste temperature per un tempo più lungo sarebbe più adatto per gli impianti di riscaldamento degli edifici.

Le misurazioni delle proprietà termiche del PCM (calore specifico della fase solida e liquida e calore latente) potrebbero essere effettuate utilizzando metodi più precisi e ricalibrando tutte le termocoppie.

Per l'incapsulamento del PCM si potrebbe provare a sviluppare forme diverse da quella utilizzata; un'idea potrebbe essere quella di impiegare una forma di un “piece of cake” (settore cilindrico) nel caso si volesse riempire un serbatoio cilindrico. Il tipo di incapsulamento è un costo che deve essere considerato. Se si riesce a trovare un buon tipo di incapsulamento, che riempia bene il serbatoio, che permetta un buon scambio termico e che sia economico, allora questo sarà facilmente commercializzabile.

Per quanto riguarda il sistema sperimentale che è stato costruito, è stato possibile effettuare solo due misure, una per il processo di riscaldamento e una per il processo di raffreddamento; sarebbe certamente più interessante effettuare più misure sui due processi consecutivamente l'una all'altra e alternarle ogni volta che il sistema raggiunge l'equilibrio. Per fare questo sarebbe necessario monitorare non solo la temperatura dell'acqua ma anche la temperatura del PCM all'interno dei boxes; una volta che entrambe le temperature sono uguali e abbondantemente al di sopra (o al di sotto) della temperatura di fusione del PCM allora si dovrebbe avviare il processo di raffreddamento (o riscaldamento).

Una tale misura non solo fornirebbe risultati più accurati in termini di capacità di accumulo termico e di coefficiente di trasferimento di calore, ma fornirebbe anche l'opportunità di vedere come il sistema risponde a diversi cicli consecutivi di riscaldamento e raffreddamento in termini di stabilità del PCM.

Index

Nomenclature

PCM	phase change material
PCMs	phase change materials
TES	thermal energy storage
TESM	thermal energy storage material
SH	sensible heat
LH	latent heat
LHTES	latent heat thermal energy storage
SHS	sensible heat storage
SHTES	sensible heat thermal energy storage
PCMboxes	phase change material boxes
PCMbags	phase change material bags
HP	heat pump

1. Aim of the study

This thesis aims to study the application of Phase Change Materials in water tanks to increase the capacity of thermal storage in buildings heating plants.

The possibility of using water as domestic hot water was excluded from the study, it was assumed to use it only for underfloor heating.

The first part of the thesis is dedicated to a wide introduction on all types of PCMs, their particular properties, their applications and in particular their use for thermal storage in water tanks.

The work involves an analysis of different way of encapsulation of the PCM (phase change material) in containers of different shapes and dimensions. The main focus was on a parallelepiped shape container to be inserted into a rectangular or cubic tank.

The study has also the objective of finding an optimal condition at a thermo-fluid dynamic level in the interaction between the PCM, its encapsulation and the water flow.

For the research in subject study, several experiments were carried out in the CeMOS laboratory. The first experience, that was performed, concerned the production of a well-known PCM. Subsequently the other experiments concerned the measurement of certain thermal properties of PCM, such as specific heats (solid and liquid phase) and latent heat. In particular, a calorimeter and the T-history method were used for these measurements, of which bibliographical references are also provided.

The research has also required the use of the Matlab software in order to perform a year-round numerical simulation of a possible heating plant to be build. In the chapter concerning this computational part of the research, the relations and methods used to calculate the heat exchange and losses that occur during the functioning of the system are explained. It was assumed to use electricity from photovoltaic panels to run the heat pump of the system; The used data were previously recorded by the CeMOS department, concerning solar radiation in Germany, in Mannheim.

Regarding the simulation of the energy demand during the year, data of a small detached house were used, previously collected by the CeMOS department.

The last part of this research involved the construction and commissioning of an experimental system. A 180 PCMbags water tank was built with inlet and outlet connections, besides the entire piping system including hydraulic pumps and the heat pump. Once the system was built, measurements were taken to estimate the thermal storage capacity of the tank.

At the end of the thesis there is a brief conclusion where some ideas about possible future work are explained.

2. Introduction on Phase Change Materials [1]

Using phase change materials (PCMs) for thermal energy storage (TES) that can be released as sensible heat (SH) and latent heat (LH) became an important aspect for energy management following the 1973–1974 energy crisis. Today, the limited reserves of fossil fuels and concerns over greenhouse gas emissions make the effective utilization of energy a key issue. Using PCMs for TES provides an elegant and realistic solution to increase the efficiency of the storage and use of energy in many domestic and industrial sectors. The application of PCMs for energy storage reduces the mismatch between supply and demand, improves the performance and reliability of energy distribution networks and plays an important general role in conserving energy.

PCMs exhibit a high enthalpy of fusion with the ability, in a relatively small volume, to store or release large amounts of energy as latent heat during melting and solidification. Additionally, practical PCMs require their upper and lower phase transition temperatures to be within the operational temperature range for a given application and possess high thermal conductivity for efficient heat transfer with congruent phase-change behaviour to avoid irreversible separation of their constituents.

During the development of PCMs, many different groups of materials have been studied, including inorganic compounds (salt and salt hydrates), organic compounds such as paraffins, fatty acids and even polymeric materials such as PEG. The relationship between the fundamental structure and the energy storage properties of these PCMs has been critically examined to determine the heat accumulation/emission mechanisms with reference to their ultimate energy storage characteristics.

2.1 Thermal energy storage (TES) methods

Thermal energy storage (TES) can be achieved by cooling, heating, melting, solidifying, or vaporizing a material with the energy becoming available as heat when the process is reversed. TES methods are classified as sensible heat thermal energy storage (SHTES) or latent heat thermal energy storage (LHTES). SHTES occurs when a material is driven to increase or decrease its temperature. The effectiveness of the method depends on the specific heat capacity of the material and, if volume is an important consideration, on the material's density. LHTES depends of a material's ability to accumulate energy densities at almost isothermal conditions and over a narrow temperature range. Such phase change thermal energy storage systems offer a number of advantages over other systems (e.g. chemical storage systems), particularly the small temperature difference between the storage and retrieval cycles, small unit sizes and low weight per unit of storage capacity. PCMs absorb energy as the phase change occurs during the heating process and then can release this energy during cooling.

2.1.1 Sensible TES

Sensible heat storage (SHS) involves storing thermal energy by raising the temperature of a solid or liquid. The principle is based on the material's change of heat capacity and temperature during the process of charging and discharging.

The amount of heat stored is a function of the specific heat of the medium, the temperature change and the mass of storage medium – Eq. (1).

$$Q = \int_{T_i}^{T_f} m\, C_p dT = mC_{ap}\left(T_f - T_i\right) \quad (1)$$

where Q – quantity of heat stored (J), T_i – initial temperature (°C), T_f – final temperature (°C), m – mass of heat storage medium (kg), C_p – specific heat (J/kg K), C_{ap} – average specific heat between T_i and T_f (J/ kg K). The storage materials absorb heat by the conventional heat transfer mechanisms of radiation, conduction and convection. As the materials cool at night or on cloudy days, the stored heat is released by the same modes. Active space heating systems commonly use tanks of water or rock bins as TESM.

Water, stored in plastic, fibreglass, or glass-lined steel containers, is the typical thermal SHS medium for solar heating systems – as it absorbs heat, its temperature increases, and the systems become warm to the touch. Water is the best SHS liquid available because of its low cost and high specific heat.

2.1.2 Latent TES

Latent heat storage is a most efficient method of storing thermal energy. Latent heat storage (LHS) relies on the storage material absorbing or releasing heat as it undergoes a solid to solid, solid to liquid or liquid to gas phase change or vice versa. The storage capacity of an LHS system with a PCM is given by:

$$Q = \int_{T_i}^{T_m} mC_p dT + ma_m \Delta H_m + \int_{T_m}^{T_f} mC_p dT \qquad (2)$$

where a_m – fraction melted, ΔH_m – heat of melting per unit mass (J/kg) and T_m – melting temperature.

LHS offers a much higher storage density with a narrower temperature range between storing and releasing heat than SHS. The ideal PCM should meet a number of criteria related to the desired thermophysical, kinetic and chemical properties:

Thermal properties:

- a melting temperature in the desired operating range,
- a high phase transition latent heat per unit volume,
- a high specific heat, to provide significant additional SHS,
- high thermal conductivity of both phases.

Physical properties:

- a small volume change on phase transformation,
- a low vapour pressure at the operating temperature,

- favourable phase equilibrium,
- congruent melting of the PCM,
- a high density.

Kinetic properties:

- no supercooling,
- a high nucleation rate,
- an adequate rate of crystallization.

Chemical properties:

- long-term chemical stability,
- a completely reversible freeze/melt cycle,
- compatibility with the construction materials,
- no corrosion influence on the construction materials,
- it should be non-toxic, non-flammable and non-explosive to ensure safety.

The PCM should be readily available in large quantities at low cost. In practice, those criteria are not fully met by most PCMs. However, recent progress in the design and characterization of novel materials for energy storage, including nanomaterials, has opened new possibilities for enhanced performance with extended lifetimes.

2.2 Classification of PCMs

Over the last 40 years different classes of materials, including hydrated salts, paraffin waxes, fatty acids, the eutectics of organic and non-organic compounds and polymers have been considered as potential PCMs. PCMs can be divided into three main groups – based on the temperature ranges over which the TES phase transition occurs: (i) low temperature PCMs – with phase transition temperatures below 15 °C, usually used in air conditioning applications and the food industry; (ii) mid temperature PCMs, the most popular – with phase transition temperatures in the range 15–90 °C with solar, medical, textile, electronic and energy-saving applications in building design; (iii) high temperature PCMs with a phase transition above 90 °C developed mainly for industrial and aerospace applications.

PCMs can be classified by their mode of phase transition: gas–liquid, solid–gas, solid–liquid and solid–solid systems, see Fig. 1. The applications of PCMs with a solid–gas or liquid–gas phase transition are limited in TES systems because of the large volume changes associated with the transition – even if they possess a high phase transition latent heat. Significantly smaller volume changes occur, usually ca. 10% or less, with solid–solid and solid–liquid transformations. This makes them economically and practically attractive as materials for TES systems despite their smaller heat of phase transition. Solid–solid PCMs employ the heat associated with the phase transition one to another crystalline form and can be considered as an alternative to solid–liquid PCMs. Generally, the heat of phase transition for solid–solid PCMs is lower than that of solid–liquid PCMs. However, employing the former group of materials can avoid the problems of PCM leakage at temperatures above the phase transition temperature, a significant technical problem with solid–liquid PCMs.

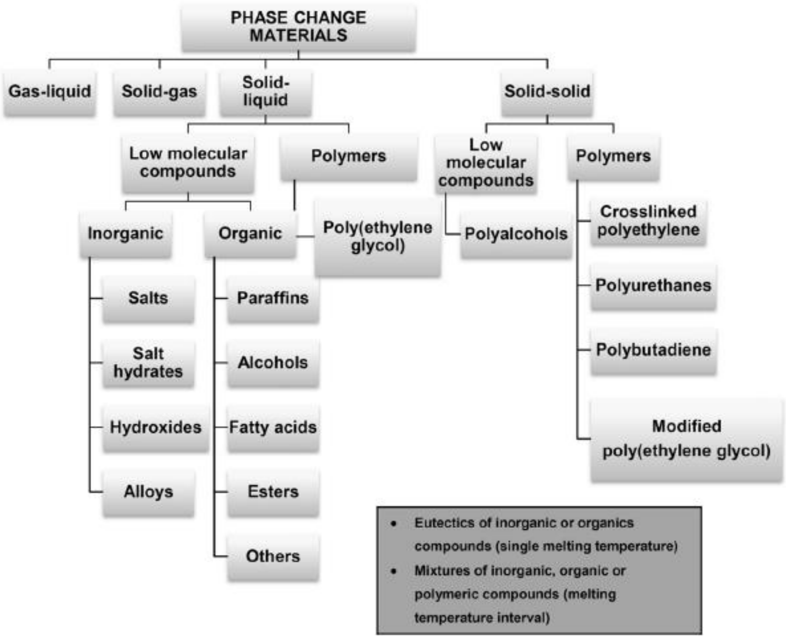

Fig. 1 - Classification of energy storage materials (adapted from [1])

Only solid-liquid PCMs will be taken into consideration in this thesis because they are the ones that allow to accumulate more energy thanks to a high heat of phase transition.

2.2.1 Solid–liquid PCMs

Many different types of solid–liquid PCMs are employed for thermal storage applications, such as water, salt hydrates, paraffins, selected hydrocarbons, polymers and metal alloys. In the following subsections, the various classes of solid–liquid PCMs will be described.

Inorganic PCMs

The various inorganic substances, eutectics and mixtures for low and high temperature applications that have been considered as potential PCMs are given in Tables 1–3. A number of the thermophysical properties, such as melting point, heat of fusion, thermal conductivity and density, is presented.

Table 1 - Inorganic compounds with potential use as PCMs (adapted from [1])

Compound	Melting temperature (°C)	Heat of fusion (J/g)
$AlCl_3$	192	280
$LiNO_3$	250	370
$NaNO_3$	307	172
KNO_3	333	266
Na_2O_2	360	314
KOH	380	150
$KClO_4$	527	1253
LiH	699	2678
$MgCl_2$	714	452
NaCl	800	492
Na_2CO_3	854	276
KF	857	452
LiF	868	932
K_2CO_3	897	235
NaF	993	750
MgF_2	1271	936

Salt hydrates. Salt hydrates with the general formula $AB\cdot nH_2O$, are inorganic salts containing water of crystallization. During phase transformation dehydration of the salt occurs, forming either a salt hydrate that contains fewer water molecules:

$ABn\cdot nH_2O \rightarrow AB\cdot mH_2O+(n-m)H_2O$

or the anhydrous form of the salt

$AB\cdot nH_2O \rightarrow AB+nH_2O$.

Table 2 - Salt hydrates with potential use as PCM (adapted from [1])

Compound	Melting temperature (°C)	Heat of fusion (J/g)	Thermal conductivity (W/mK)		Density (solid) (10^3 kg/m^3)
			Liquid	Solid	
$LiClO_3\cdot 3H_2O$	8	253			
$KF\cdot 4H_2O$	18.5–19	231			1.45
$Mn(NO_3)_2\cdot 6H_2O$	25.3	125.9			
$CaCl_2\cdot 6H_2O$	28.0–30.0	190–200	0.540	1.088	1.80
$LiNO_3\cdot 3H_2O$	30	256			
$Na_2SO_4\cdot 10H_2O$	34	256			
$Na_2CO_3\cdot 10H_2O$	33	247			
$NaCH_3COO\cdot 3H_2O$	55.6–56.5	237–243			
$CaBr_2\cdot 6H_2O$	34	115.5			2.19
$Na_2HPO_4\cdot 12H_2O$	35–45	279.6	0.476	0.514	1.52
$Zn(NO_3)_2\cdot 6H_2O$	36	146.9	0.464		
$Zn(NO_3)_2\cdot 4H_2O$	45.5				
$Zn(NO_3)_2\cdot 2H_2O$	54				
$Na_2S_2O_3\cdot 5H_2O$	48–55	201			1.75
$Na(CH_3COO)\cdot 3H_2O$	58	226			1.45
$Cd(NO_3)_2\cdot 4H_2O$	59.5				
$Na_2B_4O_7\cdot 10H_2O$	68.1				
$Na_3PO_4\cdot 12H_2O$	69.0				
$Na_2P_2O_7\cdot 10H_2O$	70	184			
$Ba(OH]_2\cdot 8H_2O$	78	266			
$(NH_4)Al(SO_4)_2\cdot 12H_2O$	95	269			
$MgCl_2\cdot 6H_2O$	117	169			
$Mg(NO_3)_2\cdot 6H_2O$	89.3	150			

Table 3 - Eutectic and non-eutectic mixtures with potential use as PCM (adapted from [1])

Mixture	Melting temperature (°C)	Heat of fusion (J/g)	Density (kg/m^3)
Eutectic mixtures			
66.6% $CaCl_2 \cdot 6H_2O$ + 33.3% $MgCl_2 \cdot 6H_2O$	25	127	
50% $CaCl_2$ + 50% $MgCl_2 \cdot 6H_2O$	25	95	
48% $CaCl_2$ + 4.3% NaCl + 0.4% KCl + 47.3% H_2O	27	188	
47% $Ca(NO_3)_2 \cdot 4H_2O$ + 53% $Mg(NO_3)_2 \cdot 6H_2O$	30	136	
40% $CH_3COONa \cdot 3H_2O$ + 60% NH_2CONH_2	30	200.5	
50% $Na_2SO_4 \cdot 10H_2O$ + 50% NaCl	18		
61.5% $Mg(NO_3)_2 \cdot 6H_2O$ + 38.5% NH_4NO_3	52	125	
58.7% $Mg(NO_3)_2 \cdot 6H_2O$ + 41.3% $MgCl_2 \cdot 6H_2O$	59	132	
53% $Mg(NO_3)_2 \cdot 6H_2O$ + 47% $Al(NO_3)_2 \cdot 9H_2O$	61	148	
59% $Mg(NO_3)_2 \cdot 6H_2O$ + 41% $MgBr_2 \cdot 6H_2O$	66	168	
14% $LiNO_3$ + 86% $Mg(NO_3)_2 \cdot 6H_2O$	72	180	
66.6% urea + 33.4% NH_4Br	76	161	
11.8% NaF + 54.3% KF + 26.6% LiF + 7.3% MgF_2	449		2160 (liquid)
35.1% LiF + 38.4% NaF + 26.5% CaF_2	615		2225 (liquid)
32.5% LiF + 50.5% NaF + 17.0% MgF_2	632		2105 (liquid)
51.8% NaF + 34.0% CaF_2 + 14.2% MgF_2	645		2370 (liquid)
48.1% LiF + 51.9% NaF	652		1930 (liquid)
63.8% KF + 27.9% NaF + 8.3% MgF_2	685		2090 (liquid)
45.8% LiF + 54.2% MgF_2	746		2305 (liquid)
53.6% NaF + 28.6% MgF_2 + 17.8% KF	809		2110 (liquid)
66.9% NaF + 33.1% MgF_2	832		2190 (liquid)
Non-eutectic mixtures			
H_2O + polyacrylamide	0	292	
50% $Na(CH_3COO) \cdot 3H_2O$ + 50% $HCONH_2$	40	255	

Depending on the melting behaviour, the salt hydrates can be classified as:

- salt hydrates with congruent melting behaviour – at the melting temperature the salt is soluble in the hydration water;
- salt hydrates with incongruent melting – at the melting temperature salt is only partially soluble in the hydration water;
- salt hydrates with semi-congruent melting – during the melting process the

solid and liquid phases that are in equilibrium have different compositions because of the transformation of the salt hydrate to a salt hydrate with a lesser amount of hydration water.

Unfortunately, a large number of salt hydrates which could be considered as potential PCMs as they possess a large phase transition latent heat and suitable melting temperature melt incongruently. Consequently, the amount of released water is insufficient to dissolve the crystalline salt formed during the dehydration process. This leads to density differences, phase separation and sedimentation in containers causing serious technical problems in practical applications.

Alloys. Metallic alloys are used as high-temperature PCMs as they offer high thermal reliability and repeatability. The largest phase transition heat, on a mass or volume basis, has been found for binary and ternary alloys of the relatively plentiful elements Al, Cu, Mg and Zn, but not all of the potential materials are suitable for use in TES system. Compared to other latent heat energy storage materials eutectic aluminium alloys were principally investigated for use as PCMs in high temperature TES systems because of their suitable phase change temperature, high latent heat density and good thermal stability.

Organic PCMs

Organic PCMs are constituted by a wide range of materials including paraffins, fatty acids and their eutectic mixtures, esters and other organic compounds. The various compounds and a selection of their thermophysical properties are shown in Tables 4‑7.

Table 4 - Paraffins with potential for use as a PCM (adapted from [1])

Paraffin	Number of carbon atoms in molecule	Melting temp. (°C)	Heat of fusion (J/g)	Density (g/cm3)
n-Tetradecane	14	5.8–6.0	227–229	
n-Pentadecane	15	9.9–10.0	206	

n-Hexadecane	16	18.0–20.0	216–236	0.773
n-Heptadecane	17	22–22.6	164–214	0.778
n-Oktadecane	18	28.0–28.4	200–244	0.776
n-Nonadecane	19	32.0	222	0.785
n-Eicozane	20	36.6	247	0.788
n-Heneicozane	21	40.2	213	0.791
n-Docozane	22	44.0	249	0.794
n-Trikozane	23	47.5	234	0.796
n-Tetracozane	24	50.6	255	0.799
n-Pentacozane	25	53.5	238	0.801
n-Hexacozane	26	56.3	256	0.803
n-Heptacozane	27	58.8	235	0.779
n-Oktacozane	28	41.2	254	0.806
n-Nonacozane	29	63.4	239	0.808
n-Triacontane	30	65.4	252	0.775

Table 5 - Fatty acid with potential for use as a PCM (adapted from [1])

Fatty acid	Number of carbon atoms in molecule	Melting temp. (°C)	Heat of fusion (J/g)	Density (g/cm3)
Caprylic acid	8	16.3	148	–
CA	10	31.3–31.6	163	–
LA	12	41–44	183–212	0.87
MA	14	51.5–53.6	190–204.5	0.86
PA	16	61–63	203.4–212	0.942
SA	18	70.0	222	0.94
Arachidic acid	20	74.0	227	–
Undecylenic acid	22	24.6	141	

Table 6 - Fatty acid eutectic mixtures with potential for use as a PCM (adapted from [1])

Fatty acid eutectic mixtures	Content (wt.%)	Melting temp. (°C)	Heat of fusion (J/g)
CA/LA	45/55	17–21	143
CA/PA	76.5/23.5	21.8	171.2

LA/MA	66.0/34.0	34.2	166.8
LA/PA	69.0/31.0	35.2	166.3
LA/SA	75.5/24.5	37	182.7
MA/PA	58.0/42.0	42.6	169.7
MA/SA	64.0/36.0	44.1	182.4
MA/SA	65.7/34.3	50–52	162.0
PA/SA	64.2/35.8	52.3	181.7

Table 7 - Other organic compounds with potential for use as a PCM (adapted from [1])

Class of compounds	Compound	Melting temp. (°C)	Heat of fusion (J/g)
Monohydroxy alcohols	1-Dodecanol	17.5–23.3	184.0–188.8
	1-Tetradecanol	39.3	221.23
Ketones	Phorone	27	123.5
Ethers	Diphenyl ether	27.2	97
Esters of fatty acids	Methyl palmitate	27	163.2
	Allyl palmitate	23	173
	Propyl palmitate	16–20	186–190
	Methyl stearate	38–39	160.7
	Isopropyl palmitate	11	100
	Isopropyl stearate	14	142
	Butyl stearate	17–23	140–200
	Ethylene glycol distearate	63.2	215.80
	Dimethyl sebacate	21	135
	Methyl-12-hydroxystearate	43	126
	Vinyl stearate	27	122
Halogen derivative	1-Iodehexadecane	22.2	131
	Chlorobenzothiazole	18.6	65
	3-Iodoaniline	23	64
Sulphur compounds	Octadecyl 3-mercapto-propionate	21	141
	Octadecyl thioglycolate	26	91
	Dilauryl thiopropionate	39	159
Amides	Acetamide	82	241

Sugars	Erythritol	117	344
	Mannitol	165	341
	Xylitol	93	280
	Sorbitol	97	110
	Granulated sugar	179	179
	White superior soft sugar	172	110
Dienes	Dicyclopentadiene	28.7	11.7
Oleochemical carbonates	Decyl carbonate	-2.2	144
	Dodecyl carbonate	19.3	200
	Tetradecyl carbonate	33.7	227
	Hexadecyl carbonate	44.9	219
	Octadecyl carbonate	51.6	223

Paraffins. Paraffins (saturated hydrocarbons with CnH2n+2 formula), which constitute the broadly used solid–liquid PCMs, possess a high latent heat storage capacity over a narrow temperature range and are considered as non-toxic and ecologically harmless. Paraffin waxes exhibit moderate TES density, but a large surface area is needed as they have low thermal conductivity. This reduces their rate of heat charging and discharging during the melting and solidification cycles. The latent heat of paraffins is molar mass-based and their various phase change temperatures give the flexibility to select an appropriate PCM for a specific LHTES application. They are economically viable and repeated cycling across the solid–liquid transition does not induce phase separation. Paraffins between C5 and C15 are liquids with the higher analogs being waxy solids with melting temperatures ranging from 23 to 67 °C. Commercial grade paraffin wax, which is a mixture of different hydrocarbons, is produced by the distillation of crude oil. In general, the longer the average length of the hydrocarbon chain, the higher the melting temperature and heat of fusion. This relationship can be employed to design the PCM properties by mixing physically different paraffins. In fact, most paraffin PCMs are mixtures of saturated hydrocarbons with different numbers of carbon atoms in the molecules.

The literature data show that after 1000–2000 cycles commercial grade paraffin waxes and other pure paraffins have stable properties and good thermal reliability. Paraffin waxes are safe, non-reactive and are compatible with metal containers as they do not promote corrosion.

Alcohols. Alcohols have been tested for energy storage applications for four decades, but recent advances in such PCMs are associated with nanomaterials or special composites with unique properties, such as the introduction of electrical conductivity.

Fatty acids. The interest in fatty acids ($CH_3(CH_2)_{2n}$-COOH) as PCMs for energy storage has increased recently as they possess desirable thermodynamic and kinetic characteristics for low temperature LHS. They exhibit a high latent heat of fusion, compared to that of paraffins, and reproducible melting and freezing behaviour, with little or no supercooling. However, fatty acids are more expensive than technical grade paraffins, are mildly corrosive and possess a disagreeable odour. With an increasing number of carbon atoms in the fatty acids molecule, the melting and freezing points, the heat of melting and the degree of crystallization gradually increase. Carboxylic acids with an even number of carbon atoms in the structure possess higher values of thermal parameters than those with odd numbers of C-atoms. The former shows a tendency for more regular alignment and a denser crystalline lattice arising from hydrogen bonding between the carboxylic acid molecules. The melting and boiling points of fatty acids are relatively high and the saturated fatty acids exhibit low phase transition volume changes with very little or no supercooling when freezing.

Esters. Fatty acid esters show a solid–liquid transition over a narrow temperature range and their mixtures can form eutectics, similar to numerous inorganic salt mixtures, with little or no super- cooling. Most of the fatty acid esters are commercially available as large quantities are produced for the polymer, cosmetics, textiles industries and other applications.

3. Potential PCMs for building applications [2]

As we know, many factors influence the indoor air temperature of a building. These include climate conditions (outdoor temperature, wind velocity, solar radiation and others), building structure and the building material´s thermophysical properties (wall thickness, area ratio of window to wall, thermal conductivity and specific heat of wall material), indoor heat source, air change rate per hour and auxiliary heating/cooling installations.

It has been shown that the difference between the indoor temperature and the comfort range determines the heating and cooling load when there is no space heating and cooling. Therefore, the heating and cooling load will decrease with decreasing this temperature difference. For a certain building placed in a specific region, the building structure parameters such as wall thickness, area ratio of window to wall, cubage of the room, are known, however the outdoor temperature and solar energy change with the different hour and day during the entire year. Then, with a certain interior heat source, the natural room temperature (i.e. the room temperature without any active cooling or heating) depends on the material thermophysical properties (thermal conductivity, λ, and specific volumetric heat, C (the product of the density by the material’s specific heat, $\rho \cdot c_p$).

If there are certain building materials whose λ and $\rho \cdot c_p$ values can make the given room meet the condition $I_{win} = I_{sum} \approx 0$, (being I_{win}, integrated discomfort level for indoor temperature in winter and I_{sum}, integrated discomfort level for indoor temperature in summer), we can call these materials ideal building materials. This means that the indoor temperature will be in the comfort range all year round without auxiliary heating or cooling.

The application of PCMs in building can have two different goals. first, using natural heat, that is solar energy, for heating or night cold for cooling; second, using artificial heat or cold sources. In any case, storage of heat or cold is necessary to match availability and demand with respect to time and also with respect power.

Basically, there are three different ways to heating or cooling a building. They are:

- PCMs in building walls;
- PCMs in other building components other than walls;
- PCMs in heat and cold storage units.

The first two options are passive systems, where the heat or cold stored is automatically realized when indoor or outdoor temperature rises or falls beyond the melting point. The last one is an active system, where the stored heat or cold is in containment thermally separated from the building by insulation, so the heat or cold is only used on demand not automatically. Some authors classified passive systems applications in the building envelope into two main categories, PCM "integrated" and PCM as "component". The main difference between them is that component can be manufactured before the building being constructed and have a particular design. For example, blinds with integrated PCM are considered as component.

4. Examples of encapsulation [3]

To encapsulate salt hydrates, usually plastic containers are selected because of material compatibility. Plastics are not corroded by salt hydrates; however, attention has to be paid to the water tightness of the material of the capsule wall. This is to make sure that the water content in the capsule and thus the composition of the salt hydrate does not change with time. Plastic encapsulations can also be used for organic PCM, but the combination of PCM and encapsulation material has to be chosen very carefully because organic materials may soften plastics.

Fig.2 shows several examples of macro encapsulation in plastic containers from different companies. Many companies produce a selection of different encapsulations. Because plastic containers can nowadays be produced easily in a high variety of shapes, there are few restrictions on the geometry of the encapsulation.

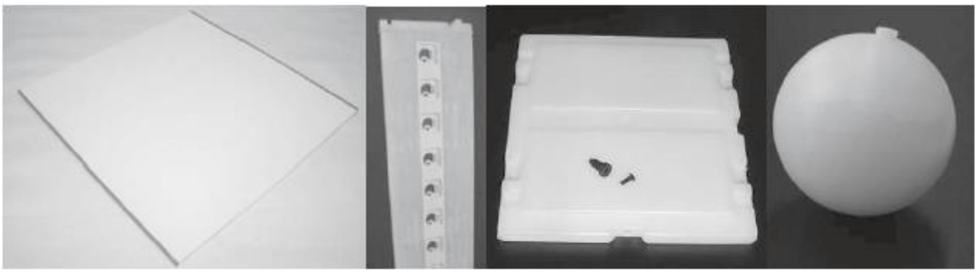

Fig. 2 - Encapsulation in plastic containers. From left to right: bar double panels, panel, flat container and balls (adapted from [3])

Another form of encapsulation shows fig.3. Here, plastic sheets form small containments for the PCM that are sealed with a plastic foil. Such encapsulations called capsule stripes or dimple sheets are useful to cover large surfaces and can be manufactured on a fully automated production line.

Fig. 3 - Encapsulation in capsule stripes for inorganic PCM (adapted from [3])

It is of course also possible to use only foils as a wall material; the resulting product is PCM encapsulated in bags. Fig.4 shows two examples. To ensure tightness of the bag regarding water, usually plastic foils combined with a metallic layer are used.

Fig. 4 - Encapsulation in bags (adapted from [3])

If good heat transfer is important, the low thermal conductivity of container walls made of plastic can be a problem. An option is to choose containers with metal walls. Metal walls also have the advantage of higher mechanical stability if a sufficient wall thickness is chosen. It is however necessary to select a suitable metal which is not corroded by the PCM. This selection should also consider that depending on the metal different options and restrictions for shaping, welding, etc exist. Fig.5 shows two examples of metal containers used to encapsulate PCM.

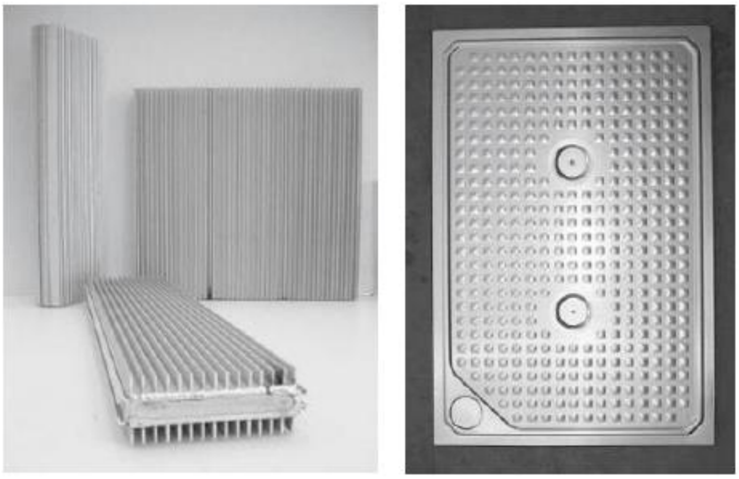

Fig. 5 - Macroencapsulation in metal containers: left, aluminium profiles with fins for improved heat transfer, and right, coated aluminium plate (adapted from [3])

On the left is a ClimSel Thermal Battery: a hollow aluminium profile with cooling fins that is filled with PCM. The batteries can be connected to each other, as shown in the background. On the right is a coated aluminium plate filled with PCM.

5. Stored Heat of materials [3]

The *stored heat* between two temperatures is the most important characteristic of PCM materials and objects, as the final goal in an application is to store heat. Before starting with the detailed discussion, it is necessary to go through some definitions.

5.1 Basics of calorimetry

The stored heat can be given with respect to the volume or mass in case of a material, or with respect to a given object. The *calorimetric formula*

$$dQ = \frac{dQ}{dT} \cdot dT = C \cdot dT \tag{3}$$

defines the relation between the stored heat and the heat capacity C (e.g. J/K). The heat capacity of a material can be given with respect to mass (e.g. J/kg·K), volume (e.g. J/m^3·K) or amount of the material (e.g. J/mol·K). If the heat capacity is with respect to mass, volume, or amount, it is called specific heat capacity and c is used instead of C. The heat capacity depends also on the boundary conditions; for constant pressure, it is denoted as C_p, and for constant volume as C_V. Because of the relation between the enthalpy H, internal energy U, pressure p, and volume V

$$H = U + pV \tag{4}$$

and the *first law of thermodynamics*

$$dU = dQ - pdV \tag{5}$$

follows

$$dH = dU + d(p \cdot V) = dQ - pdV + pdV + Vdp = dQ + Vdp \tag{6}$$

For constant pressure follows then

$$dH = dQ \tag{7}$$

And consequently also

$$\Delta H = \Delta Q \tag{8}$$

Further on

$$\left.\frac{dH}{dT}\right|_p = \left.\frac{dQ}{dT}\right|_p = C_p \tag{9}$$

For solids and liquids, which under usual conditions are incompressible, the term $V \cdot dp$ can be neglected in eq.6. Then, independent of the pressure conditions, eq.7, eq.8, and eq.9 are valid. Changes of enthalpy ΔH and of heat ΔQ are therefore often used synonymously when dealing with solids and liquids. From a physics point of view, there is however an important difference between H and Q: heat is something that only shows up in the transfer of thermal energy and the amount transferred depends on the path between the initial and the final state of the system. Enthalpy H is a thermodynamic potential and therefore characteristic of a state.

The correct expression is therefore that the heat stored or lost is equal to the enthalpy increase or reduction of the storage material.

Methods to determine the change of heat in any kind of process are called *calorimetric methods*. A *calorimeter* usually works in one of the following ways shown in Fig.6, based on the calorimetric formula (eq.3):

- The calorimeter actively supplies heat to the sample via an electrical resistance heater and measures the temperature change of the sample.
  The electrical energy supplied is calculated from the voltage and current of the heater.
- The calorimeter actively supplies heat to the sample via a thermal resistance and a temperature difference between the sample and its surrounding. Further on, it measures the temperature change of the sample.

The heat supplied to the sample across the thermal resistance is calculated from the temperature gradient across the thermal resistance. The value of the resistance can be calculated. However, usually it is determined via a calibration using standard materials with a known heat capacity or melting enthalpy.

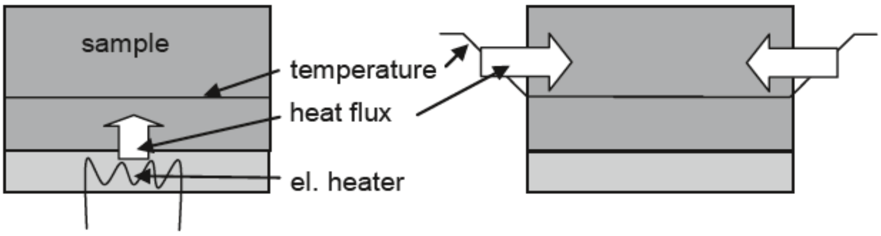

Fig. 6 - Supply of the heat elettrically (left), or by a heat flux from the outside (right) (adapted from [3])

An advantage of the electrical heating is that it needs no calibration. On the other hand, it can only be used for heating, while with a thermal resistance there is also the possibility of measuring upon cooling when the temperature of the surrounding is below the sample temperature. There are several *modes to operate calorimeters* to determine the heat storage capacity within a temperature interval of interest. They differ in the resolution of the data on the heat supplied to the sample and the corresponding temperature change:

1. *Interval mode*: heating or cooling is between the start and the end of the temperature interval of interest, indicated on the left in Fig.7 by “|”. Then

$$\Delta Q = \int_{T_{start}}^{T_{end}} C_p dT = C_p \cdot \Delta T = C_p \cdot (T_{end} - T_{start}) \qquad (10)$$

It is important that the sample is isothermal at the start and end temperatures, otherwise these states are not well defined, and the heat supplied is not determined correctly. The heat supplied or extracted for the temperature change can be measured with high accuracy; the temperature resolution of the stored heat however is very poor. The heat capacity value determined is an average value for the whole interval. Fig.7 shows this for the case of a material with a melting temperature, and not a melting range.

2. *Step mode*: heating or cooling is as with the interval mode, but the whole interval of interest is now divided into small intervals, called steps. For these steps, the same treatment as described for the interval mode before is applied. This increases the temperature resolution of the stored heat. The resolution is equal to the height of the temperature steps; however, the start and end of each step must again be an isothermal state, otherwise the change in heat in each step is not determined correctly.

3. *Dynamic mode*: the interval is scanned by continuously heating or cooling according

$$dQ = \frac{dQ}{dT} \cdot dT = C_p \cdot dT \qquad (11)$$

There are no steps to wait for thermodynamic equilibrium anymore. The heating or cooling rate has to be slow enough to assure thermodynamic equilibrium within the sample, however. If not, the heat supplied at each data recording (equal to the enthalpy change dH, eq.7) cannot be assigned to the measured temperature. Too high heating or cooling rates cause significant errors in the data of the heat stored as a function of temperature. The resolution of the data itself is only restricted by the data recording system.

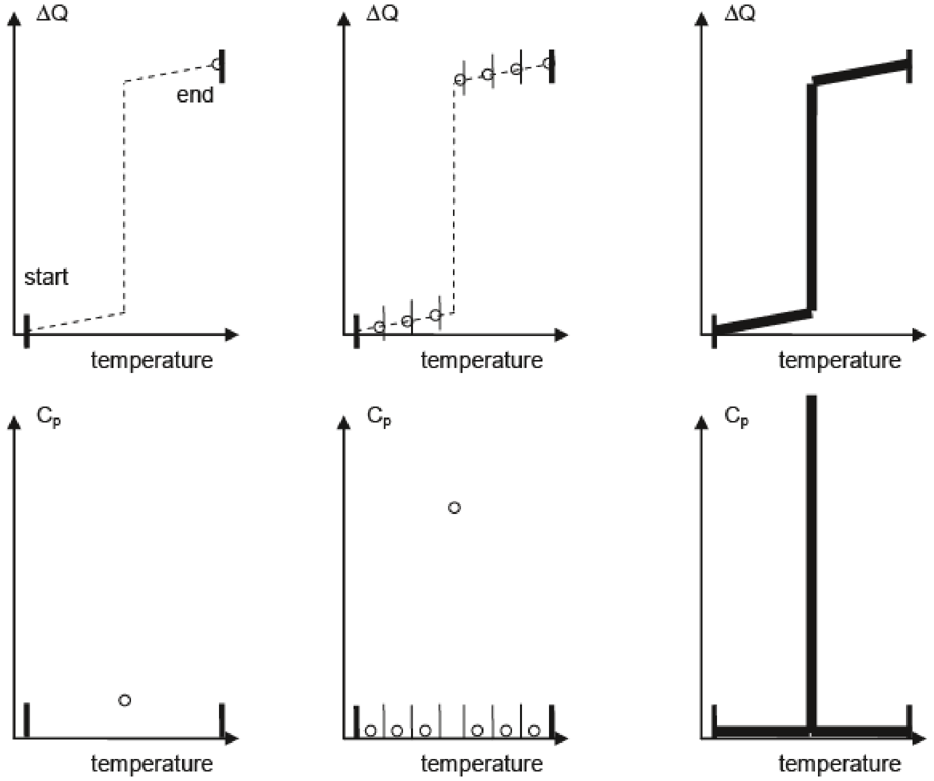

Fig. 7 - Data sets for interval (left), step (center), and dynamic mode (right) for the case of a material with a melting temperature. The total heat ΔQ supplied to the sample (=ΔH) over the whole interval is the same, but the resolution of the data ○ increases from left to right (adapted from [3])

From the data of the heat supplied to the sample and the corresponding temperature change the heat capacity can be calculated. Actually, in the case of a melting temperature the heat capacity, which is the 1st derivative of the stored heat with respect to temperature, would be infinite. Therefore, many people do not like to call the values a heat capacity, even if there is a melting range instead of a melting temperature. However, for a melting range it is not possible to distinguish the temperature ranges of melting and of only sensible heat storage. Any attempt to do it anyway leads to confusion and uncertainties as the past has shown. Further on, even for a melting temperature the measurement will never result in an infinite value. Years of experience have shown that the best way is to strictly follow the definition and use the heat capacity throughout, even in the presence of a melting temperature.

Fig.7 shows data sets for interval (left), step (centre) and dynamic mode (right) for the case of a melting temperature. The total heat supplied to the sample over the whole interval results from adding up the heat supplied in each interval. As the top row of diagrams shows, it is the same for all measurement modes, but the resolution of the data ○ increases from left to right. The influence of the resolution on the heat capacity data shown in the lower row of diagrams is dramatic. It is obvious that the interval mode gives the worst resolution because it averages over the whole measurement interval where, due to the phase change, dramatic differences in the heat capacity occur. Between step and dynamic mode, there is no significant difference in the range of sensible heat storage. In the range of phase change, the width of the measurement interval has a strong influence on the peak value of the heat capacity data. This effect can be dramatic when pure substances with a melting temperature are analysed, but it is usually less pronounced when measuring PCM because most PCM have a melting range.

5.2 General aspects in doing a measurement

From what was discussed up to this point in chapter 5, it is possible to summarize that aspects related to doing a measurement include general aspects of calorimetry and the materials investigated. Three main aspects have to be considered:

1. The sample has to be representative for the investigated material

This originates from the definition of a material property.

To assure that the sample is representative, the sample must be larger than typical inhomogeneities of the material.

2. Correct determination of the exchanged heat and temperature of the sample

This originates from the use of the calorimetric formula.

For the temperature, the correct determination is usually assured by a calibration procedure, where standard materials with known melting temperatures are used. This procedure has to be repeated from time to time. Usually the temperature is not measured within, but only close to the sample. This can lead to an offset between the measured and the real sample temperature.

For the heat flow, the correct determination is usually also assured by a calibration. If a measurement has to be very accurate, the calibration should be done just before or after a sample measurement.

3. Thermodynamic equilibrium in the sample

Thermodynamic equilibrium in the sample requires first that *the sample is isothermal*, otherwise the heat flux cannot be attributed to a single temperature indicated at the sensor. Therefore, the measurement should be done slow enough, or the sample should not be too large. This can be in conflict with the necessity to have a sufficiently large sample to be representative for the investigated material.

Further on, the sample should be in *reaction equilibrium*, otherwise the enthalpy at the measured temperature has no defined value, and consequently enthalpy differences are also not well defined. This refers to two aspects: first, dynamic processes have to proceed to a stable state, and second, there should only be one stable state at the same temperature. There are several occasions causing problems with regard to reaction equilibrium, for example very slow reactions, metastable states like amorphous instead of crystalline structures, subcooling, and different crystalline structures.

5.3 Problems in doing measurements on PCM

Besides the general aspects just summarized that apply to any material, PCM pose additional problems or larger problems due to their high phase change enthalpy.

Regarding point 1, saying that the sample has to be representative for the investigated material, subcooling can be a problem. Subcooling can depend on the sample size and therefore the sample size should be typical for the application if possible.

Regarding point 2, the correct determination of the exchanged heat and temperature of the sample, PCM will give a large signal in the temperature range where the sample melts, and a small signal outside that range. The calibration therefore should be done for large signals.

Regarding point 3, the thermodynamic equilibrium in the sample, the measurement on PCM can cause severe problems. The requirement of reaction equilibrium is violated during subcooling of a sample, or if upon cooling crystals form slowly. This means the heating / cooling rate should be small. To get the sample isothermal can also take a lot of time with a PCM during the phase change, because of the large amounts of heat involved and the usually low thermal conductivity of PCM. If not done properly, there will be significant errors as Fig.8 shows. When the temperature of the sample is measured at the sample surface, which is usually the case, the heat released or supplied to the sample is then attributed to a wrong temperature, too low when cooling and too high when heating.

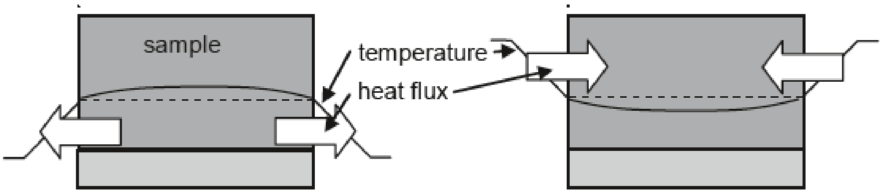

Fig. 8 - Left: temperature profile in a cooling measurement for a material storing only sensible heat (- - -) and a PCM during phase change (–). Right: the same for a heating measurement (adapted from [3])

Outside the melting temperature range, this effect is relatively small; because only sensible heat is stored, the temperature gradients remain small. While most calorimeters are constructed to give accurate results for sensible heats of “ordinary” materials, a significant offset can be observed in the melting range of PCM with their special, high phase change enthalpy. Upon cooling, the situation can even be worse.

In most cases, interval and step mode are not critical, as isothermal conditions are attained when waited for long enough. In dynamic mode, where also many data points lie in the melting and solidification temperature range of the PCM, different measurement results are obtained on heating and cooling (Fig.9, left). This is often called hysteresis; however, most people understand *hysteresis* as a property of the material / sample only. Effects, which are only due to the measurement conditions, are usually not called hysteresis, but *apparent hysteresis*.

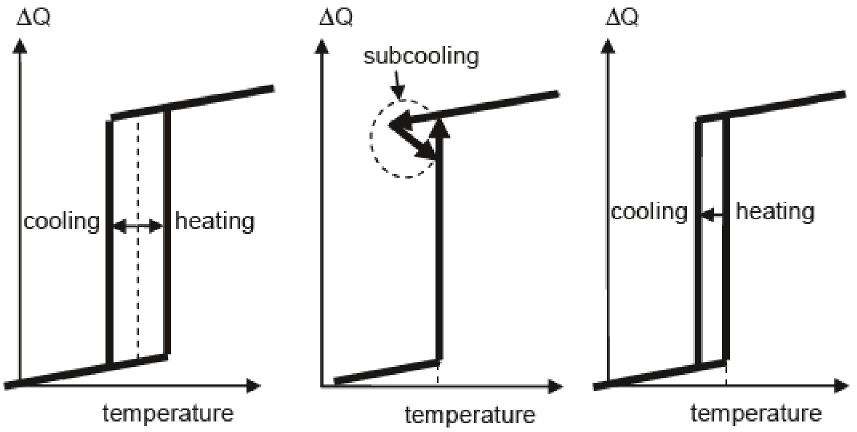

Fig. 9 - Left: apparent hysteresis caused by non-isothermal conditions. Center: real hysteresis as a material property caused by subcooling. Right: real hysteresis by slow heat release or a real difference between the phase change temperatures (adapted from [3])

To find out if an observed hysteresis is real or only apparent, that means if it is a property of the material or only due to the measurement apparatus or procedure, it is necessary to have isothermal conditions in the sample. Therefore, the heating and cooling rate should be small, or the sample size should be small. However, small sample size contradicts the requirement of having a representative sample, and small heating and cooling rates will lead to a low signal to noise ratio. Therefore, it often cannot be avoided to have different results from heating and cooling measurements. To get at least an idea what the result would be if temperature equilibrium were attained, it is necessary to measure always upon heating and cooling and with a small heating and cooling rate as possible. The closer the result, the better temperature equilibrium was attained. A comparison of results from measurements with different heating rates indicates also how close temperature equilibrium was attained. There are several effects due to the material, which cause real hysteresis.

The most common one is subcooling. Subcooling will lead to different results for heating and cooling; however, it is not a shift of the results to higher temperatures on heating and lower temperatures on cooling. Subcooling is restricted to the temperature range where solidification is started, as fig.9 shows. Another cause of hysteresis is when the latent heat is released too slowly on cooling, e.g. because the crystal lattice forms very slowly or because diffusion processes are necessary to homogenize the sample. The temperature of the sample then drops below the melting temperature. Upon melting, a similar effect is usually not observed (Fig.9, right) because during melting the kinetic effects proceed much faster. Another possible cause of hysteresis is when upon solidification the sample forms a different solid phase than the one it was at the beginning of melting process. This can be an amorphous phase, or a different crystalline structure.

Up to now, the discussion and the diagrams discussed the case of a melting temperature. Because PCM are usually not pure substances and therefore usually have a melting range, it is not possible to detect from any single measurement what exactly the underlying effects are and to eliminate the deviations in the data caused by not having isothermal conditions, reaction equilibrium, etc. It is therefore strongly recommended to try to measure at least as close as possible to isothermal conditions and to make measurements on heating and additionally on cooling.

The problems in doing measurements on PCM, discussed here on a theoretical basis, will then be discussed in connection with the measurement systems and real measurement results.

6. Use of water-phase change material storage in conventional solar water heating systems [5]

Domestic water heating, which constitutes a significant share of the residential energy consumption, is an excellent application for utilizing solar energy. However, due to the intermittent, unsteady, and time-dependant characteristics of solar radiation, the widespread use of solar water heating systems relies heavily on the availability of reliable and feasible energy storage methods.

Solar thermal energy had been traditionally stored in the form of sensible heat by raising the temperature of water or rocks for later use. Despite the obvious simplicity of such storage methods, they are inefficient as their storage capacities are limited. In contrast, solar thermal energy can be stored in the form of latent heat by using suitable phase change materials, which can offer high storage capacity per unit volume, and per unit mass. This is essentially due to the fact that for most materials, the latent heat of fusion is very much larger than their enthalpy change (for example: the ratio of the latent heat to the specific heat of water is around 80). The melting of a phase change material (PCM) enables the absorption of large amounts of heat which can be excessively available during the daytime. This stored heat can then be released to the surrounding medium during the evening and night hours as the PCM changes its phase again from liquid to solid. Such method of storage is also advantageous in reducing the temperature fluctuations in a solar thermal system by absorbing the extra heat at peak radiation hours to release it when solar radiation is absent.

A wide range of PCMs can be used for latent heat storage applications, including salt hydrates, paraffin waxes, fatty acids, and sugar alcohols. For use in domestic solar water heating applications, paraffin waxes represent the most suitable option due to their congruent melting temperatures, availability, low cost, and non-corrosiveness. However, they usually suffer from relatively high volumetric expansion ratios and low thermal conductivity values. The poor thermal conductivity can be overcome by using the PCM through geometries with large surface area to volume ratios. Over the past two decades, the area of latent heat thermal energy storage has generated a great deal of interest. Detailed reviews have been presented of phase change materials, applications, and theoretical and experimental investigations. Different designs of integrated and compact phase change material solar collectors have been proposed and experimentally evaluated. Alternatively, the use of different PCMs with different configurations in the storage tanks of solar collector systems has been experimentally investigated under various conditions.

I. Al-Hinti et al. experimentally investigated the effect of using paraffin wax as a phase change material in containers packed in the storage tank of a conventional solar water heating system. The investigation includes a set of day-long experiments representing different practical application scenarios. The suggested storage configuration is simple and can be easily used with existing conventional systems without major or expensive modifications.

A schematic diagram of the experimental setup is shown in Fig. 10. The setup is essentially similar to conventional, commercially available, solar water heating systems with a few differences.

It consists of four south-facing flat plate 1.94 m * 0.76 m * 0.15 m collectors with a tilt angle of 30°. The collectors, which have ordinary single glass covers and black painted absorber plates, are connected to the main water supply and the hot water storage tank through a set of three valves enabling open-loop and closed-loop operation. A standard 90W circulation pump, with a maximum capacity of 10 l/min, is also available on the collectors-storage tank loop to enable forced circulation investigations, in addition to natural circulation.

The galvanized steel storage tank is cylindrical in shape having a length of 675 mm, an inner diameter of 450 mm and a volume of 107.4 l. It is insulated with 75-mm thick layer of rock wool insulation. Fig. 11 shows a detailed cross-sectional view of the storage tank. The tank contains a total of 38 thin walled, cylindrical, aluminium containers. Each container has a volume of 1.3 l and contains 1.0 kg of paraffin wax which was used in this investigation as the PCM.

The thermophysical properties of the paraffin wax are given in Table 8. The PCM containers are arranged in the tank on two levels, each containing 19 containers, with the aid of two perforated sheet metal separators.

The choice of these containers was meant to reach a relatively large heat transfer surface area in comparison with the volume of the PCM, and to minimize the thermal resistance between water and the PCM. The total volume of the PCM containers is 49.4 l, with water occupying the remaining 58 l in the storage tank. The bottom section of the storage tank also contains an auxiliary 2 kW electrical heater, in order to enable controlled conditions investigations.

The measurement system includes a total of seven pre-calibrated K-type thermocouples: One at the inlet line and one at the outlet line of the storage tank, three distributed at the upper, middle, and lower sections of the storage tank, one thermocouple inserted in a PCM container at the central section of the tank, and one to measure the ambient air temperature.

All thermocouples are connected to an HP 34970A-type data logger connected to a PC to enable the continuous recording of the temperature readings during various test scenarios. In the experiments described in the following section, temperature readings were continuously recorded with 1, 5, or 10 min intervals between each reading and the other, depending on the experiment requirements.

Two flow meters with an accuracy of ±2% are also available at the inlet and outlet lines of the storage tank to measure the water flow rates when needed.

All the experiments were conducted during the period extending from 1 to 24 April 2008 at the campus of the Hashemite University. This site is located at 32.1°N and 36.2°E, with an altitude of around 620 m. The climate is semi-arid and is characterized by low annual rain fall and around 3300 h of sunshine per year. The annual-average daily solar radiation is around 5.5 kWh/m^2.

The hourly average radiation for the month of April is shown in Fig. 12, with the months of January and August shown for comparison purposes. It can be seen that the month of April represents the yearly average climatic and radiation conditions of the site.

Table 8 - Thermophysical properties of the phase change material (adapted from [5])

Melting point	Latent heat of fusion	Density (solid phase)	Density (liquid phase)	Specific heat	Thermal conductivity
52 °C	230 kJ/kg	820 kg/m3	780 kg/m3	2.4 kJ/kg K	0.25 W/m K

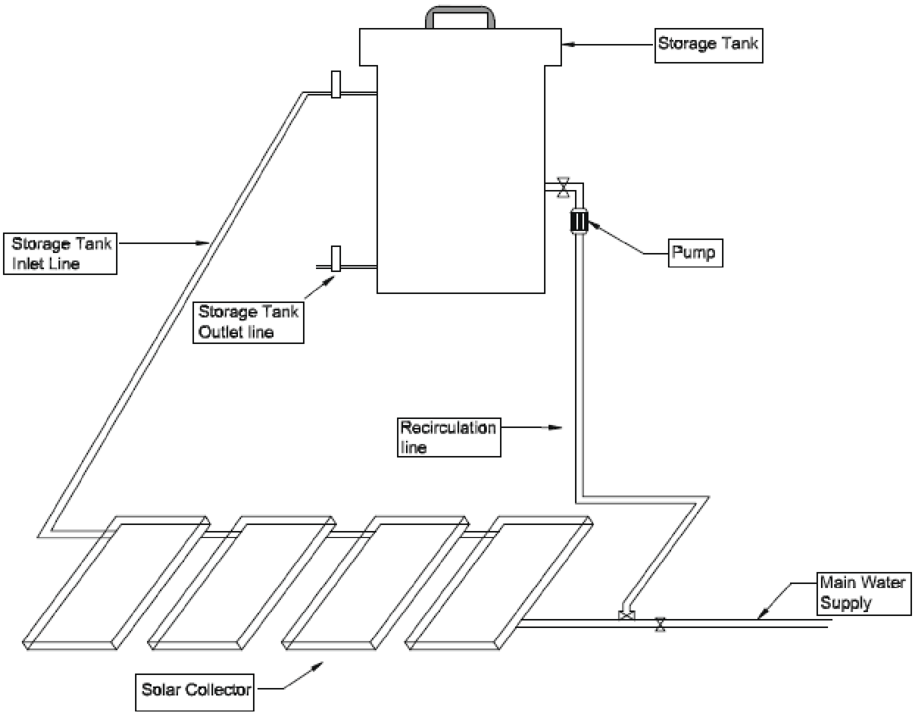

Fig. 10 - Schematic of the experimental setup (adapted from [5])

6.1 Storage performance with controlled heat input

Fig. 13 shows the time variation of the water temperature at the tank midpoint section, the PCM temperature, and the ambient air temperature, during a controlled heating conditions experiment.

In this experiment, the storage tank was separated from the system by closing the valves on the inlet and the outlet lines. The electrical heater was turned on for a period of 3 h to reach a maximum water temperature of 76 °C. Afterwards the heater was turned off, and the temperature measurements continued for a further 20 h.

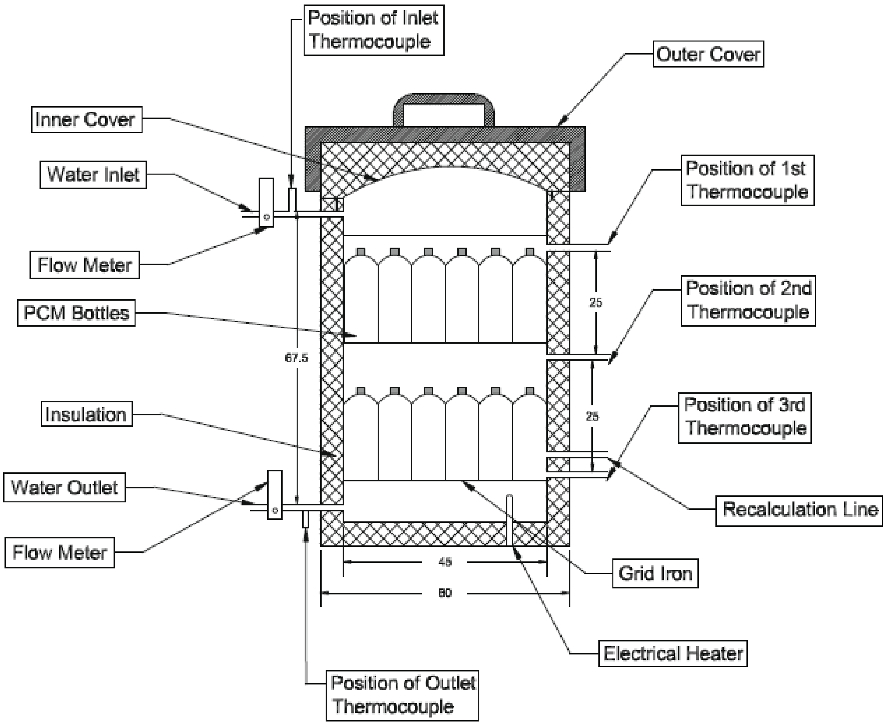

Fig. 11 - Cross sectional view of the storage tank with PCM containers (adapted from [5])

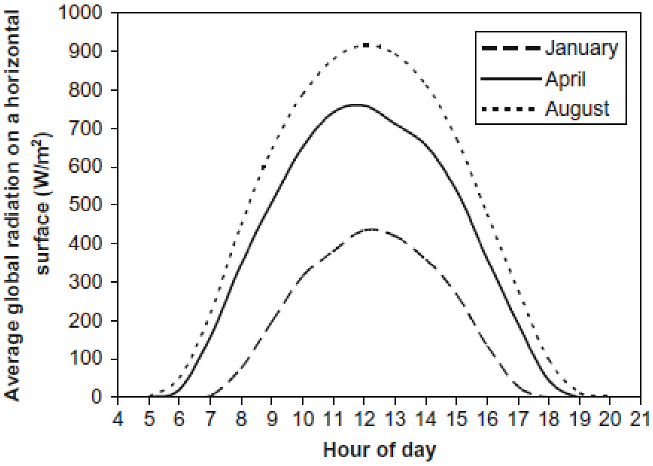

Fig. 12 - The hourly average radiation for January, April, and August at the experiment site (adapted from [5])

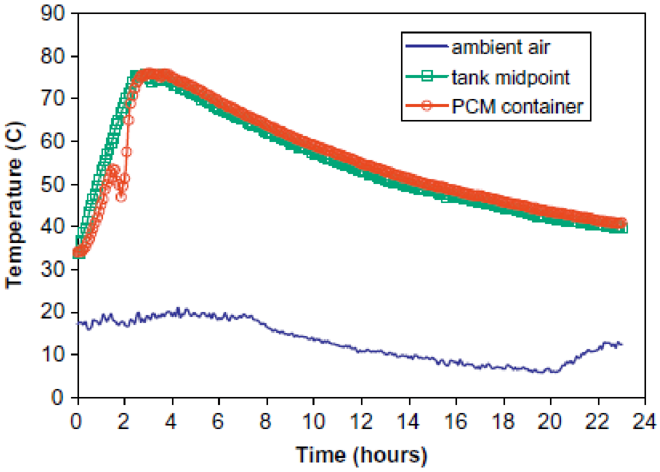

Fig. 13 - Temperature–time variations in the storage tank during controlled energy (adapted from [5])

It can be seen that at the beginning of the heating period, the water temperature increases at a faster rate in comparison with the PCM, which is initially in the solid phase. Then a sudden drop in the temperature of the PCM temperature is witnessed as it reaches a temperature of around 50 °C, which is close to its reported melting point. This can be explained by realizing that at this stage the PCM is undergoing phase change and therefore it is absorbing large amounts of heat without increasing its temperature. Following this, the temperature of the PCM starts to increase at a faster rate to catch up with the water temperature at the end of the heating stage. In less than 1-h time after the heater is switched off, the water temperature drops below the PCM temperature and continues to be 1-2 °C lower until the end of the experiment. During this stage, the PCM continues to release the stored heat to the surrounding water, and thus reducing the rate at which the temperature of water decreases.

In order to investigate the validity of this discussion and the extent of the advantage obtained by using the PCM, the same experiment was repeated under similar ambient conditions but with the PCM containers removed from the storage tank and the remaining tank volume filled with water. Fig. 6 shows the time variation of the difference between the water temperature at the tank midpoint section and the ambient air temperature, with the existence of the PCM and without it.

It can be seen that although the difference between the water temperature and the ambient temperature reaches a maximum of around 58 °C at the end of the heating process in both cases, water gains and looses heat at a slightly slower rate in the presence of PCM during the first 8 h of the experiment.
A significant difference between the two cases becomes apparent after that, as the water temperature reaches around 50-55 °C. This is attributed to the release of the stored latent heat during the gradual solidification of the PCM at this range of temperatures. The temperature advantage of the PCM case reaches 13-14 °C after 16 h of the start of the experiment. It is obvious that at 17 h after the heater was switched off, the temperature of water in the presence of the PCM was still 36 °C higher than the ambient temperature, in comparison to a difference of only 22 °C in the case without PCM.

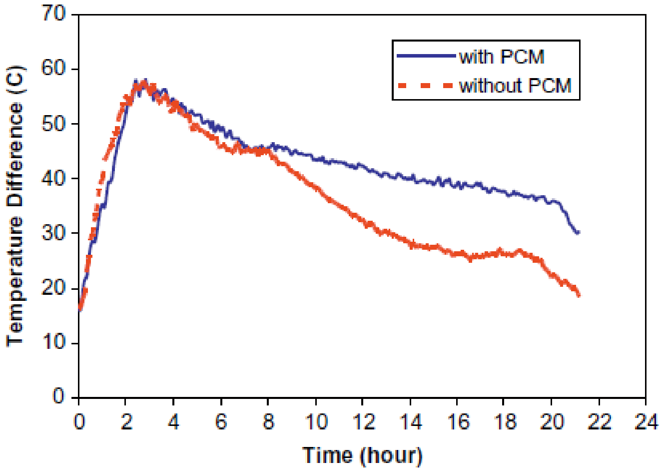

Fig. 14 - Time variations of the temperature difference between the tank midpoint and the ambient, with and without the PCM containers, during controlled energy input experiment (adapted from [5])

6.2 Storage performance with closed-loop solar system

Although the advantage of water-PCM storage was clearly demonstrated under the controlled conditions of the previous experiment using the electrical heater as the energy source, the performance of the PCM in the storage tank needs to be tested under real operational conditions.

Fig. 15 shows the time variation of the water temperature at the midpoint section of the storage tank, the temperature of the PCM, the inlet temperature to the storage tank, in addition to the ambient air temperature. These results were recorded with the storage tank connected to the flat plate collectors in a closed loop with natural circulation over a continuous period of 24 h which started at 8:00 am on 6 April 2008. No water was discharged from the system through the outlet line.

The intermittent characteristics of the solar radiation absorbed by the system are evident in the fluctuating inlet water temperature reaching the tank from the collector plates. These fluctuations are effectively smoothed in the storage tank as shown from the water and PCM temperatures. Although the ambient temperature drops at night hours to as low as 13 °C, the water temperature in the tank does not drop below 45 °C at any time which is considered acceptable for most domestic applications. A 1-h time lag is noticed between the maximum ambient temperature, and possibly solar radiation as well as seen from the inlet temperature, and the maximum water temperature in the tank.

The slowing water and PCM temperature gradient when solar radiation is absent is clear as the PCM approaches its melting temperature.

Fig. 16 shows the results of a similar experiment that was started at 8:00 am on 14 April 2008, with one difference: the circulation pump was operated for 10 min after 90 min of the start of the experiment. The purpose of this experiment was to investigate the effect of limited periods of forced circulation on the performance of the system in general and on reducing the time lag between the peak radiation and the peak water temperature. It is obvious that such effect is minimal and is only limited at the time of pump operation only as the whole system temporarily approaches an almost uniform temperature, but the temperature variations continue after that with a trend similar to that observed in the natural circulation experiment. The only exception is that following the forced circulation, the PCM temperature becomes slightly higher than the water temperature throughout the experiment.

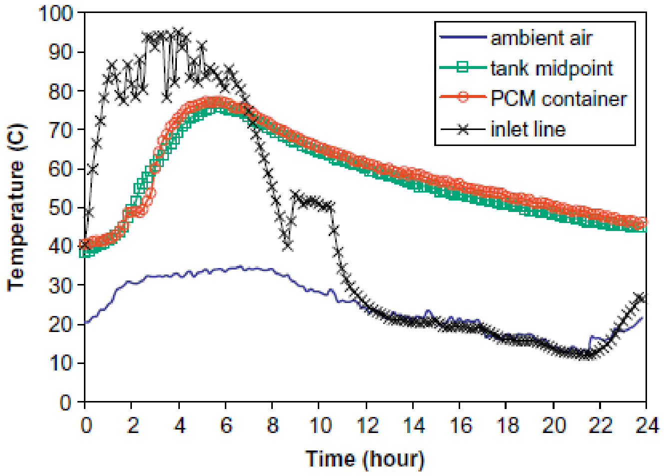

Fig. 15 - Temperature–time variations in the storage tank when connected in a natural circulation closed loop with the solar heating system (adapted from [5])

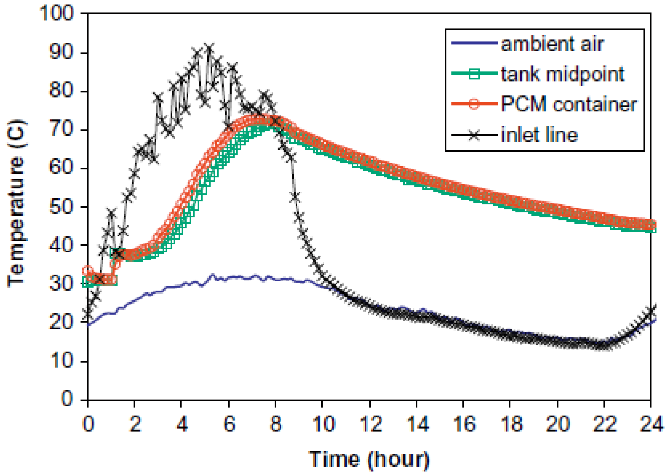

Fig. 16 - Temperature–time variations in the storage tank when connected in a closed loop with the solar heating system, with a 10 min period of forced circulation (adapted from [5])

6.3 Storage performance with open-loop solar system

For a real-life application of a solar water heating system, hot water is withdrawn from the storage tank for consumption during certain times during the day. The effect of such intermittent demand on the performance of the system is shown in Fig. 17. The results were obtained from a 24-h experiment that was started at 8:00 am on 11 April 2008. Water was withdrawn from the system according to the pattern shown in Table 9, which is supposed to simulate suggested domestic day-time consumption for a small family.

The water withdrawn from the system through the bottom of the storage tank was directly compensated by water from the main water supply.

It can be seen that such withdrawal pattern has a limited effect on the PCM or the water temperature in the tank. Due to the natural stratification of water in the storage tank driven by density differences, and since the withdrawn batches were taken during the time of the day where solar radiation was available, the inlet temperature to the tank from the collector plates was in fact higher than the temperature of the discharged water from the bottom of the tank. However, the effect on the average water temperature was not significant since the relative volume of the withdrawn water was small in comparison with the total volume of water in the system. In general, it can be said that withdrawing moderate amounts of water from the storage tank on sufficiently spaced intervals of time during the day when solar radiation is available, does not adversely affect the final water temperature or the overall performance of the system.

An extreme case of consumption was tested in an experiment designed with the aim of examining the effect of the PCM on maintaining acceptable water temperatures, even with the absence of input solar energy. In this experiment, which was started at 8:30 am on 23 April, the system was operated on a closed loop basis, with natural circulation until 2:00 pm during the day when the discharge of the tank was completely opened to discharge 60 l of water in one batch, which is more than the water storage capacity of the tank. Afterwards, the inlet and outlet valves to the tank are closed to isolate it from the system. Such scenario can identify how the system can perform in the case of night time consumption with the inlet water temperature to the tank is lower than the average temperature of water inside it. The results are shown in Fig.18.

As the discharge valve is opened, the inlet water temperature to the tank from the collector plates, which is compensating for the withdrawn water, sharply drops from 79 °C to 42°C due to the inability of the collector plates to sufficiently heat of the incoming water into the system. As a result, the average water temperature in the tank drops from 71 °C to 51 °C, while the PCM temperature drops by only 12 °C from 72 °C to 60 °C.

Due to the obvious temperature difference, heat is transferred at high rates from the PCM to the water, until steady conditions are achieved after about 90 min, with the PCM and water temperatures maintaining a 1 °C difference to the end of the experiment. It can be seen that 12 h later, the water temperature in the tank was still 44 °C, which is only 7 °C less than the starting temperature following the complete discharge. Such temperature recovery pattern and the later reduced temperature drop is attributed to the continuous release of heat from the PCM to the surrounding water.

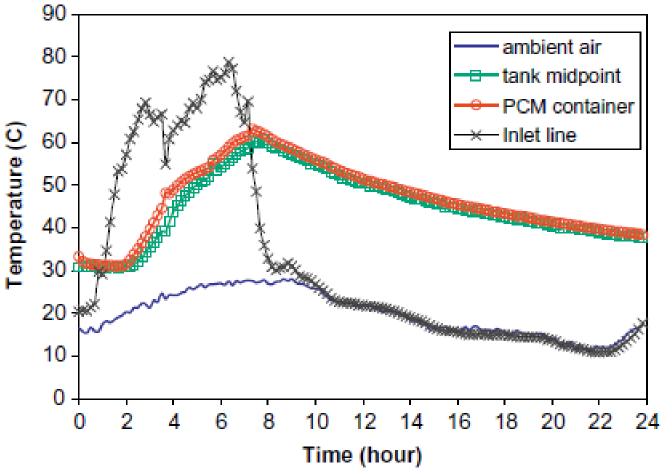

Fig. 17 - Temperature–time variation in the storage tank when connected in an open loop with the solar heating system, with structured withdrawal pattern (adapted from [5])

Table 9 - Hot water consumption pattern used in the open-loop investigation (adapted from [5])

Time	9:30am	11:30 am	01:30 pm	03:00 pm	04:30 pm
Volume of withdrawn water (l)	10	10	15	10	10

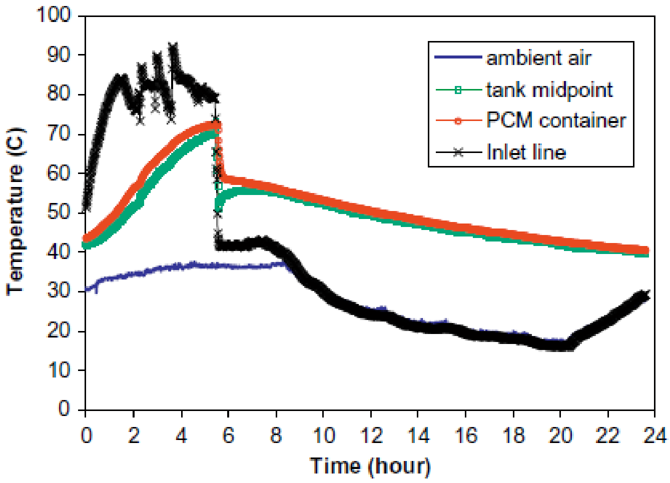

Fig. 18 - Temperature–time variations in the storage tank when connected in an open loop with the solar heating system, with one batch full capacity withdrawal (adapted from [5])

6.4 Experiments' Conclusions

The use of paraffin wax as a phase change material in small aluminium containers packed in conventional water storage tanks represents an approach for simple and inexpensive thermal energy storage. Such storage can be reliably used with conventional and existing solar water heating systems. The suitability of the melting temperature of paraffin wax enables the storage of excess energy available in daytime hours as latent heat, and then the release of this stored heat to maintain the water temperature in an acceptable range for most domestic applications.

Controlled energy input experiments using electrical heating revealed that the PCM advantage 14 h following the termination of input energy can reach 14 °C in comparison with conventional sensible heat storage. When used with variable solar energy input from conventional flat plate collectors, the water-PCM storage succeeded in keeping the water temperature over 45 °C under all operational and climatic conditions. A 1-h time lag was noticed between peak ambient temperature and solar radiation on one hand, and the peak water temperature in the tank on the other.

The effect of limited periods of forced circulation on the performance of the system in general and on reducing the time lag between the peak radiation and the peak water temperature was found to be minimal. It was also found that day-time consumption of moderate amounts of hot water withdrawn from the storage tank on sufficiently spaced time intervals does not adversely affect the final water temperature or the overall performance of the system. Finally, it was demonstrated that in cases of extreme consumption during evening hours, the existence of PCM can partially recover the temperature of water, and thus resulting in extending the effective operational time of the system.

7. PCM production process

This chapter describes the process that leads to the production of PCM.
Some PCM was produced to perform certain measurements and experiments (T-history method, calorimeter measurements and encapsulation tests).
The aim of the process was to obtain a PCM-mix with a melting temperature at about 26/27 °C as close as possible to
$48\%\ CaCl_2 + 4.3\%\ NaCl + 0.4\%\ KCl + 47.3\%\ H_2O$
that is a well-known eutectic mixture.
The tools used in the experiment were:

- 20 litres Pot
- electric stove
- 3 beakers
- spoon
- container
- hummer
- press to crumble materials
- balance
- PCMbox made of PVC
- 2 thermocouples
- 2 digital trackers
- Drill.

Chemical Materials used to create the PCM:

- 6,51 kg $CaCl_2*2H_2O$
- 3,19 kg H_2O
- 0,20 kg KCl
- 0,05 kg NaCl
- 0,05 kg $Ba(OH)_2$.

The process began with the mixture of $CaCl_2*2H_2O$ with water. The amount of $CaCl_2*2H_2O$ (solid) was put into a pot together with water, and they were heated and mixed at a temperature of 60°C until the solution was completely uniform.

KCl is very hydroscopic and when exposed to the environmental temperature it becomes harder and made of several blocks of different dimension. In order to have a good dissolution of this substance, a hummer and then a motorised press were used to crumble it until a powder was obtained.

Fig. 19 - Manual breakage of KCl (left), and result after the motorised press (right)

Once the powder was obtained, 200 g of KCl was added to the solution. Since the powder sometimes tends to form solid aggregates in the pot, they must be broken in smaller ones with the aim to dissolve better the solid parts and blend them.

The following step consisted in the addition of NaCl and $Ba(OH)_2$. They did not involve problems but as the water was already rather saturated with $CaCl_2*2H_2O$ and KCl it was difficult and it took a long time to dissolve them in the solution. Again, to obtain a more uniform liquid mixture with less solid aggregates, the liquid was stirred continuously for 30 minutes at 60°C. The controlled low temperature was fundamental to avoid water evaporation because, to obtain the right PCM, all concentrations and quantities must be correct.

Fig. 20 - Stirring of the liquid mixture

Fig. 21 - Some aggregate of KCl, NaCl and Ba(OH)2

Once the PCM was obtained from the addition of all listed materials, it was left in the pot for one night because the PVC box for the PCM was not ready to be filled yet.

The pot was covered with a cap to avoid exposition of the PCM to the humidity. The day after when the pot was opened there were some solid parts formed during the night, especially attached to the pot's walls. This happened because of the crystallization process due to the ambient temperature of the laboratory that remained always under 27 °C. An example of these solid parts can be seen attached to the pot's wall in Fig.22. Successively these formations were crumbled into fine powder that solved with the other liquid parts.

Fig. 22 - PCM with crystalline parts at the pot walls

7.1 Temperature Measurements over time and encapsulation

A sample of 20 cl was collected inside a glass container covered by a cap with a hole. A thermocouple was then introduced into this hole to measure the temperature every 30 seconds. The sample was placed in a refrigerator at a constant temperature of about 5/6 °C.

The initial temperature of the sample measured by the thermocouple was 35.9 °C. The objective was to completely solidify the PCM inside the container, therefore it took time for the temperature to drop to 20 °C.

Once the temperature of 20 °C had been reached, the sample was taken out from the refrigerator, in a completely solid state, and placed in an oven with a temperature of 50 °C, with the aim of melting the PCM again. The entire measurement process lasted more than 6 hours. The temperature behaviour within this time frame is described by the graph (Fig.23) whose data were taken from the digital tracker device and exported to excel.

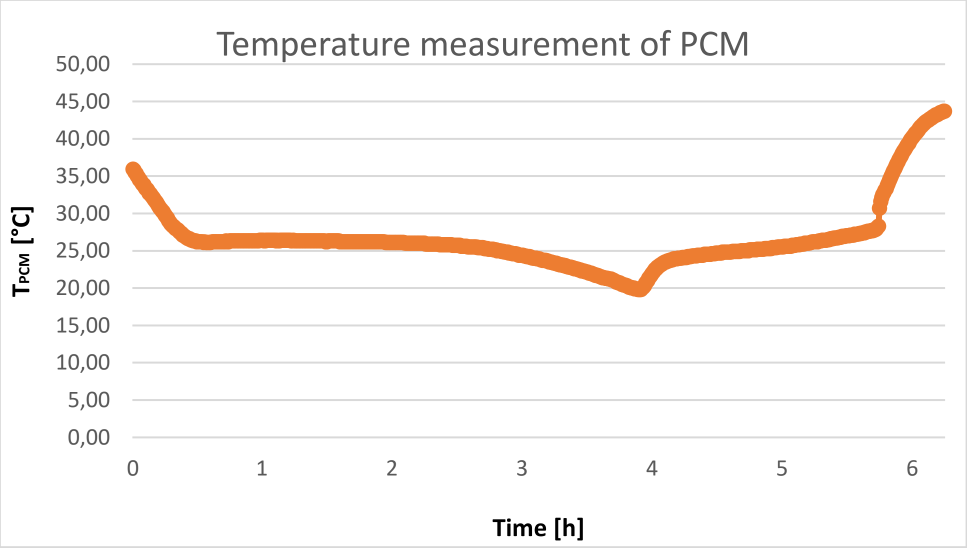

Fig. 23 - Measuring temperature of the PCM probe

From the graph you can perfectly see the latent behaviour of the material, during cooling and heating. The melting temperature was about 26/27 °C as originally expected.

For this study a PCM box made of PVC was also developed as already said. The dimensions of the box were the following: 100 cm long, 11,1 cm wide and 5,4 cm thick. The box originally was built only with lateral walls, the two caps, at the top and the bottom, were initially separated. To close the system was used a special glue for PVC materials pasting these two covers at the walls. Then in the middle of the box, as it can be seen from the Fig.24 , a hole was made with a drill in order to insert a temperature probe (thermocouple) to measure the temperature change over time.

Fig. 24 - PCM box (first encapsulation)

The PCM was inserted into the bag, from one side and filled almost until it was completely full, leaving 6 cm of space to avoid problems of expansion of the mixture itself, during the phase change. Later it was closed from both side with the glue and left for some time in a vertical position to make sure it was not leaking.

After putting the PCM liquid into the bag the system was left for one night exposed to the ambient temperature (approximately at 20/21°C) to see if the day after it was fully solidified. As expected, the following day it was completely solid. From this point on the study consisted in the analysis of the behaviour of this PCM. This means that it was put in a climate chamber were the temperature can be controlled by the user. In fact, for three days the PCM was subject to this temperature program: every 8 hours the temperature of the chamber changed from 15°C to 50°C and vice versa. The purpose of this program was to see complete cycle of the PCM from liquid to solid and from solid to liquid, for more than ones. During the whole experiment lasted two days, the probe collected the temperature of the PCM with a time step of 30 seconds from one measure to another. Therefore, it was possible to draw the temperature curve with the time in the x axis, but also see if the system was stable or not during a working cycle.

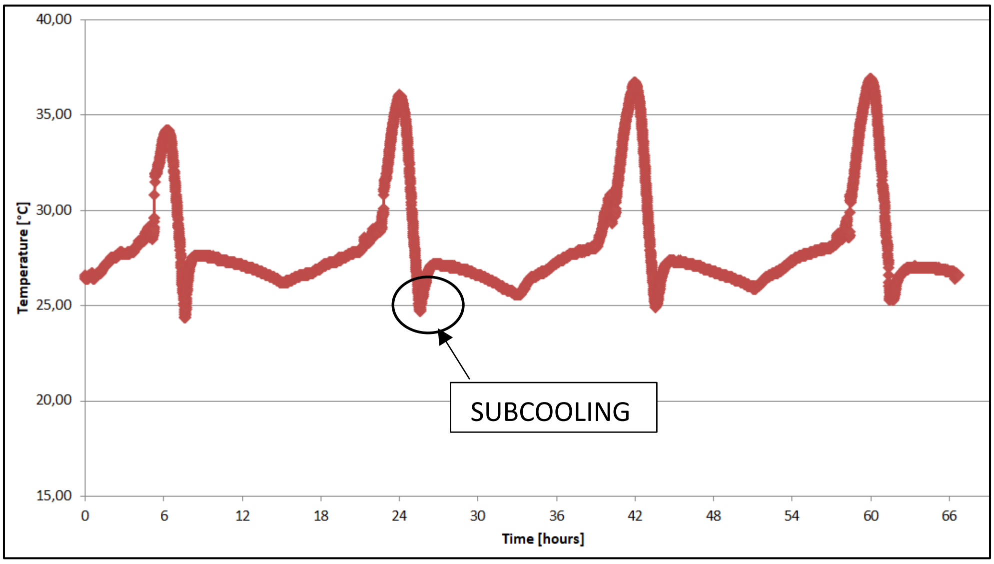

Fig. 25 - Climate chamber measurement

However, although the heating and cooling cycles showed good stability for PCM, the same could not be said for the designed encapsulation. The change in volume of PCM during the multiple phase changes caused the breakage of the junction made with PVC glue at the bottom of the encapsulation.

For this reason, the PVC encapsulation described above has been discarded with regard to the construction of the system that will be described later.

From the gathered data given by the thermocouple during the measurement in these three days, one could see that 8 hours at 50°C were enough to melt completely the PCM in the box. On the contrary, 8 hours at 15°C were insufficient to solidify the material. This last behaviour can be explained with the phenomenon of subcooling, clearly visible in the graph of Fig.25. During the cooling time the temperature goes significantly below the melting temperature until the material starts to solidify and release heat. If this temperature is not reached, the PCM does not solidify and we would not have the latent behaviour.

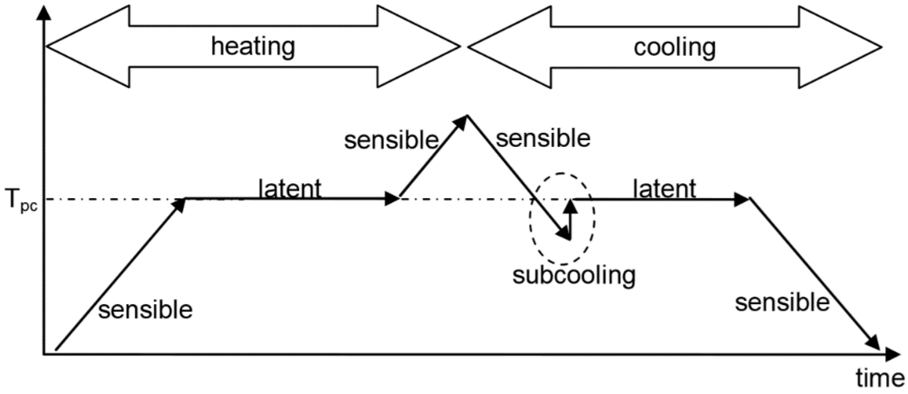

Fig. 26 - Schematic temperature change during heating and cooling of PCM (adapted from [3])

7.2 Subcooling [3]

Here following a brief explanation of subcooling will be given, or better the reasons why some materials do not solidify right away when cooled below the melting temperature. Solidification means that the amount of solid phase grows because the liquid phase at the interface with the solid phase solidifies. However, this has to start at a certain point and the starting can be a problem. At the very beginning, there is no or only a small solid particle, also called nucleus. For the nucleus to grow by solidifying liquid phase on its surface, the system has to release heat to get to its energetic minimum. There is however a competition between the surface energy, which is proportional to the surface area and therefore to r^2 (r is the radius of the nucleus), and the heat released by changing the phase, which is proportional to the volume and therefore to r^3. At small radius, it is possible that the heat released by crystallization is smaller than the surface energy gained. That means there is an energetic barrier; only when a nucleus of sufficiently large radius is present solidification starts. For this, in some cases temperatures significantly lower than the melting temperature are necessary. Based on this, nucleation is divided into two cases:

- *Homogeneous nucleation* means nucleation solely started by the PCM itself. Homogeneous nucleation includes nucleation by low enough temperatures and a second possibility, that particles of the solid PCM are added to the subcooled PCM. The latter one is sometimes also called *secondary nucleation*.
- *Heterogeneous nucleation* means nucleation not by the PCM itself. Origins of heterogeneous nucleation can be special additives intentionally added to the PCM, but also impurities, or cracks at the wall of the vessel that contain solid PCM.

The most common approach to get rid of subcooling on the level of the PCM is to add special additives, also called nucleator, to the PCM to cause heterogeneous nucleation. Nucleators have been developed for most well investigated PCM, and reduce subcooling typically to a few K.

Most nucleators are materials with a similar crystal structure as the solid PCM to allow the solid phase of the PCM to grow on their surface, but a higher melting temperature to avoid deactivation when the PCM is melted. The problem with this method is that usually a similar crystal structure also means a similar melting temperature. Therefore, many nucleators are only stable up to a temperature 10 K to 20 K above the melting temperature of the PCM. There are also other nucleators where the mechanism is completely unknown. The fact that there is still no reliable theoretical approach makes the search for a new nucleator time consuming. Examples of nucleators for some of the most important PCM are given in Farid et al. 2004 and in Lane 1983. Lane 1983 also gives an in-depth description of nucleation, crystallization, and nucleators. The difficulty of finding a nucleator can be circumvented if the PCM is locally cooled to a sufficiently low temperature to always have some solid phase left that acts as homogeneous nucleator. The necessary local cooling can be done by a Peltier element or by the cold finger technique. The cold finger technique uses a cold spot in the containment, caused for example by an intentionally bad insulation, to always have some solid PCM. It is therefore only useful when the melting temperature of the PCM is higher than the temperature of the ambient.

8. Measurements of PCM properties with calorimeter

This chapter describes the calorimeter measurement method; The aim is to measure the latent heat, the specific heat of the liquid phase and the specific heat of the solid phase of the PCM.

Each variable wasn’t directly measured but calculated from the temperature change of the water and the PCM. Water is used as a reference fluid in both measurements because of its easy availability and due to the fact that its thermofluid-dynamic properties are known.

Three measurement sequences were performed to calculate the Cp of the solid PCM, the Cp of the liquid PCM and the latent heat.

In particular, the latter one was deducted from the total energy exchanged subtracting the sensible heat of the solid part and the liquid part without phase change.

The melting temperature of PCM, which is around 26.5/27.5 °C, is known in advance. In this way it is possible to know, by measuring the temperature, when the material is completely solid and when it is completely liquid. Otherwise this approach could not be valid.

The calorimeter is an instrument that can be schematized as a confined volume thermally insulated from the external environment. Inside, three thermocouple probes are inserted to measure the water temperature in different points of the volume.

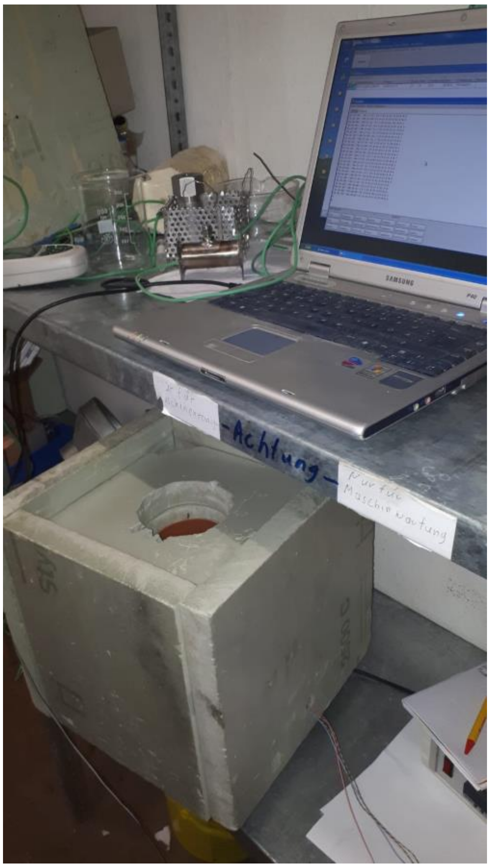

Fig. 27 - Calorimeter connected to the computer

The PCM was inserted inside a capsule, tailored for the calorimeter. Where it was possible an additional probe was inserted to measure the temperature of the PCM. The materials and tools used were:

- Calorimeter;
- Steal capsule to contain the PCM, equipped with a temperature probe in the middle of the volume;
- 3 temperature probes for the water;
- PCM with a well-known melting temperature;
- Water;
- Digital Tracker;
- Computer collecting data second by second;
- resistance heater;
- magnetic stirrer.

Fig. 28 - PCM capsule (sample) on the left and temperature digital tracker on the right.

8.1 Working method

For this work two type of measurements were made. The first group consists of three tests carried out on the same PCM material collected into three different samples (Test 1, Test 2, Test 3).

Then, another test was done (Test 4) on a PCM already stored in some bags in the lab, similar to the material of other measurements.

Before starting the measurement, the mass of the water of the PCM and of the steel capsule must be known. For all of these 4 measurements, a mass of 320g of water, was considered.

The choice to use exactly 320g of water comes from the fact that the losses of the calorimeter was calibrated for this precise mass of water.

Water's and PCM's temperatures were measured second by second and collected in a TXT file on a computer connected with the digital tracker shown in Fig.27.

The weight of the steel capsule and of the PCM materials for each experiment are reported in the table below:

Table 10 – Mass of the PCM and the capsule

	Mass of PCM	Mass of steel capsule
Test 1	52,210 g	187,605 g
Test 2	53,407 g	187,605 g
Test 3	53,407 g	187,605 g
Test 4	56,570 g	188,480 g

In every measurement, the most important thing is to wait for the entire system, thermally insulated from the external environment, to reach a state of thermodynamic equilibrium (no more heat exchange between water and PCM and constant temperature in the whole system).

8.2 Measurement of the Cp solid

To calculate the Cp of the PCM when it is solid, it is important that the thermodynamic transition inside the calorimeter remains in the range of temperature where it is known that the PCM does not change phase.

This first measurement then started with the PCM in a solid state and remained solid throughout the measurement.

The PCM inside the steel capsule was refrigerated overnight to ensure that the PCM and steel started at the same temperature during the measurement.

Knowing in advance that the melting temperature of the PCM is around 27°C, it is important that the water starts at 26°C for example, so that one can be sure that the PCM will never reach the melting point.

The following table shows some of the temperatures recorded during the measurement:

Table 11 – Recorded temperatures ($c_{p,solid}$ measurement)

T_{water_1} [°C]	T_{water_2} [°C]	T_{water_3} [°C]	T_{PCM} [°C]
25,100	25,500	25,400	7,400
25,000	25,400	25,400	7,500
24,900	25,300	25,300	7,600
24,900	25,300	25,300	7,600
24,900	25,200	25,200	7,700

24,800	25,200	25,200	7,900
24,700	25,200	25,100	8,100
24,800	25,100	25,100	8,200
24,800	25,100	25,000	8,400
…	…	…	…
23,600	24,000	24,100	23,000
23,600	24,000	24,100	23,000
23,600	24,000	24,100	23,000
23,600	24,000	24,100	23,000
23,600	24,000	24,200	23,000
23,500	24,000	24,200	23,000
23,500	24,000	24,200	23,000
23,500	24,000	24,100	23,000
23,500	24,000	24,100	23,000
…	…	…	…
23,400	24,000	24,300	23,800
23,400	24,000	24,300	23,800
23,400	24,000	24,300	23,800
23,400	24,000	24,200	23,800
23,300	24,000	24,200	23,800
23,300	24,000	24,200	23,800
23,300	24,000	24,200	23,800
23,300	24,000	24,200	23,800
23,300	24,000	24,300	23,800

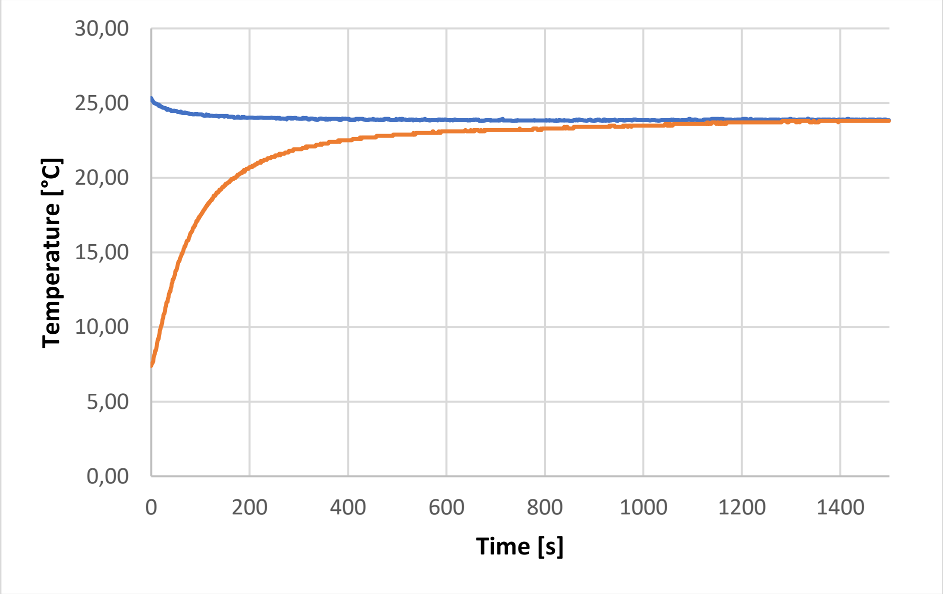

Fig. 29 - Data for the Cp solid

From the graph above it is possible to take the starting and the finishing moments of the measurement for the calculation of the Cp. Hence, a Matlab script was adopted, taking the temperatures data from Excel file. In the code, the equation used for the calculation is shown below:

$$C_{p,s_{PCM}} = \left(\frac{k}{m_{PCM}}\right) \cdot \left(\frac{T_w - T_{w0}}{T_{m0} - T_m}\right) - \left(\frac{m_{steel}}{m_{PCM}}\right) \cdot C_{p_{steel}} \cdot \left(\frac{T_{m0} - T_m}{T_{m0} - T_m}\right) \quad (12)$$

Where:

- $\mathrm{m_{PCM}}$ si the mass of PCM;
- $\mathrm{m_{steel}}$ is the mass of steel capsule and $\mathrm{C_{p_{steel}}}$ is its heat capacity;
- $\mathrm{T_{w0}}$ is the starting temperature of the water;
- $\mathrm{T_w}$ is the water temperature measured for each time-step;
- $\mathrm{T_{m0}}$ is the starting temperature of the PCM;
- $\mathrm{T_m}$ is the water temperature measured for each time step.

Finally, the variable k, in this case, simply refers to the mathematical expression of water:

$$\mathrm{k = m_{water} * C_{p_{water}} = 0{,}320\ [kg] * 4{,}187 \left[\frac{kJ}{kg * K}\right] = 1{,}493}$$

For this calculation the value of the $\mathrm{C_{p_{steel}}}$ was taken equal to 0.5 $\left[\frac{kJ}{kg*K}\right]$.

8.3 Measurement of the Cp liquid

For the evaluation of the Cp liquid of the PCM, the starting conditions are the following. The PCM must be all in the liquid phase and the water has to be hotter than the melting temperature. To satisfy these conditions it was used a water heater where the PCM was located for a while, reaching the temperature of 40°C. Meanwhile since the water has to be at a higher temperature than the melting point (27°C), with an electric resistance placed within the calorimeter the water arrived at 28°C. Although here it is stressed again that it is not important for the water to reach a precise value but a value above the melting with the aim to cool down the PCM without starting the melting process.

The following table shows some of the temperatures recorded during the measurement:

Table 12 - Recorded temperatures ($c_{p,liquid}$ measurement)

T_{water_1} [°C]	T_{water_2} [°C]	T_{water_3} [°C]	T_{PCM} [°C]
29,900	29,600	29,700	39,470
29,900	29,700	29,600	39,470
30,000	29,800	29,700	39,370
30,000	29,800	29,700	39,370
30,000	29,800	29,700	39,370
30,000	29,900	29,700	39,370
30,100	29,900	29,800	39,370
30,000	29,900	29,800	39,270
30,000	29,900	29,800	39,270
…	…	…	…
30,600	30,800	30,700	31,370
30,700	30,800	30,700	31,370
30,600	30,800	30,800	31,370
30,700	30,800	30,700	31,370
30,700	30,800	30,700	31,370
30,700	30,800	30,700	31,370
30,700	30,800	30,700	31,370
30,600	30,800	30,700	31,370
30,700	30,800	30,700	31,370
…	…	…	…
30,600	30,700	30,700	30,670
30,600	30,700	30,700	30,670
30,600	30,700	30,700	30,670
30,600	30,700	30,700	30,670
30,600	30,700	30,700	30,670
30,600	30,700	30,700	30,670
30,600	30,700	30,700	30,670
30,600	30,700	30,700	30,670
30,600	30,700	30,700	30,670

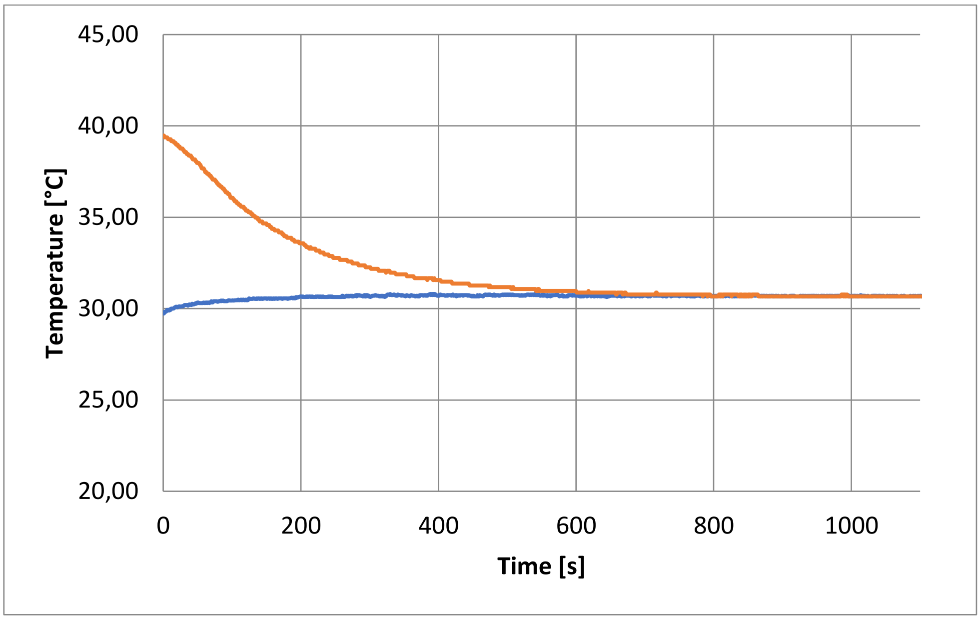

Fig. 30 - Data for the Cp liquid

To evaluate the Cp of the PCM when it was liquid, the same Matlab code was used. In fact, the same calculation shown before was used.

8.4 Measurement of the latent heat

This measure is important for two aspects. The main reason is obviously to discover the amount of latent heat of the PCM during the phase change, but there is another qualitative information that can be evaluated from this test, the T-time curve. In this case the water was at 40°C and the PCM at the moment of the insertion in the Calorimeter was at 20°C (solid state). The explanation for these choices is that the water must be much hotter than the melting temperature in order to completely melt the PCM, that starts from its solid phase while inserted in the Calorimeter. At the end, the water will be cooled down and, the PCM will finish the melting process and already start the liquid sensible behaviour. The measurement ends when the two materials reach approximately the same temperature, meaning that the heat transfer process is nearly finished. This test could also be done starting from the liquid phase of PCM and with cold water (for example 10°C) reaching the solid phase of PCM. However, there would have been some complications with this last approach. The first one is that the solidifications requires more time than the liquefaction. Moreover, in this case there would have been a different T-time curve due to the subcooling phenomenon. In conclusion with the T-time curve the latent heat of the PCM can be calculated.

The following table shows some of the temperatures recorded during the measurement:

Table 13 - Recorded temperatures (latent heat measurement)

T_{water_1} [°C]	T_{water_2} [°C]	T_{water_3} [°C]	T_{PCM} [°C]
39,000	39,400	39,517	21,072
38,800	39,300	39,417	21,072
38,900	39,300	39,417	21,172
38,800	39,300	39,417	21,272
38,800	39,300	39,417	21,272
38,800	39,200	39,317	21,272
38,700	39,100	39,217	21,372
38,600	39,100	39,217	21,472
38,600	39,000	39,017	21,472
…	…	…	…
33,100	33,400	33,617	27,372
33,200	33,400	33,717	27,472
33,200	33,400	33,717	27,472
33,100	33,400	33,617	27,372
33,100	33,400	33,617	27,372
33,000	33,400	33,617	27,372
33,100	33,400	33,617	27,472
33,100	33,400	33,617	27,472
33,100	33,400	33,617	27,472
…	…	…	…
31,900	32,200	32,417	32,172
31,900	32,200	32,417	32,172
31,900	32,200	32,417	32,072
31,900	32,200	32,417	32,072
31,900	32,200	32,417	32,072
31,900	32,200	32,417	32,172
31,900	32,200	32,417	32,072
32,000	32,200	32,417	32,172
31,900	32,200	32,417	32,172

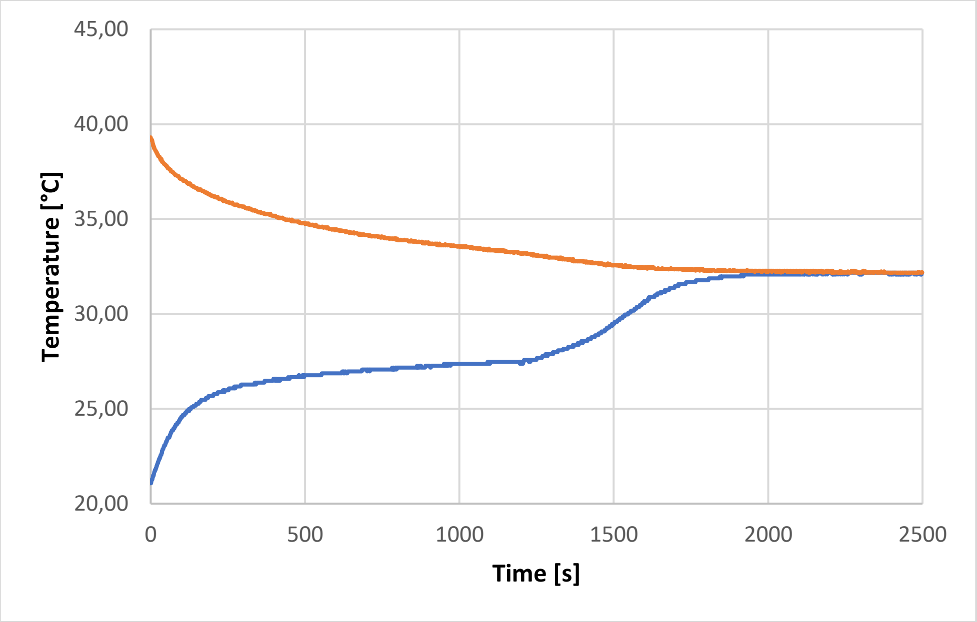

Fig. 31 - Data for the latent heat.

For what concerns the calculation of the latent heat of fusion a different Matlab code was used. In this case the script needs to know the values of the Cp,s and Cp,l of the PCM calculated before, the temperature of melting, that can be deduced from the graph, and also the moments of the start and the end of the measurement. The equation implemented within the script is shown below:

$$\begin{aligned} m_{PCM} \cdot H_m = \; & k \cdot (T_w - T_{w0}) - m_{steel} \cdot C_{p_{steel}} (T_{m0} - T_m) + \\ & - m_{PCM} \cdot C_{p,l_{PCM}} \cdot (T_m - T_S) - m_{PCM} \cdot C_{p,s_{PCM}} \cdot (T_S - T_{m0}) \end{aligned} \tag{13}$$

8.5 Data evaluation

In this chapter are reported all the measurements of Cp,solid, Cp,liquid and the latent heat that were done. All the results for each test are reported here below:

Test 1

Mass of steel capsule=187.82 [g]

Mass of PCM=52.21[g]

Cp solid=0.9765 [kJ/(kg·K)]

Cp liquid=0.8319 [kJ/(kg·K)]

Latent heat=47.8759 [kJ/kg]

Test 2

Mass of steel capsule=187.82 [g]
Mass of PCM=53.407[g]
Cp solid=1.8965 [kJ⁄(kg·K)]
Cp liquid=2.3678 [kJ⁄(kg·K)]
Latent heat=134.9619 [kJ/kg]

Test 3

Mass of steel capsule=187,60[g]
Mass of PCM=53,407[g]
Cp solid=1.6425 [kJ⁄(kg·K)]
Cp liquid=2.3777 [kJ⁄(kg·K)]
Latent heat=131.6871 [kJ/kg]

Test 4

Mass of steel capsule=188.48[g]
Mass of PCM=56.57[g]
Cp solid=0.5960 [kJ⁄(kg·K)]
Cp liquid=2.3433 [kJ⁄(kg·K)]
Latent heat=133.7284 [kJ/kg]

The range of values was taken between the beginning of the test (instant 0) and the moment where the water temperature and the PCM temperature were significantly close to each other and also where these temperatures remain the same (before and after that point).

These criteria were applied in order to get rid of irrelevant data from the experiment that could affect the results. In fact, the effect of this approximation is to end up to the measurement before it really ends, cutting off the last data of the heat transfer where actually the heat transfer is already finished.

At the end, there must be taken an average value from all the test. Therefore, here there are two different tables. In both cases were calculated the arithmetic mean and the standard deviation of the Cp solid/liquid and the latent heat. In the first table the data from all the experiments were taken into consideration, meanwhile the second table does not count the first test that is the one most affected by errors.

Table 14 – Tests' Results

	Cp solid [kJ/(kg · K)]	Cp liquid [kJ/(kg · K)]	Latent heat [kJ/kg]
Test 1	0,9765	0,8319	47,8759
Test 2	1,8965	2,3678	134,9619
Test 3	1,6425	2,3777	131,68
Test 4	0,5960	2,3433	133,7284
Medium value	1,277875	1,980175	112,0616
Standard deviation	0,491625	0,574138	32,09283

At this point some considerations can be done. The values obtained from the experiments are similar each other, with the exception of the first test. In fact, the first test, is affected by some errors. There were made two type of errors: the first is that the data storage started with a delay, due to a problem in the connection of the temperature sensors with the computer. The other one was that the system had not been used for a while before the measurements, and as a result the system was not well calibrated and so it gave out weird values. After that measurement the Calorimeter and the sensors were re-calibrated. For these reasons it is more interesting to focus on the results obtained in the next tests, that are more reliable and accurate.

Table 15 – Tests' Results.

	Cp solid [kJ/(kg · K)]	Cp liquid [kJ/(kg · K)]	Latent heat [kJ/kg]
Test 2	1,8965	2,3678	134,9619
Test 3	1,6425	2,3777	131,68
Test 4	0,5960	2,3433	133,7284
Medium value	1,3783	2,3629	133,4568
Standard deviation	0,521556	0,013089	1,184511

As a result, considering the second table, the results show a stable trend for the Cp liquid and the latent heat around the average value, despite the Cp solid reported some different values. However, all these values could be considered successful compared to the values of the well-known salt-hydrate PCM taken from the literature.

Table 16 – Salt-hydrate PCM's benchmark values (adapted from [1])

$CaCl_2*6H_2O$		
Cp solid =1.42 [kJ/(kg · K)]	Cp liquid= 2.10 [kJ/(kg · K)]	Latent heat Hm=190 [kJ/kg]

9. T-History method [6]

The T-history method, first proposed by Zhang et al. 1999, is a simple and economic way for the determination of the stored heat as a function of temperature of PCM. Its origin is based on the determination of phase diagrams. When a sample of a material is cooled down and its temperature history (T-history) is recorded, as shown in Fig.32, any change in its thermophysical properties that leads to a release of heat will result in a change of its temperature history. For example, the release of the latent heat of solidification will ideally result in a sample temperature that remains constant for some time, until the latent heat is released. This system is renowned for its simplicity and low cost in terms of measurement time and materials.

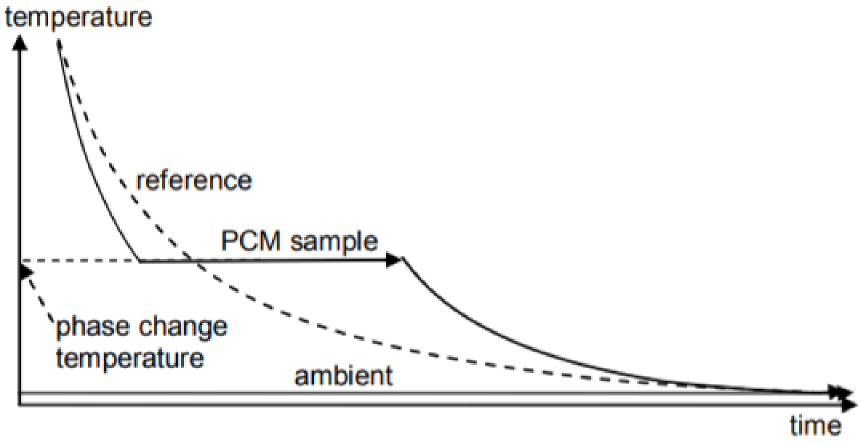

Fig. 32 - T-history of a sample with a latent heat effect, and a reference with only sensible heat, during cool down at constant ambient temperature

For a long time, this method has been used to find the phase change temperatures of mixtures, data that are necessary to draw phase diagrams. Because the heat exchanged was not measured, it was not a calorimetric method. That changed when Zhang et al. 1999 further developed the idea to be able to get quantitative information on the heat stored. For that, the heat flux during cool down had to be determined. This was done using two identical setups, one with the sample, and one with a reference material (Fig.33).

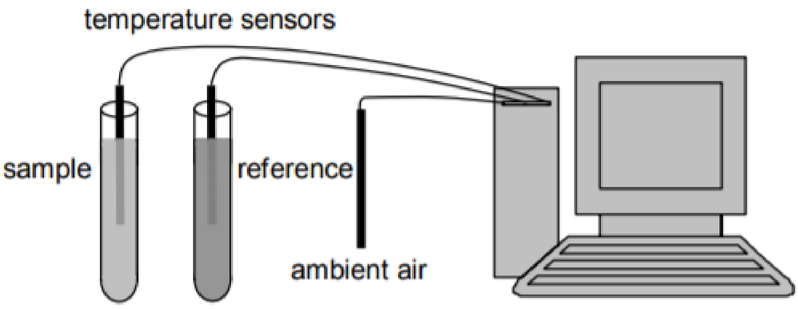

Fig 33. Schematic figure of an experimental T-history method set-up

The experimental procedure is as follows. The sample, and a reference (water in this case) with known thermal properties, are subject to ambient air. Their temperature history upon cooling down from the same initial temperature to the ambient temperature is recorded, as Fig.32 shows. A comparison of both curves, assuming identical heat transfer coefficients between sample and ambient, as well as reference and ambient, allows the determination of the heat stored within the sample from the known heat capacity of the reference material. In the same way also the temperature curves during the heating up can be measured, starting with the PCM in a solid state until it is liquid.

The determination is based on the following calculations: The heat flux from the sample to the environment, the ambient air, is

$$\dot{Q} = \frac{1}{R_{th}} \cdot \left(T_{sample} - T_{ambient}\right) = -C_{sample} \cdot \frac{d}{dt} T_{sample} \qquad (14)$$

To get a quantitative value of the heat flux, the unknown thermal resistance R_{th} has to be determined. For that, the reference with known heat capacity is used. The reference gives

$$\dot{Q} = \frac{1}{R_{th}} \cdot \left(T_{reference} - T_{ambient}\right) = -C_{reference} \cdot \frac{d}{dt} T_{reference} \qquad (15)$$

If the sample and reference have the same geometry and are placed in the same environment, R_{th} has the same value for the sample and the reference. From the temperature history and heat capacity of the reference $C_{reference}$, R_{th} can be calculated by eq.15. The heat capacity of the sample can then be calculated from the temperature history of the sample and eq.14. There are several methods to evaluate the signal of a T-history measurement based on the formulas just described. They differ in what the result is, like one value for the heat capacity of the solid or a temperature dependent value, the way subcooling is treated, and the mathematical procedure.

9.1 Method of calculation: determinations of the heat of fusion, specific heat

The calculation method for the phase change from liquid to solid of PCM will be shown below, but an approximately equal procedure can be used for the phase change from solid to liquid.

If a tube containing a liquid PCM whose temperature is uniform and equal to T_0 ($T_0 > T_m$, T_m is the melting temperature of the PCM) is suddenly exposed to an atmosphere whose temperature is $T_{\infty,a}$ (which can be time dependent), the temperature versus time curve of the PCM, i.e. the T -history curve, is as shown in Fig.34, where ΔT_m $(=T_m - T_s)$ is the degree of supercooling.

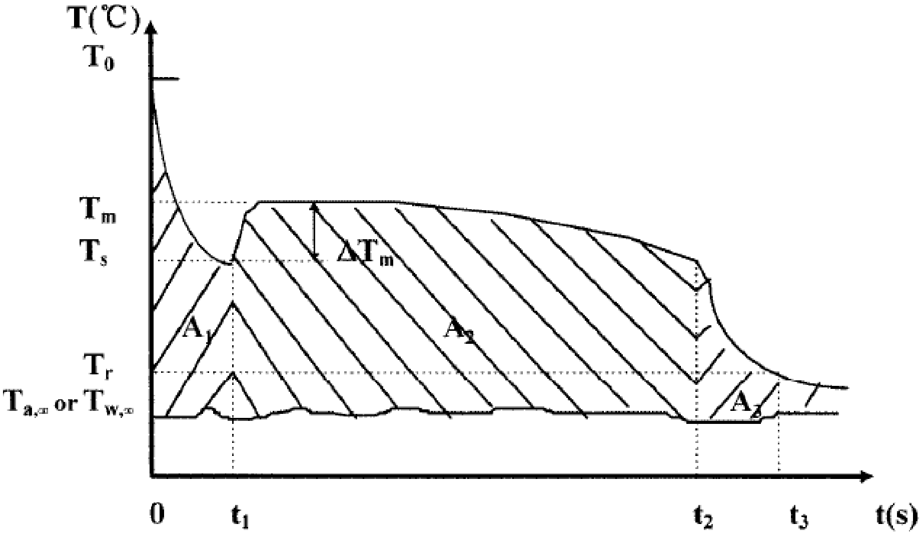

Fig. 34 - A typical T-history curve of a PCM during a cooling process (with subcooling)

When Bi ($=hR/(2k)$, i.e. the Biot number, where R is the radius of a tube, k the thermal conductivity of PCM and h the natural convective heat-transfer coefficient of air outside a tube) is less than < 0.1, the temperature distribution in the sample can be regarded as uniform and the lumped capacitance method can be used. Hence, we have

$$(m_t c_{p,t} + m_p c_{p,l})(T_0 - T_s) = hA_c A_1 \tag{16}$$

where m_p and m_t are the masses of the PCM and tube, respectively, $c_{p,,l}$ and $c_{p,t}$ are the mean specific heats of the liquid PCM and of the material of the tube, respectively, and A_c is the convective heat-transfer area of a tube; $A_1 = \int_0^{t_1} (T - T_{\infty,a}) dt$. We have also

$$m_t H_m = hA_c A_2 \tag{17}$$

where H_m is the heat of fusion of the PCM and $A_2 = \int_{t_1}^{t_2} (T - T_{\infty,a}) dt$ ($t_1 \rightarrow t_2$ is the time during which a phase-change process occurs) and

$$(m_t c_{p,t} + m_p c_{p,s})(T_s - T_r) = hA_c A_3 \tag{18}$$

where $c_{p,s}$ is the mean specific heat of the solid PCM, $A_3 = \int_{t_2}^{t_3} (T - T_{\infty,a}) dt$ and T_r is the reference temperature.

If a tube containing pure water is suddenly exposed to the same atmosphere as that mentioned above, its cooling curve is as shown in Fig.35. Considering that $Bi < 0.1$, similarly, we have

$$(m_t c_{p,t} + m_w c_{p,w})(T_0 - T_s) = hA_c A'_1 \tag{19}$$

$$(m_t c_{p,t} + m_w c_{p,w})(T_s - T_r) = hA_c A'_2 \tag{20}$$

Where m_w and $c_{p,w}$ are the mass and mean specific heat of water, respectively, $A'_1 = \int_0^{t'_1} (T - T_{\infty,a}) dt$ and $A'_2 = \int_{t_1}^{t'_2} (T - T_{\infty,a}) dt$.

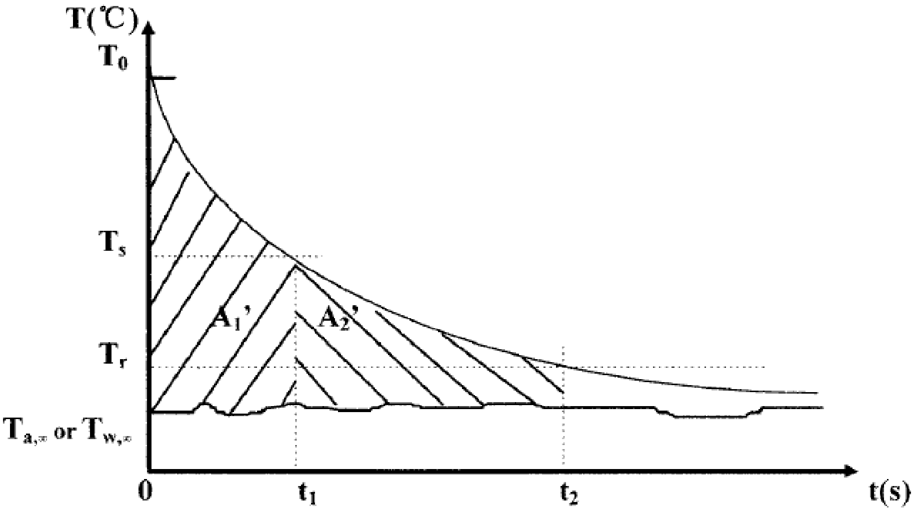

Fig. 35 - A typical T- history curve of water during a cooling process

In fact, using equation (19), the natural convective heat transfer coefficient of air outside a tube *(h)* can be obtained. It is about 5-6 [$Wm^{-2}K^{-1}$], so the condition about $Bi \leq 0.1$ can be satisfied when $k_s > 0.2$ [$Wm^{-1}K^{-1}$] (k_s of salt hydrates are all larger than 0.3 [$Wm^{-1}K^{-1}$]).

From equations (16)-(20), one obtains:

$$c_{p,s} = \frac{m_w c_{p,w} + m_t c_{p,t}}{m_p} \frac{A_3}{A'_2} - \frac{m_t}{m_p} c_{p,t} \tag{21}$$

$$c_{p,l} = \frac{m_w c_{p,w} + m_t c_{p,t}}{m_p} \frac{A_1}{A'_1} - \frac{m_t}{m_p} c_{p,t} \tag{22}$$

$$H_m = \frac{m_w c_{p,w} + m_t c_{p,t}}{m_t} \frac{A_2}{A'_1} (T_0 - T_s) \tag{23}$$

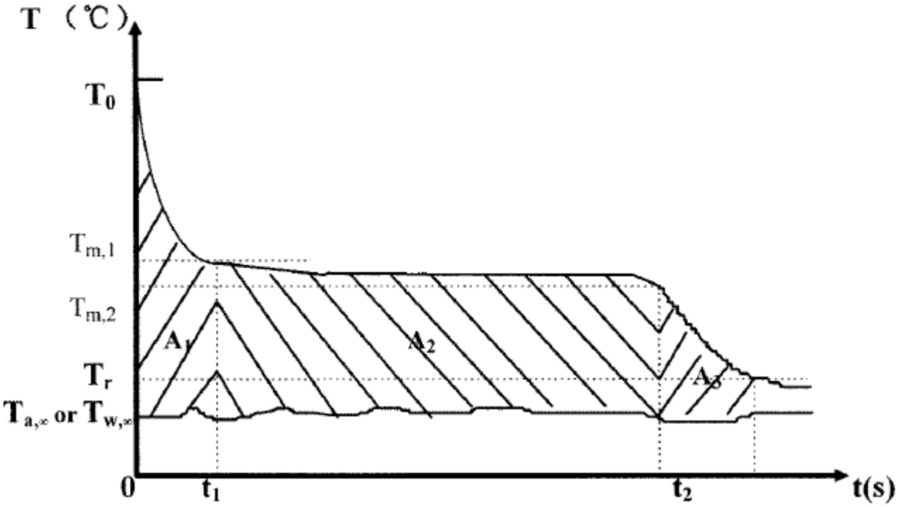

Fig. 36 - A typical T- history curve of a PCM during a cooling process (without subcooling)

For PCMs without supercooling (see Fig.36, where the temperature range of the phase-change process is between $T_{m,1}$ and $T_{m,2}$), the expressions for $c_{p,l}$ and $c_{p,s}$ are the same as those above, but the heat of fusion should be rewritten as follows:

$$H_m = \frac{m_w c_{p,w} + m_t c_{p,t}}{m_p} \frac{A_2}{A'_1} \left(T_0 - T_{m,1}\right) - \frac{m_t c_{p,t}\left(T_{m,1} - T_{m,2}\right)}{m_p} \qquad (24)$$

Compared with methods available such as conventional calorimetry methods, the method presented in this paper has the following salient features: the experimental system is simple; it is able to measure lots of samples and obtain several thermophysical properties of each PCM sample through a group of tests; the precision of measurement satisfies the need for engineering applications; and the phase-change process of each PCM sample can be observed clearly.

The results agree well with those in the literature. This method is useful for rapid measurement of PCM candidate for use in engineering applications of latent thermal storage. The method is applicable to a larger range of temperature if an oil bath or other suitable liquid bath were used instead of a water bath.

9.2 Measurements with T-history method

Two different types of PCMs were analysed. The first was the one prepared in the laboratory, the second was the one taken from the PCMbags that were into an old cylindrical storage tank. These two PCM types are very similar in terms of composition and in terms of melting temperature and both are salt hydrates, so what is expected is that the results of the measurements are quite similar.

For the first type of PCM two samples were taken to be analysed while from the old tank three samples were taken from three different bags.

9.2.1 First type of PCM measurement

The laboratory experiment involved two measurements. The first measurement started with water and PCM at the ambient temperature of the laboratory, thus with the PCM in a solid state. Water and PCM were placed in an oven at a constant temperature of 35°C until both arrived in thermal equilibrium with the environment.

The temperature of all the test tubes was measured and saved every 10 seconds using 3 thermocouples and 2 digital trackers.

The second measurement started immediately after the first one: the cables were disconnected from the digital tracker for more than 30 seconds in order to finish the first measurement; water and PCM were taken from the oven and placed inside a fridge and the cables were then reconnected to the digital tracker.

In this way, two temperature curves were obtained. The first with the PCM that starts at the ambient temperature of the laboratory (solid state) and reaches a state of equilibrium with the oven at 35 °C (liquid state). The second with the PCM that starts at a temperature of about 35 °C (liquid state) and reaches a state of equilibrium with the fridge (solid state).

Materials and tools used were:

- 3 test tubes;
- 3 thermocouples;
- a support to keep the tubes in a vertical position;

- 2 digital tracker;
- water;
- PCM with a melting temperature of about 27 °C;
- a balance;
- a programmable temperature oven;
- fridge.

One tube was filled with water, the other two with PCM. All tubes were weighed before and after being filled, in order to know precisely the mass of the tubes, water and PCM.

For the T-history method it is very important that the water and the PCM inside the tubes have all the same volume, so that the heat exchange surface is the same for all the samples; the three tubes were thus all filled to the same level.

Due to the non-availability of a temperature probe, during this first experiment the ambient temperature was not measured, and so the last temperature measured from the water was taken as ambient temperature for the calculations. This approximation can lead to large errors especially in the calculation of c_{pliq} and c_{psol}.

The results of the first two analysed samples are shown below.

Table 17 - First experiment results

Sample		heating (oven)	cooling (fridge)
PCM 1	c_{pliq} [kJ/(kg*k)]	2,701	3,090
	c_{psol} [kJ/(kg*k)]	5,529	0,543
	Hm (latent heat) [kJ/kg]	150,474	156,841
PCM 2	c_{pliq} [kJ/(kg*k)]	8,045	3,432
	c_{psol} [kJ/(kg*k)]	4,371	1,352
	Hm (latent heat) [kJ/kg]	156,278	159,837

As one can see, the values of c_{pliq} and c_{psol} vary greatly from measure to measure and therefore cannot be considered as a result. Moreover, the values itself are really high, discording to the known properties of the material from the state of the art.

What can be taken into consideration as a result is the value of the Hm (latent heat); it does not vary much from measurement to measurement and its calculation is independent from the values obtained of the specific heats of the liquid and solid phase. This time, on the contrary with the c_p, the results are acceptable, according with the standards. There were taken as a benchmark values, as already reported, the following data from a common salt-hydrate, similar to the one used in these two experiments:

Table 18 – Salt-hydrate PCM's benchmark values (adapted from [1])

$CaCl_2*6H_2O$		
c_{psol} =1.42$\left[\frac{kJ}{kg \cdot K}\right]$	c_{pliq}= 2.10 $\left[\frac{kJ}{kg \cdot K}\right]$	Hm =190 $\left[\frac{kJ}{kg}\right]$

It was then calculated a Hm that varies between 150,5 and 159,8 [kJ/kg].

Below are graphs of the temperature behaviour of a PCM sample and water during the cooling process and the heating process.

Graphs of the temperature behaviour of one PCM sample and water during the cooling and heating process are shown below.

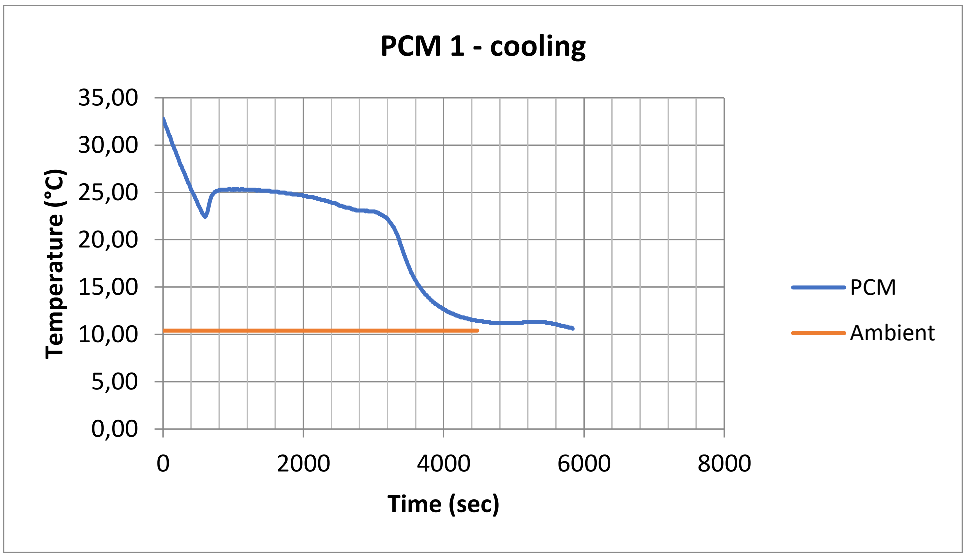

Fig. 37 - Behaviour of PCM during the cooling process

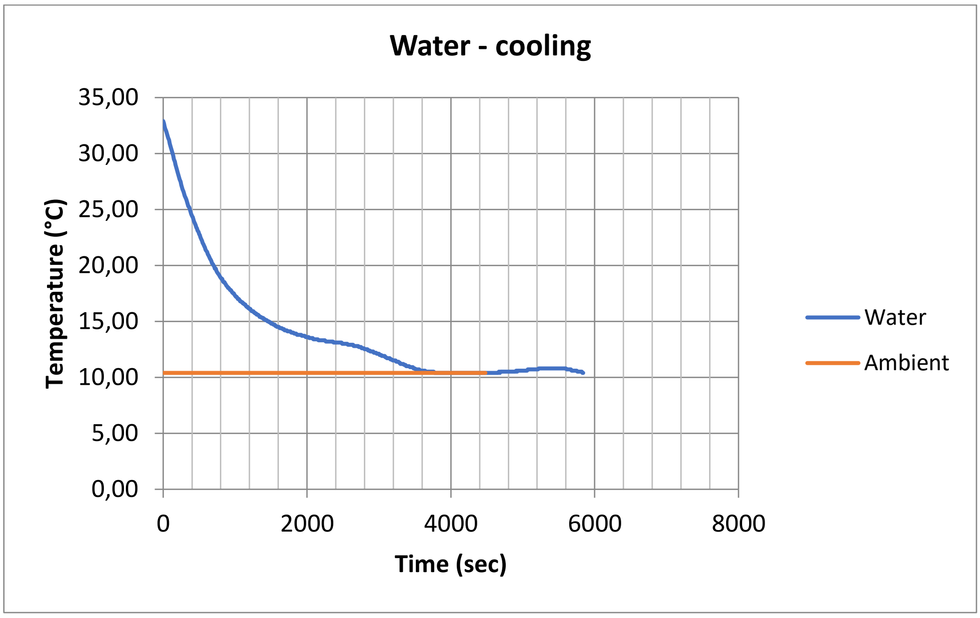

Fig. 38 - Behaviour of water during the cooling process

From the graph in Fig.37 one can see the effect of subcooling, where the temperature curve has a peak down and then goes up and start the crystallization process at a temperature above 25 ° C.

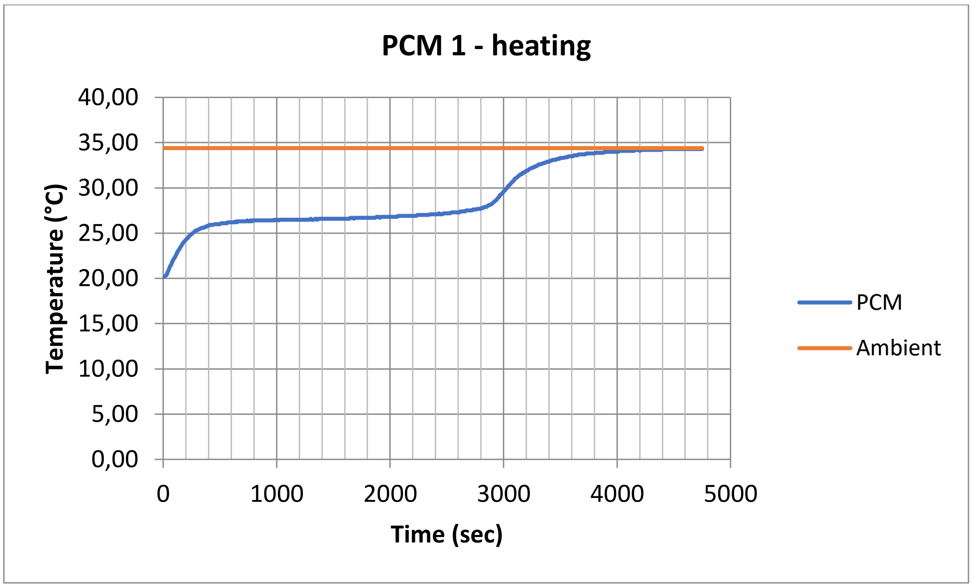

Fig. 39 - Behaviour of PCM during the heating process

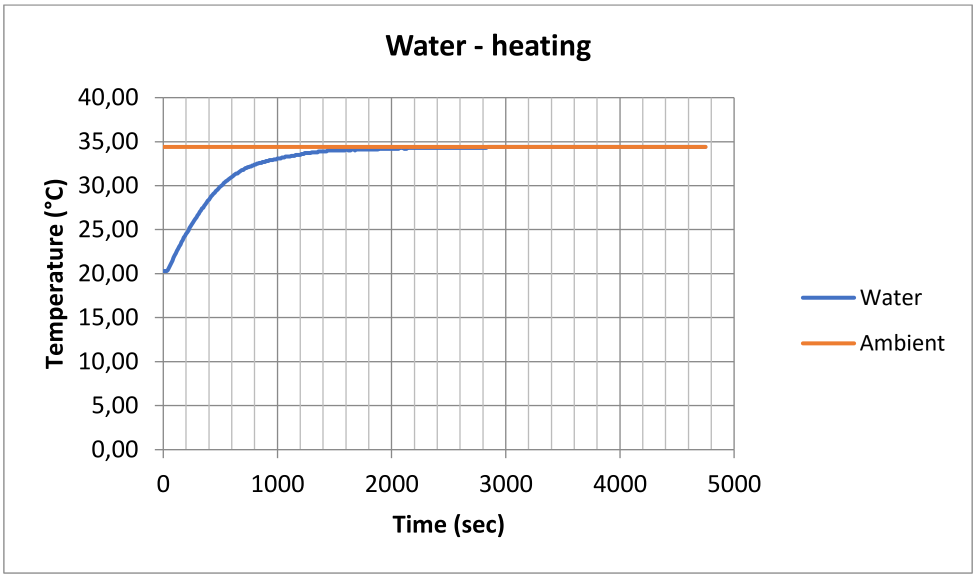

Fig. 40 - Behaviour of water during the heating process

The latent behaviour of the PCM is clearly visible in the graph in Fig.39. The melting process starts at a temperature of just over 25 °C and ends at around 28 °C.

9.2.2 PCMbags Measurement

As already mentioned for this experiment, three different PCM tubes have been analysed.

Compared to the previous experiment in this case, the ambient temperature was also tracked to see if with that it was possible to obtain more stable values of specific heats. With the aim of collecting more data, three measurements were made and not two.

The temperature was tracked during a first cooling process, a heating process and a second cooling process. Compared to the first experiment the duration of the data storage was longer this time for each measurement (the two cooling and the heating). So far, with a more accurate values for the PCM and the water in addition to a more precise value for the Ambient temperature the results obtained are better.

The results obtained are shown in the following tables:

Table 19 - PCMbags measurement, first cooling

	$c_{psol}\left[\frac{\mathrm{kJ}}{\mathrm{k_g \cdot K}}\right]$	$c_{pliq}\left[\frac{\mathrm{kJ}}{\mathrm{k_g \cdot K}}\right]$	$\mathrm{Hm}\left[\frac{\mathrm{kJ}}{\mathrm{k_g}}\right]$
PCM 1	1,72247	2,712264	136,5345
PCM 2	1,445714	2,832004	159,9437
PCM 3	1,609243	1,871091	211,5706
average value	1,592476	2,471786	169,3496
Standard deviation	0,097841	0,400464	28,14733

Table 20 - PCMbags measurement, second cooling

	$c_{psol}\left[\frac{\mathrm{kJ}}{\mathrm{k_g \cdot K}}\right]$	$c_{pliq}\left[\frac{\mathrm{kJ}}{\mathrm{k_g \cdot K}}\right]$	$\mathrm{Hm}\left[\frac{\mathrm{kJ}}{\mathrm{k_g}}\right]$
PCM 1	2,031852	2,765701	187,1066
PCM 2	1,766887	3,717862	132,0066
PCM 3	1,836399	3,671457	179,3367
average value	1,878379	3,385007	166,15
Standard deviation	0,102315	0,41287	22,76224

Table 21 - PCMbags measurement, heating

	$c_{psol}\left[\frac{\mathrm{kJ}}{\mathrm{k_g \cdot K}}\right]$	$c_{pliq}\left[\frac{\mathrm{kJ}}{\mathrm{k_g \cdot K}}\right]$	$\mathrm{Hm}\left[\frac{\mathrm{kJ}}{\mathrm{k_g}}\right]$
PCM 1	2,858645	2,916305	150,0048
PCM 2	4,022728	1,751326	136,5037
PCM 3	2,838412	2,045067	150,7849
average value	3,239928	2,237566	145,7645
Standard deviation	0,521866	0,452493	6,173844

The results from the measurements give approximately values for the latent heat in the same range of the first experiment. Meanwhile both for the Cp solid and Cp liquid the values are lower. However, the values for the Cp, as happened for the first experiment, are slightly different from the expected ones. In fact, for the first cooling the average value of Cp solid and Cp liquid are very close to the standards expected. Also, the Cp liquid from the heating and the Cp solid from the second cooling measurement are good results. On the contrary the other measurements for the Cp values are a little too high. At the same time for all the three measurements good results came out for the latent heat.

As a conclusion the graphs for the cooling and the heating are shown here below.

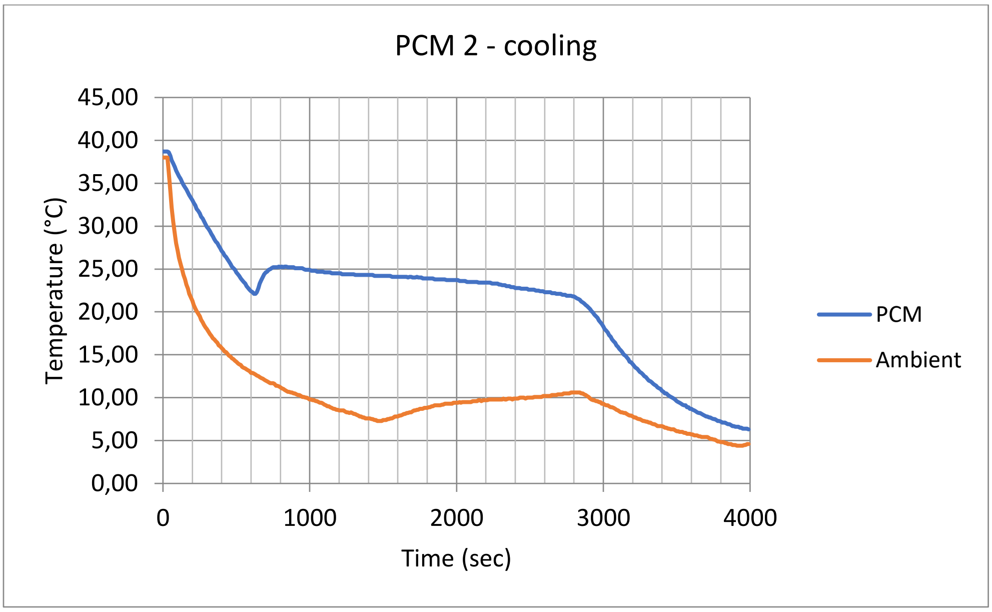

Fig. 41 - PCM2 - cooling

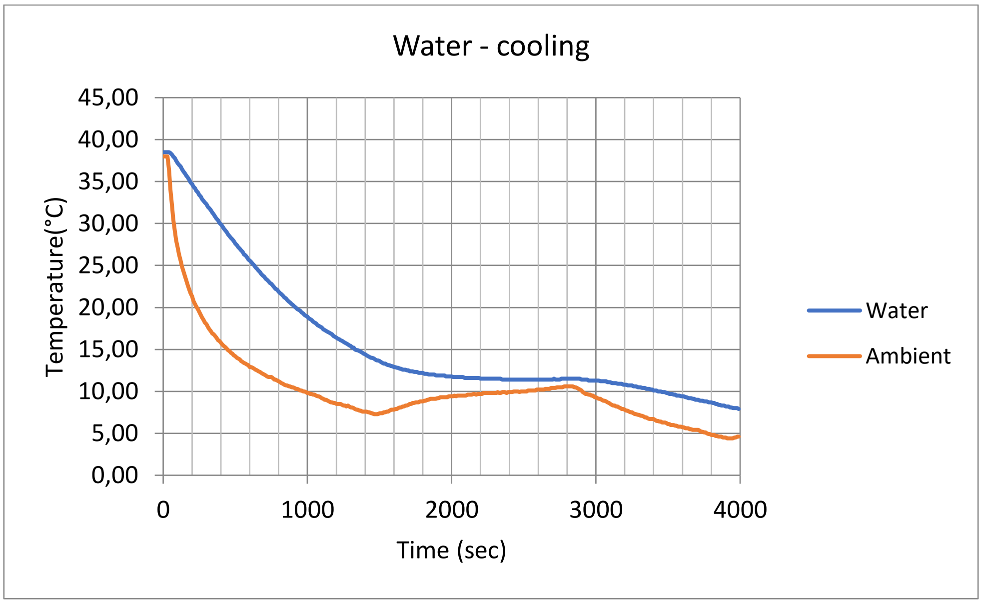

Fig. 42 - Water - cooling

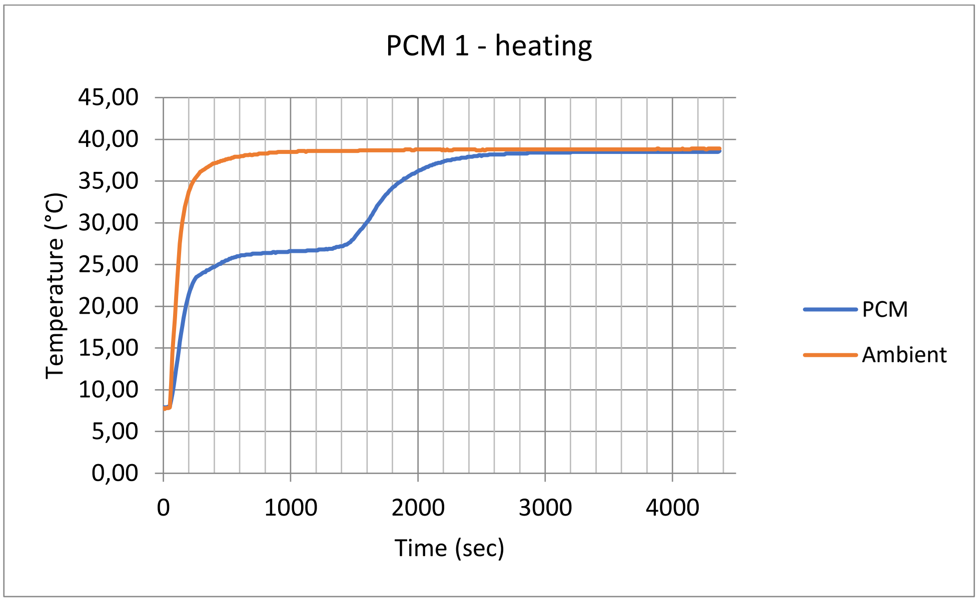

Fig. 43 - PCM1 – heating

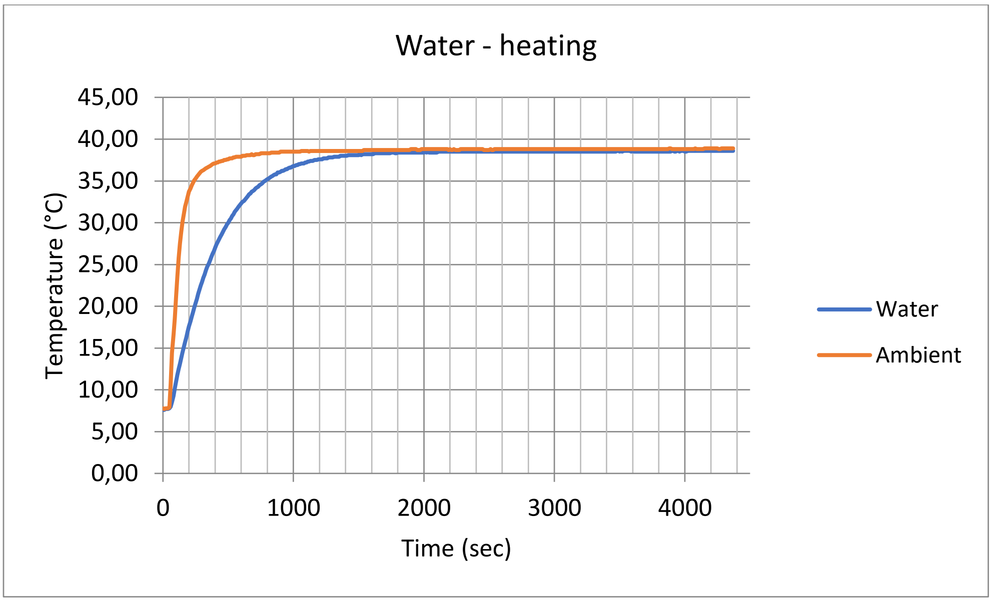

Fig. 44 - Water- heating

10. Year-round Matlab simulation of the system

In these paragraphs are reported and discussed the simulation for the calculations of the parameters of the systems, with the aim to discover the consumptions, costs of energy and other interesting values. This evaluation is useful to have a long-term projection of how the systems should work while implemented. For the simulations it was necessary to use data set to describe the weather condition for each day, and some other parameters to describe the system. These data are useful to have a realistic value of the heat energy demand from the house; in this case they were provided by the CeMOS department. In addition, even the amount of solar irradiance was taken because the system is supposed to be installed in a house where there is a solar power system to run the heat pump. In this way the calculation was made pretty realistic. In every simulation the following objects are always present: there is always a solar panel, a heat pump and the water tank with PCMboxes inside.

10.1 Solar energy

In the calculation the system works in this way; the heating is given by the system, only if there is an effective energy demand from the house. This hypothesis may sound obvious, but it is not, because there could be even a system where one wants to have always a fixed value of energy in the tank, without caring if the house really needs this energy or not. When there is the energy demand coming from the house the water will be heated up by the PCMboxes. If the PCMboxes are not enough hot the pump is used. If there is not energy demand no heating is given to the house and the water will decrease its temperature. During the simulations, when the heat pump has to run there are three possible scenarios. First of all let us define three indicators for the heat pump: the nominal energy of the pump “I_{wp}” ,the sun energy “I_i”, the energy limit to make the pump run with solar energy “I_{grenz}”.

The cases of the working methods for the pump are the following. If the energy from the sun is higher than the energy limit from the pump, $(I_{grenz} < I_i)$ then the electricity from the solar panel is used to make the pump run. Here there are two more cases that can happen when $I_{grenz} < I_i$.

It can happen that $I_{wp} > I_i$, that means the solar energy is not enough to make the heat pump run, therefore some energy must be taken from the grid in order to reach the nominal energy of the pump, I_{wp}. As a result, from the grid $I_{wp} - I_i$ is taken, and of course this is counted as a cost.

In the other case $I_{wp} \leq I_i$ the solar energy is high enough to run the heat pump and so it is not necessary to buy electricity from the grid. Thus, the surplus of solar energy, $I_i - I_{wp}$, can be sold on the grid.

Meanwhile if the solar energy is below the limit for the pump: $I_{grenz} > I_i$ the pump must be run with all the energy coming from the grid. However, this amount of electricity I_i, that it is not enough to run the pump, is sold to the grid.

$if\ EnergyDemand > 0$	
$if\quad I(i) > I_{grenz}$	
$if\quad I_{WP} > I(i)$ $Q_{energy\ to\ buy} = I_{WP} - I(i)$ $Q_{energy\ sold} = 0$ $else$ $Q_{energy\ to\ buy} = 0$ $Q_{energy\ sold} = I(i) - I_{WP}$ end	Energy loop A.1
$else$	
$Q_{energy\ to\ buy} = I_{WP}$ $Q_{energy\ sold} = 0$	Energy loop A.2
end	
$else$	
$Q_{energy\ to\ buy} = 0$ $Q_{energy\ sold} = I(i)$	Energy loop A.3

10.2 Heat losses

This calculation model was provided with heat losses. Here as heat losses basically were considered only two type of losses: heat losses caused by the distribution system, in this case pipes, and heat losses caused by storing. The formula describing these losses were taken from the European rules for the calculation of energy buildings systems.

Starting from the heat losses of distribution ($Q_{d,loss}$) one has:

$$Q_{d,loss} = \sum_{i=1}^{M} L_i \cdot U_i \cdot (T_{water} - T_{amb}) \cdot t_i \tag{25}$$

Where:

1. L_i = length of the considered pipe track
2. U_i = Transmittance of the considered pipe
3. T_{water} = temperature of the water in the pipe
4. T_{amb} = temperature of the ambient air
5. t_i = time of utilization of the circuit

For the storing heat losses (Q_{store}), one has:

$$Q_{store} = \frac{S_s}{d_s} \cdot (T_{store} - T_{amb}) \cdot t_i \cdot \lambda_s \tag{26}$$

Where:

1. S_s =external area of the tank
2. d_s =thickness of insulator installed on the tank
3. T_{store} = temperature inside the tank
4. T_{amb} = temperature of the ambient air
5. λ_s = thermal conductivity of the insulator
6. t_i = time period of calculation

Now are described the specific materials considered for the calculations of the losses. These values remained the same in all the calculations. Starting from the losses of distribution, hence from the pipes, it was supposed that the pipes were not insulated from the ambient. However, it was also supposed that the pipe circuit was located inside a room with the tank insulated from the external environment, for instance in a basement.

For this case, the norm provides a formula to calculate the value of U_i considering only the temperature difference form the water in the pipes and the outside air, and the diameter of the pipe-circuit:

$$U_i = 3{,}24 \cdot \pi \cdot d \cdot (T_{water} - T_{amb})^{0.3} \tag{27}$$

As diameter for the pipes was taken a value of $d = 5cm$ and a value for the ambient temperature $T_{amb} = 15°C$ .The last fixed value was the length of the pipes that was $L_i = 10m$.

The variable T_{water} changed for every loop of calculation meanwhile the term t_i is the time step of the loop.

Hence for the storage losses the considerations already made for T_{amb} remained the same. It was supposed that the tank was insulated with a substrate of stone wool, with a thickness of $2cm$. In this way the value of the thermal conductivity was $\lambda_s = 0.037 \left[\frac{W}{m\ K}\right]$ and the thickness substrate of insulator was $d_s = 2cm$. The last value to set up is S_s : in this case the external area of the tank was measured as $S_s = 4.42\ m^2$, and this was set as a parameter for all the simulations.

10.3 COP evaluation

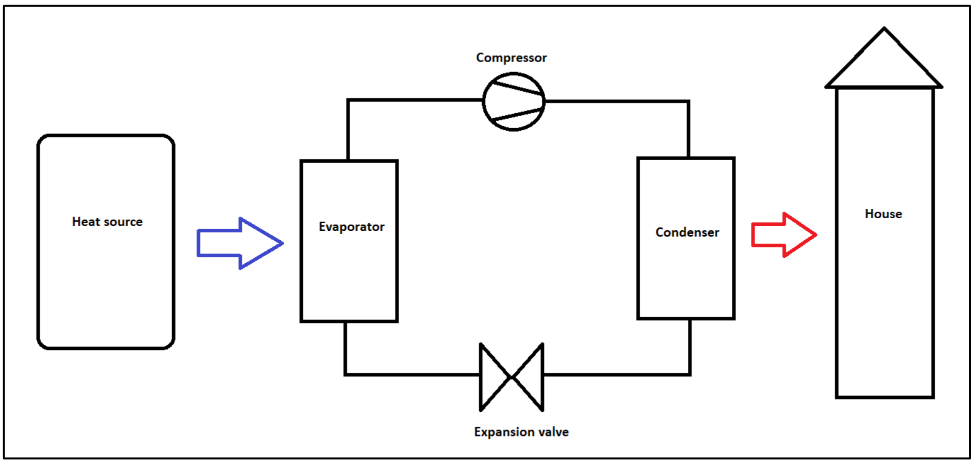

Fig. 45 - Schematic description of the plant

The functioning of the heat pump can be schematized as in the picture above (Fig.45). There is a heat source, in this work case represented by a water tank, a heat pump and a house. This chapter deals with the description of the Heat Pump used in the Matlab code.

Within all simulations made, to simulate the behaviour of the heat pump, it was necessary to implement a function for the COP (coefficient of performance), defined as the ratio between the heat delivered to the high temperature ambient and the amount of energy consumed to transport it.

The lower is the temperature difference between the source temperature and the temperature in the flow of the heating system, the greater will be the COP. Therefore, the temperature difference can change by increasing/decreasing one of these two temperatures. If the temperature flow of the heating system is lowered by 1 °C the coefficient of performance increases by 2.5 % and it increases by 2.7 % if the source temperature is increased by 1 °C.

From experimental data provided by the CeMOS department it was found a polynomial function of this temperature difference.

Table 22 – COP in function of ΔT

ΔT [K]	COP
50	3,07
45	3,5
40	3,99
35	4,55
30	5,19
25	5,9
20	6,71
15	7,63
10	8,67

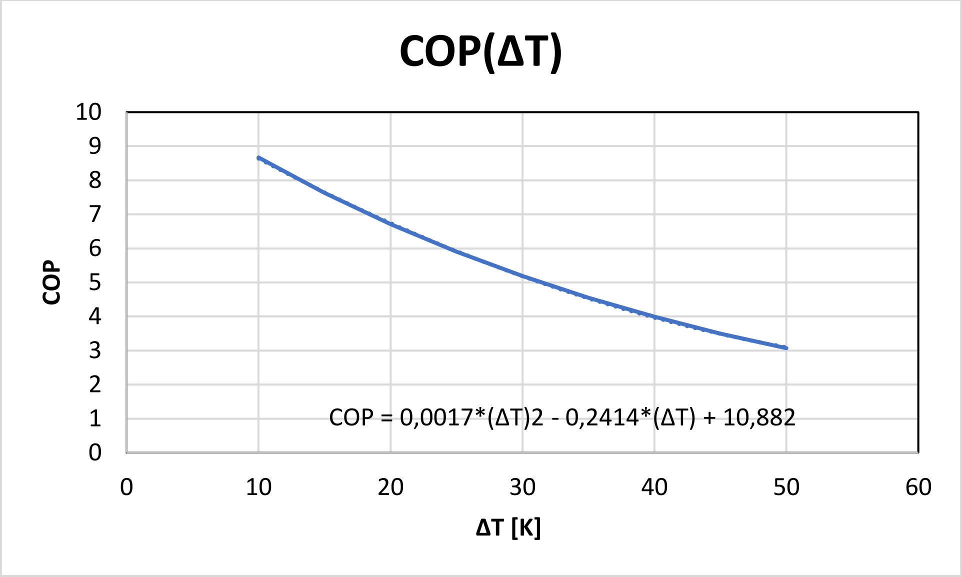

Fig. 46 - Graph of the polynomial expression of the COP

So far, in the simulation, it was used, as a formula to calculate the COP, the polynomial expression obtained from the experimental data set:

$$COP = 0{,}0017 * (\Delta T)^2 - 0{,}2414 * (\Delta T) + 10{,}882 \quad (28)$$

Where in the code the value of ΔT was calculated for every loop, taking into account the outside temperature of the day $T_{a(i)}$, the temperature of the system (T_{PCM} or T_{water}) and a fixed value that represents the temperature difference between the heat source and the temperature flow of the house circuit ($dTWUT$).

$$\Delta T = T_{PCM(i)} - T_{a(i)} + dTWUT \quad (29)$$

Where $dTWUT = 10°C$. In this way the simulations consider the weather conditions for the calculation of the COP. As a consequence, the Heat Pump is described more realistic rather than using a fixed value for the COP for the whole year-round simulation and it is also possible to see the effect of the working temperature on it.

10.4 Materials properties

As mass of water it was taken 350 kg that is in fact the real value of water in the tank. The total PCM mass was calculated as it follows:

$$m_{PCM} = Volume_{total} * \rho_{PCM} = 324\ [kg] \tag{30}$$

Where the density was accounted as $\rho_{PCM} = 1800\ \left[\frac{kg}{m^3}\right]$, and the Volume was estimated taking the number of PCM boxes=180 multiplied by considering each box made of 1 litre. Then $Volume_{total} = \frac{180}{1000} = 0.18\ m^3$. In the table below are reported some fundamental parameters considered for the water and the PCM.

Table 23 – Some fundamental parameters considered for the simulation

$Cp_{l_{PCM}} = 2100\ \left[\frac{J}{kg * K}\right]$	$T_{high} = 30\ [°C]$
$Cp_{s_{PCM}} = 1420\ \left[\frac{J}{kg * K}\right]$	$T_{low} = 25\ [°C]$
$Cp_{water} = 4190\ \left[\frac{J}{kg * K}\right]$	$T_{melt} = 27\ [°C]$

Where for T_{low} it refers to the minimum temperature wanted for the storage tank. On the contrary T_{high} stands for the maximum value admitted for the storage tank, meanwhile T_{melt} refers to the melting temperature of the PCM. On the left are reported the values for the Cp solid and liquid of the PCM and the Cp of water.

$Q_{low} = 0$
$Q_{melt_s} = \left(m_{PCM} * cp_{s_{PCM}} + m_{water} * cp_{water}\right) * (T_{melt} - T_{low})\ [J\ ]$
$Q_{melt_l} = Q_{melt_s} + H_{PCM}\ [J\ ]$
$Q_{high} = Q_{melt_l} + \left(m_{PCM} * cp_{l_{PCM}} + m_{water} * cp_{water}\right) * \left(T_{high} - T_{melt}\right)$
$h_{value} = 140000\ \left[\frac{J}{kg}\right]$
$H_{PCM} = h_{value} * m_{PCM} = 45360000\ [J\ ]$

10.5 System Simulation

In the figure below it is shown how the functioning is organized. The water flows from the tank to the house and again to the tank passing through the heat pump. This model gives accurate results and close to the reality and it does not request a high computer demanding because the script is short and simple.

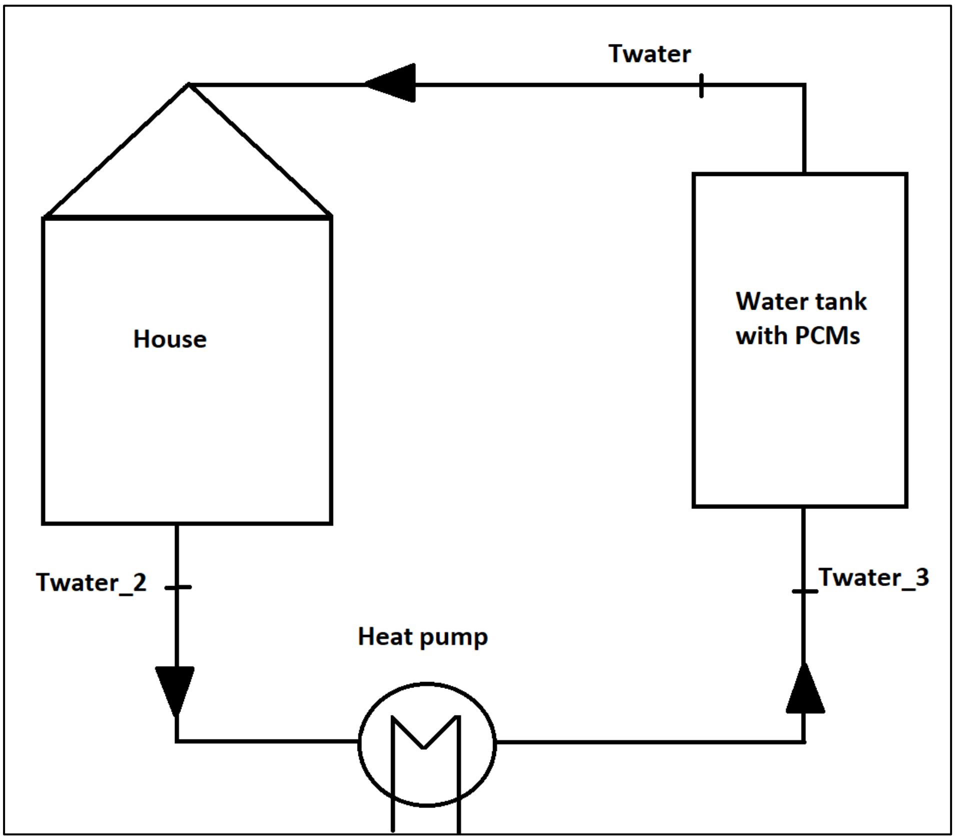

Fig. 47 - Schematic structure of the system

Therefore, to describe the working circle of the system it is necessary to use three temperature for the water, one for every heat exchange. So far, there are three different variables $Twater, Twater_2\ and\ Twater_3$ that describe the water temperature in 3 different situations. Hence, there is one variable left for the PCM temperature in the tank, T_{PCM}.

The other fundamental difference introduced for this script is the use of a new formula for the heat exchange between the water and the PCMboxes in the tank. The formula is the following:

$$Q = A * U * (T_{PCM} - T_{water3}) * t \tag{31}$$

Where Q is the total heat exchange; A is the surface area where the heat exchange takes place, in this case the bags surface. Then t is the time for the heat exchange in the tank. The value for the global coefficient of heat transfer was estimated equal to $U = 50\ \left[\frac{W}{m^2\ K}\right]$.

The values of these variables were taken from the properties of the real system. Starting from the properties of one bag, here reported, the total mass of PCM and the area for the heat exchange were calculated.

$Volume_{onebag} = 0{,}025 * 0{,}28 * 0{,}19 = 0{,}00133\ m^3$
$\rho = 1800\ \frac{kg}{m^3}$
$m_{PCM_{onebag}} = Volume_{onebag} * \rho = 2{,}394\ \ kg$
$Area = 0{,}28 * 0{,}90 * 2 + 0{,}28 * 0{,}025 + 0{,}025 * 0{,}19 = 0{,}13\ m^2$

Hence the total mass of PCM was calculated easily multiplying the mass of a single PCMbox with the number of the boxes (180) disposed in the tank. In the same way even the surface area of the heat exchange A was determined.

The mass of water in the tank was estimated to be $M_{waterTank} = 350\ kg$ and the mass flow of water circulating in the pipe circuit was imposed of a value $m_{water} = 0.39\ \frac{kg}{s}$.

The temperature references in the script are:

$T_{low} = 25\ °C$
$T_{melt_S} = 26.5\ °C$
$T_{melt} = 27\ °C$
$T_{melt_L} = 27.5\ °C$
$T_{high} = 33\ °C$

And the energy references, depending from these temperatures, are:

$Q_{melt,S} = (m_{PCM} * Cp_{s,PCM}) * (T_{melt,S} - T_{low})$
$Q_{melt,L} = Q_{melt,S} + H_{PCM}$
$Q_{high} = Q_{melt,L} + (m_{PCM} * Cp_{l,PCM}) * (T_{high} - T_{melt,L})$

Then the script starts with the working loop. The main feature of this code is that the control for the switch of the heat pump is made at the beginning of the loop, and then all the heat exchanges are calculated.

The heat pump is switched off when:

- $Twater\ >\ Thigh$;
- $I(j) \leq\ I_{grenz}\ and\ Twater\ \geq\ Tlow$;
- $EnergyDemand = 0$.

These conditions are described in the script below and the control works for every loop:

```
if $EnergyDemand(j) > 1$
    $I_{act} = I_{WP};$
        if $I(j) > I_{grenz}$
            if $T_{water} > T_{high}$
                $I_{act} = 0;$
            else
                $I_{act} = I_{WP};$
            end
        else
            if $T_{water} < T_{low}$
                $I_{act} = I_{WP};$
            else
                $I_{act} = 0;$
            end
        end
else
    $I_{act} = 0;$
```

Then after this section, with the heat pump working or not, are described all the heat exchanges that occur in every section of the whole circuit. For this reason, each water temperature can now be calculated. One can see that for the PCM the energy Q_{PCM} is evaluated instead of the temperature T_{PCM}. This was made because it was discovered that if it was calculated firstly the temperature (and it had been done in a first version of the code) then the PCM behaviour would not look pretty realistic though. In fact, the temperature of the PCM showed some unrealistic behaviours in the melting area where the temperature did not show a melting behaviour with a horizontal line but still a sensible behaviour. As a consequence, the control introduced was made on the energy and lately from the energy, the temperature of the PCM was calculated. This gave an accurate description of the phenomena of the heat exchange.

$T_{water2} = T_{water} - \left(\frac{EnergyDemand(j) + Qdistr2}{\dot{m}_{water} * Cp_{water}}\right)$
$T_{water3} = T_{water2} + \left(\frac{HeatPumpEnergy - Qdistr3}{\dot{m}_{water} * Cp_{water}}\right)$
$T_{water} = T_{water3} + \left(\frac{Q - Qdistr - Qstor}{m_{waterTANK} * Cp_{water}}\right)$
$Q_{PCM} = Q_{PCM} - Q$

Where $Qdistr$ represents losses in the system segment that goes from the tank to the house, $Qdistr2$ represents losses in the system segment that goes from the house to the heat pump, $Qdistr3$ represents losses in the system segment that goes from the heat pump to the tank.

$Qstor$, instead, symbolizes losses that occur in the tank during the storage.

All losses were calculated in the same way described before, thus taking into account the length of each segment of the system, a constant temperature (15 °C) of the basement were the major part of the system have been supposed to be located and the external surface of the storage tank.

Hence, at the end of the loop it was calculated the temperature of the PCM from the energy:

```
$if\ Q_{PCM} \leq Q_{melt_s}$
        $T_{PCM} = T_{low} + \left(\frac{Q_{PCM}}{m_{PCM} * cp_{s_{PCM}}}\right)$
$elseif\ Q_{melt_s} < Q_{PCM}\ \&\&\ Q_{PCM} \leq Q_{melt_l}$
        $T_{PCM} = T_{melt_s} + \frac{Q_{PCM} - Q_{melt_s}}{m_{PCM} * cp_{interp}}$
$else$
        $T_{PCM} = T_{melt_l} + \left(\frac{Q_{PCM} - Q_{melt_l}}{m_{PCM} * cp_{l_{PCM}}}\right)$
$end$
```

10.6 Results of the simulation

Below are reported the output graphs and simulation results. To highlight the behaviour of the PCMboxes and their effect on the system, the PCM temperature, the water temperature and the heat exchange in tank are plotted over time. The calculation of the money spent to buy electricity from the grid and the money earned from the sale of electrical energy from renewable sources are also reported.

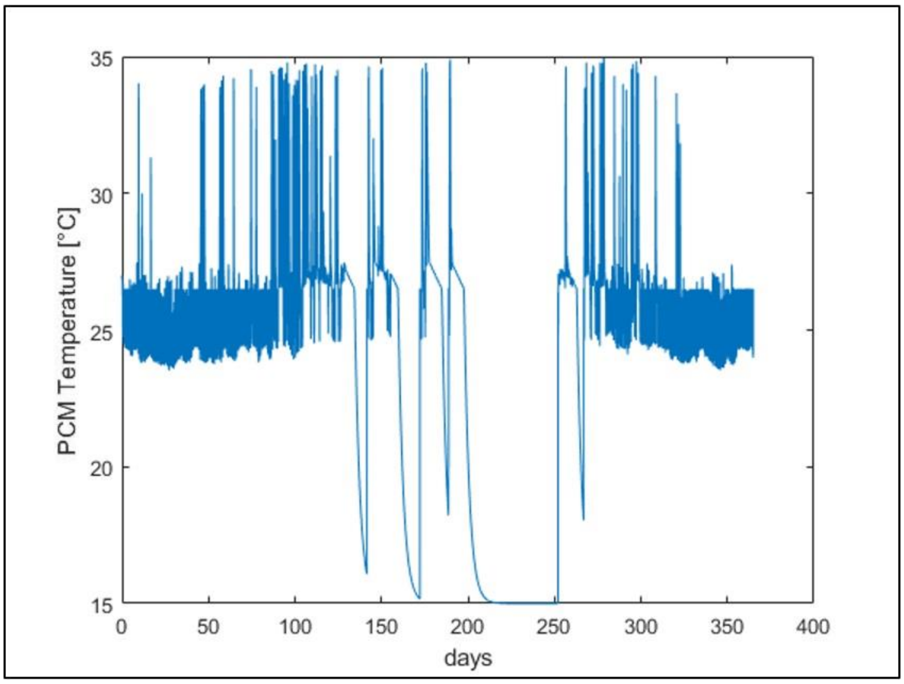

Fig. 48 - PCM Temperature graph

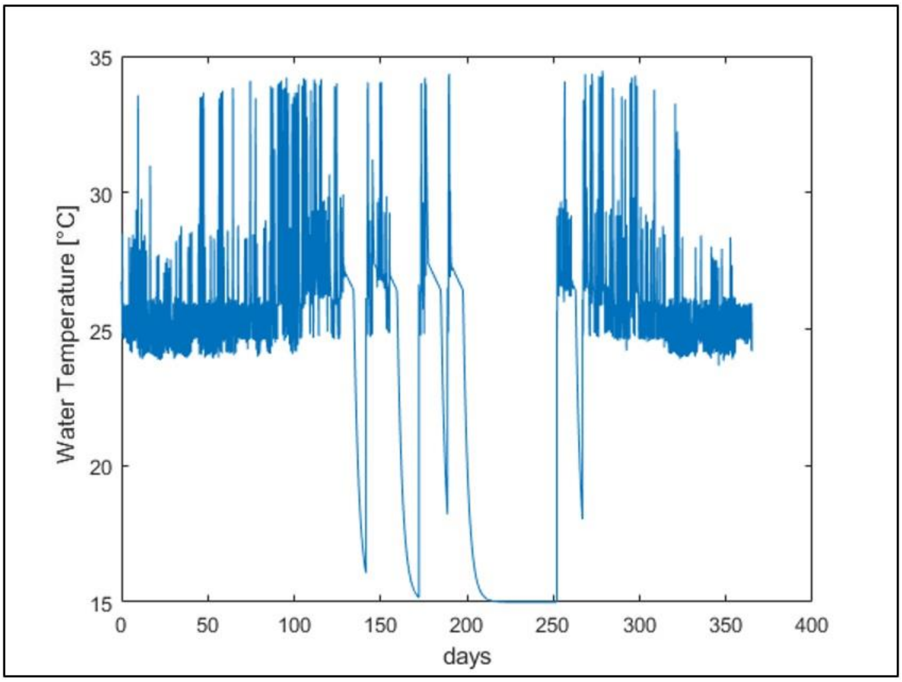

Fig. 49 - Water temperature graph

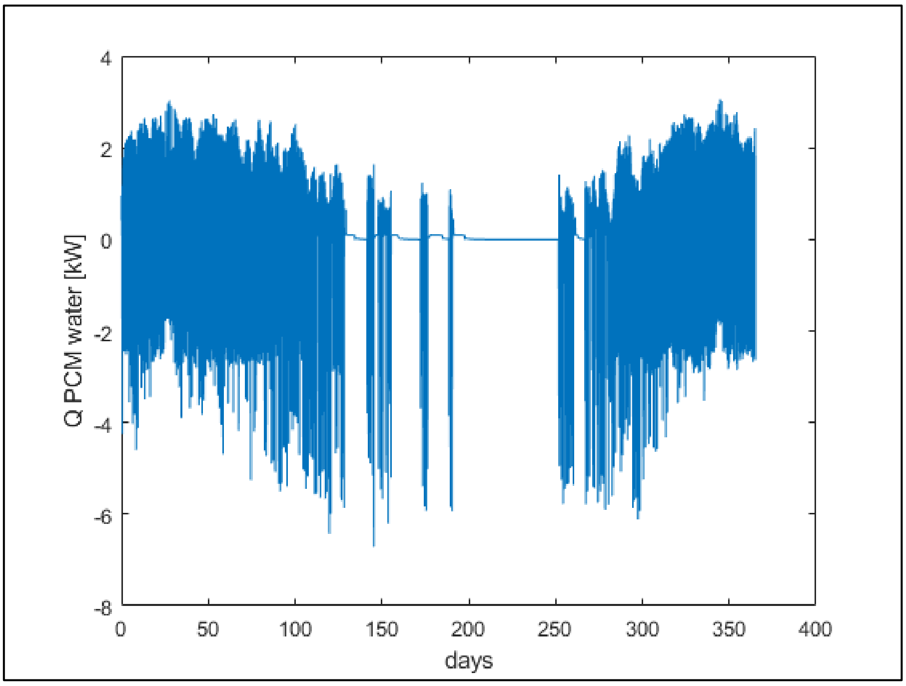

Fig. 50 - Heat exchange in the tank graph

$Costs\ for\ the\ heat\ pump = 268{,}44\ [\epsilon]$
$Earned\ money\ = 598{,}108\ [\epsilon]$
$Average\ COP = 6{,}771$

The year-round evaluation of the system reported positives values. The result of the simulation shows that the net gain from the sale of electrical energy from renewable sources on the grid is even greater than the total cost of the electricity bought from the grid to run the heat pump throughout the year. As a consequence, this work shows that in general the implementation of PCMboxes in a water tank for floor heating systems in the domestic applications is successful.

10.7 Parametric study

Finally, it was carried on a study using different combinations for the main values of the system. All the weather conditions and the energy demand for each hour remained the same in order to have the chance to compare the results from different system set up. The parameters changed are:

-I_{grenz} (the energy limit to make the pump run)

-Mass of water

-Mass of PCM

Starting from the energy limit, I_{grenz} this term was multiplied by $1{,}0.5, 0.2$. So far three possible different values for the energy limit were used. The aim was to make the pump run for more time rather than the original value I_{grenz}. At the same time also the materials were changed, either the water or the PCM. For these two parameters it was set up a brief count: starting from the number of PCMboxes the amount of water and of PCM was calculated from the script in the way described below.

The value of one PCMbox is well known from the relation: $m_{PCMonebag} = Volume_{onebag} * \rho_{PCM} = 2{,}394\ \ kg.$

Then the number of boxes used changed within this range: $50{,}100{,}200{,}450$. For the water it was simply imposed that the litres of water were calculated also from the number of PCMboxes, multiplying this number for these values:

0.5,1,2. As a result, in every simulation the litres of water were a half of the boxes, the same number or double of it. All these changes were evaluated in the simulations changing one value and taking the others fixed. Here are reported only as an example, the results obtained with the study of number of boxes=100.

Table 24 - results for 100 PCMboxes

mass of water [l/box]	I_{grenz} [W]	Gains [ϵ]	Costs [ϵ]	net gain [ϵ]	COP average
0,5	1* I_{grenz}	-	-	-	NaN
0,5	0,5* I_{grenz}	-	-	-	NaN
0,5	0,2* I_{grenz}	-	-	-	NaN
1	1* I_{grenz}	894,176	295,521	598,655	6,8067
1	0,5* I_{grenz}	891,634	293,848	597,786	6,7482
1	0,2* I_{grenz}	893,525	300,802	592,723	6,7199
2	1* I_{grenz}	877,946	289,296	588,65	6,8563
2	0,5* I_{grenz}	877,269	292,62	584,649	6,7827
2	0,2* I_{grenz}	878,547	298,476	580,071	6,7508

The same study with the same conditions was even performed considering a null quantity of PCM inside the tank. The number of boxes was still 100 but in the script the mass of the materials was set up as zero. These are the results for that case:

Table 25 - Results with number of boxes=100 and no PCMboxes

mass of water [l/box]	I_{grenz} [W]	Gains [ϵ]	Costs [ϵ]	net gain [ϵ]	COP average
0,5	1* I_{grenz}	909,243	290,465	618,778	6,9763
0,5	0,5* I_{grenz}	908,834	292,176	616,658	6,9687
0,5	0,2* I_{grenz}	908,892	294,339	614,553	6,9582
1	1* I_{grenz}	905,957	320,955	585,002	7,0052
1	0,5* I_{grenz}	905,521	323,092	582,429	6,9757
1	0,2* I_{grenz}	905,578	326,023	579,555	6,9532
2	1* I_{grenz}	902,199	331,403	570,796	6,951
2	0,5* I_{grenz}	902,07	334,455	567,615	6,9151
2	0,2* I_{grenz}	902,441	338,209	564,232	6,8931

One can see that in the Table 24 the results of the first three row, with litres of water=0.5 per box, reported numerical errors and so the COP value diverged together with costs and gains. This error is caused because the system has a really low mass of water comparing to the PCM and also the house energy demand remained the same, together with the heat pump. This fact reproduces a scenario where water can be heated up too much from the pump and so it does not cool down as it should be later and so the temperatures values then go up dramatically. Apart from this error the others are pretty accurate and reliable. Now it is possible to compare results each other and make deductions. What will be reported here considers all the other behaviours registered for the number of boxes 50,200,450. The general trends are:

Table 26 - Parameter study results summarised

Fixed Variables	Unfixed Variable (increasing)	Net gain	$COP_{average}$
N_{box} M_{water}	I_{grenz}	increases	increases
I_{grenz} M_{water}	N_{box}	decreases	No constant behaviour
I_{grenz} N_{box}	M_{water}	decreases	Mostly decreases

This evaluation described in the table is valid also for the NO PCMboxes cases as well. So far from the first line it is showed that when I_{grenz} gets higher the system has benefit because the heat pump runs less. Meanwhile when the number of PCMboxes are too high respect to the water in the tank, and the same when the water is too much compared to the PCMboxes, the system reports a low decrease in net gain and most of the time the COP has a bad influence too.

Then, last but not least, a comparison from the two tables must be done to see if there are positive aspects using the PCM or not. In fact, when the PCMboxes are implemented in the system one can see that the net gain is higher compared to the same case without PCMboxes, and the COP is a bit lower. This is definitely positive because it means that the system works better with the PCM even if the heat pump shows a low decrease of the COP during the whole year. Moreover, this means that if the system had a more efficient heat pump these results could be even more meaningful with a higher net gain in the PCM cases. For example, we can compare the results obtained with 180 boxes, like the system built up in the lab, with PCMboxes and without:

Table 27 - Comparison with the system of 180 boxes, with and without PCMs

180 boxes with PCM	180 boxes without PCM
Costs for the HP$= 268{,}44\ [\epsilon]$	Costs for the HP$= 340{,}4\ [\epsilon]$
$Earned\ money\ = 598{,}108\ [\epsilon]$	$Earned\ money\ = 558{,}4\ [\epsilon]$
$Average\ COP = 6{,}771$	$Average\ COP = 6{,}823$

11. System construction and its functioning

After the study and discussion of the numerical simulations, together with the measurements carried on in the laboratories about the PCM materials, a reproduction of the system was done. The construction of the system was carried on observing how the material behaves and how different are the results from what one has expected to obtain from the theory. It is important to say that the reproduction of such system was not, as often happens, perfectly tailored to the simulations carried on. During the constructions some problems and imperfection occurred and were fixed in many ways, but however not all the several parts of the system perfectly match with the CFD and Matlab simulations. On the other hand, the system built was really similar to the one simulated and so there is the possibility to compare results and make discussion about it.

11.1 Organization

The system required a wide range of materials. Starting with a list of the prime materials, then all the work that had been done will be discussed, step by step, from the beginning to the end of the construction. After the description of how the system was built, the measurements done will be explained and the results reported and discussed. In the end there is some space for the conclusions about the whole work.

Prime Materials:

-2 tanks of 1000 litres (IBC container);
-pipe circuit for water inlet at the bottom of one tank;
-180 PCMboxes;
-2 water pumps;
-metal sheets;
-metal grid at the bottom of the tank to sustain the PCMbags entire block.

These are the main materials used. For the test were used some instruments to evaluate some values like temperature, mass flow.

Starting with the properties of the tank (IBC container), it has a capacity of 600 litres and its dimensions are: $80cm\ height$, $68cm\ width$ and $117cm\ depth$.

The PCM used for this system construction is the well-known already obtained in the lab, the salt hydrate with a melting temperature of 26/27°C:

Table 28 – Salt-hydrate PCM's benchmark values (adapted from [1])

$CaCl_2*6H_2O$		
Cp solid =1.42 $[\mathrm{kJ}/\mathrm{k_g} \cdot \mathrm{K}]$	Cp liquid=2.10 $[\mathrm{kJ}/\mathrm{k_g} \cdot \mathrm{K}]$	Latent heat =190 $\left[\frac{\mathrm{kJ}}{\mathrm{kg}}\right]$

With a PCM density of ρ=1800 $\left[\frac{kg}{m^3}\right]$.

All the bags were filled with this material. Each bag has a dimension of $2{,}5\ cm\ width$, $20\ cm\ depth$ and $28\ cm\ height$ where the height is considered the longest distance from the bottom to the top of the whole box. Each bag had a capacity of one litre. As a consequence, to calculate the total amount of PCM's mass it was simply required to multiply the density of one PCM for the capacity of one bag and finally for the total number of bags.

For the weight of one box:

$$\rho = 1800\ \left[\frac{kg}{m^3}\right] \cdot 0{,}001\ \left[\frac{m^3}{l}\right] = 1{,}8\ \left[\frac{kg}{l}\right]$$

Then multiplying for the total number of boxes here it comes the PCM's total mass, that is

$$PCM_{total\ mass} = 1{,}8\ \left[\frac{kg}{l}\right] \cdot 180 = 324\ [kg]$$

Considering the volume of each PCMbox, that is

$$Volume_{bag} = 0.025 * 0.2 * 0.28 = 0.0014\ [m^3]$$

Multiplying this value for the number of bags one obtain the total volume occupied by the PCMboxes. In numbers

$$Volume_{tot} = 0.0014 * 180 = 0{,}252\ [m^3]$$

It is also useful to calculate the area of contact between the water and the PCMbox, to evaluate the heat transfer.

In this case

$$Area_{bag} = 0.136\, m^2\ ,\ Area_{tot} = 24.48\, m^2$$

Here below are the photos of some of the materials and parts of the storage tank.

Fig. 51 - Water tank (IBC container)

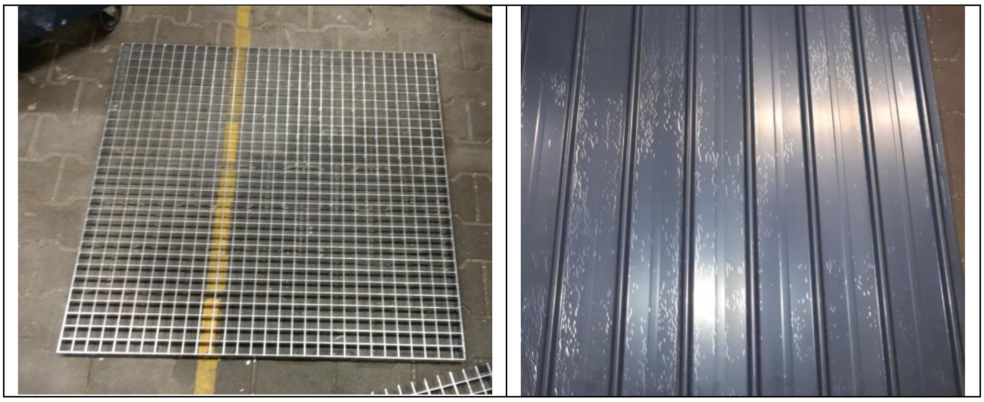

Fig. 52 - Metal grid support (left) and metal sheets (right)

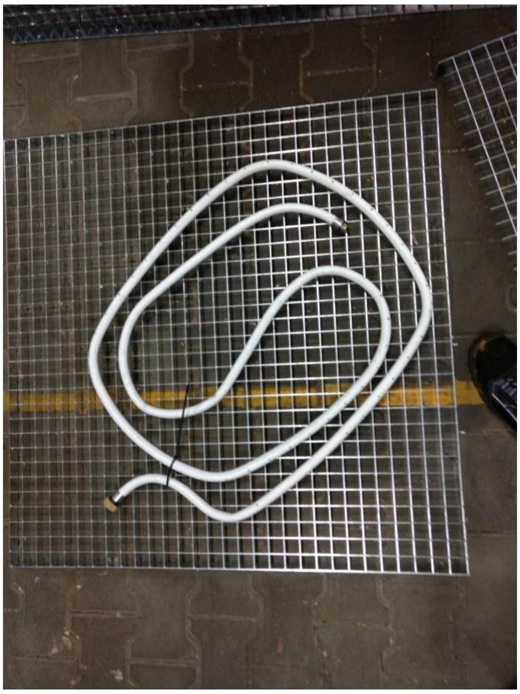

Fig. 53 – Tube for water inlet for the bottom of the tank

11.2 Construction of the tank

The first step was to drill holes in the pipe. The pipe was modelled as in Fig.53 in order to have a uniform distribution of the fluid-flow from the bottom of the tank to the top. Every $5cm$ there were made holes in the pipe of $3.3mm$ diameter. In total the holes were 92. As can be seen from Fig.53 the pipe was modelled to cover the entire floor area of the tank, it was made of aluminium and so able to maintain that certain shape. After that the metal grid was installed above the water pipe inlet (at the bottom of the tank) as a metal support (Fig.54).

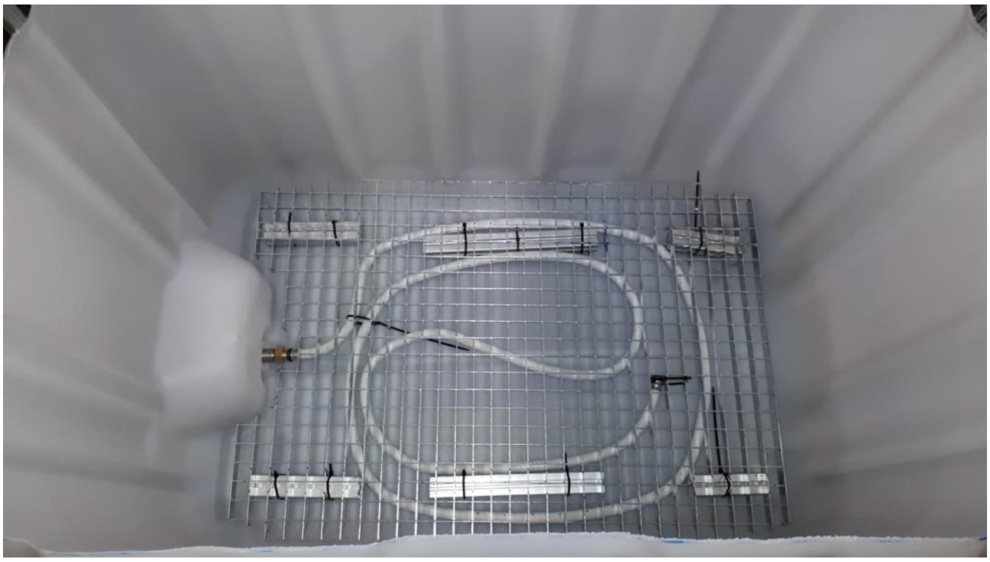

Fig. 54 – Bottom tube and grid with metal supports

Thanks to six metal supports the grid was fixed at approximately $6cm$ above the tank base. This distance was kept for two reasons. The first, as already explained, is because there was the necessity to have a steel grid to put all the first layer of boxes, but also to distance the pipe from the grid and have in this way a more uniform water flow going from the bottom to the top of the tank. Hence after the basement support for the PCMboxes was built and stable, the filling of first floor of PCMs started. The tank was filled in this way: the boxes were positioned in 18 rows each one made of 5 bags; also, between each row metal sheets were located to separate one row from another (Fig.55).

Fig. 55 - Disposition of each row of the boxes (top view)

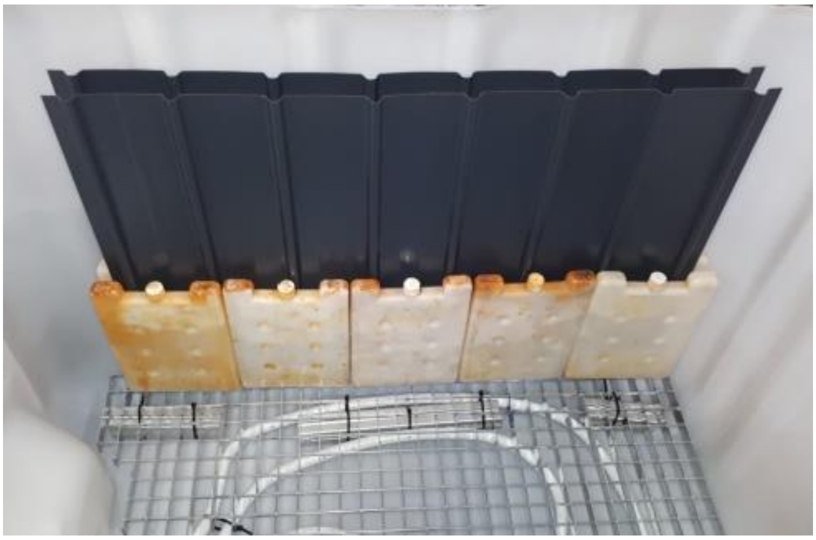

Fig. 56 - Disposition of each row of the boxes lateral view

The filling went on until all the first floor was completely full of boxes. Then the second floor was made just locating the boxes above the ones of the first floor. In Fig.57 it is shown the tank completely full.

Fig. 57 - System with all the PCMboxes

11.2.1 Test of the water inlet

Once the system was built the first test performed was the observation of the inflow distribution of the tank. To accomplish this evaluation, it was necessary to use a substance able to colour the water, a dye. In this case it was used “Amido naphthol Red G, Azophloxine” a red dye made for tracking the fluid flow. Its chemical formula is $C_{10}H_{13}N_3Na_2O_8S_2$.

Hence to see how the water inflow distribution from the bottom was, the empty tank was filled with dyed water, pumped in, until it was full. This test was useful to see if the water flow was uniform and equally distributed into all the area of the tank. In fact, as shown in some figures below, the water came out non uniformly from all the region of the tank. In fact, nearly from the beginning of the fulfilment a huge amount of red water came out from the first holes of the pipe. That area was redder than all the others, meaning that a big part of the water flow came out in the first part of the pipe without reaching the end. Due to the fact that all the layers were very compacted, it was difficult to see directly the behaviour of the water inside the tank; this simply evaluation from outside seemed to be reliable enough. Therefore, from outside it was possible to see qualitatively the colour distribution (see figures below).

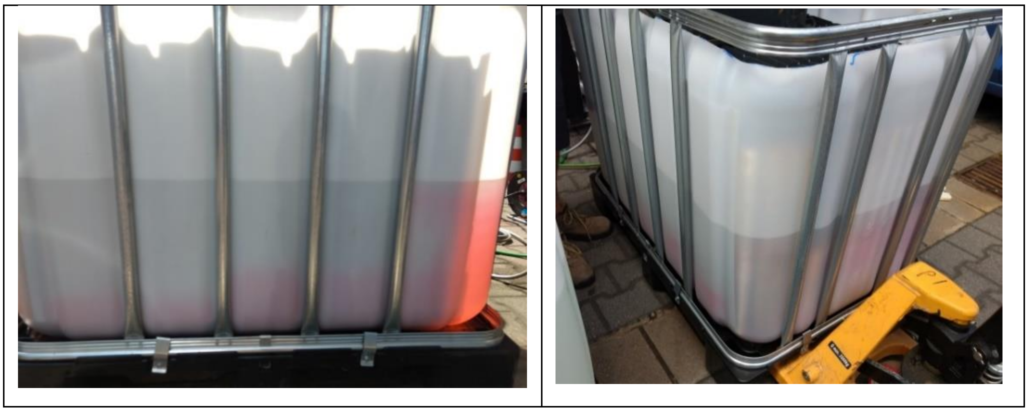

Fig. 58 - Colour evaluation of the fluid flow (lateral and back view)

Fig. 59 - Colour evaluation of the fluid flow (front and top view)

From the figures above can be seen exactly what was just described before. In Fig.58 on the left is shown the side of the tank where the red water immediately came out from the initial holes of the pipe and looking on the left of the picture the red colour starts fading, while on the right the areas where the water was not or was lightly coloured are represented. Finally, the water reached the top of the tank and the red colour was uniformly distributed all over the area.

11.3 System set up

Once the tank was completed and its flow distribution tests were successfully carried out, the assembly of the system went on with the construction of the pipe circuit with an installed heat pump. An already made pipe circuit, where there were installed two circulating pumps, a heat pump and a heat exchanger was recycled. Then the heat exchanger was removed because not needed.

Fig. 60 - Pipes circuit

Fig.60 shows a pipe circuit without the heat pump because it was temporary removed and added later over the four wooden blocks.

The plan was connecting the tank with PCMboxes to one side of the circuit and another tank with only water to the other side. In this way the heat pump could run because it needs a source to extract heat from.

Finally, the general electric panel control was connected. From the display of this panel control it was possible to monitor the temperatures throughout the whole circuit, the mass flow and the work of the two water pumps.

Fig. 61 - Electric panel (left) and heat pump (right)

Another important set up was the outlet connection for the PCM tank. As described before this tank is equipped with a peculiar water inlet pipe system located in the bottom of the tank. Consequently, the water outlet must only be at the top. For this reason, it was built a pipe system like the one shown in Fig.62.

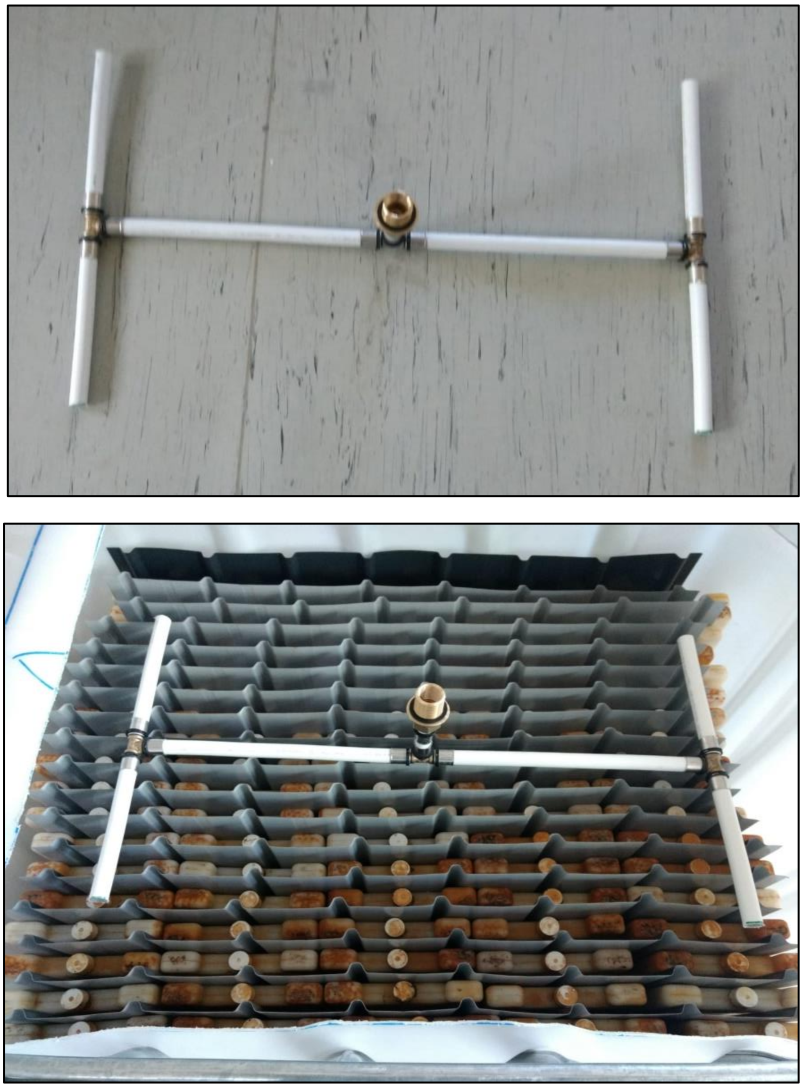

Fig. 62 - Water outlet system

This pipes structure for the water outlet system will be then connected to the CAP of the IBC container. The water outlet consists basically of 4 pipes that suck water in; thus, the water can flow out from the tank thanks to a pipe system. In this way the outflow from the tank was more uniform, not only from one point but equally from 4 parts of the tank.

Finally, the whole system is shown in the figure below.

Fig. 63 - Whole system built

The PCM tank is located on the left and the water tank is located on the right. The PCM tank was filled with 350 litres of water, and the water tank with 600 litres. Below it is reported a scheme for the system that shows all the temperature probes and flowmeters disposed around the system.

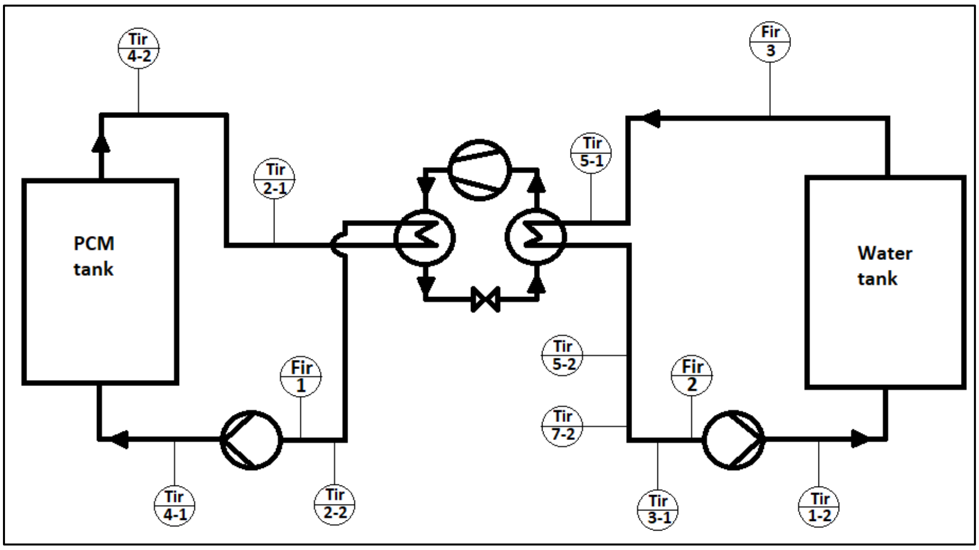

Fig. 64 - Layout of the system (heating process)

In Fig.64 the “Tir” sensors are temperature probes, and “Fir” sensors are flowmeters. In the middle is represented the heat pump circuit, in this case during the heating up mode. When a cooling down measurement was required it was done simply by the inversion of the condenser with the evaporator.

11.4 Functioning and measurements performed

In order to test the PCM tank two measurements were performed, one for the heating process and one for the cooling process. Both the measurements took a long time because it was necessary to complete respectively the entire liquefaction and solidification of the whole block of PCMboxes. They were made in this order because the PCM was already solid therefore starting with the heating process was the most logical solution.

11.4.1 Heating process

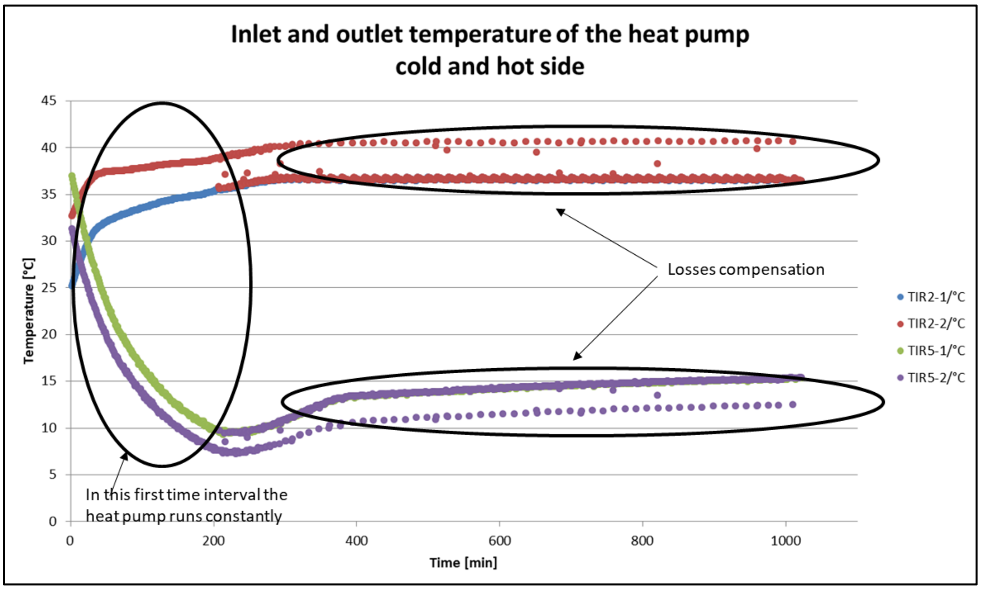

Fig. 65 - Temperatures plot for the heating process

In the Fig.65 it is possible to see four temperature that are the those saved minute by minute by the computer of the control panel.

In the graph above Tir2-1 and Tir2-2 are respectively the outlet and the inlet temperatures of the water that is circulating in the PCM tank circuit. Meanwhile Tir5-1 and Tir5-2 are respectively the outlet and inlet temperatures of the water circulating in the water tank circuit.

During the heating of the PCM tank, the water goes up reaching a value imposed by the user, in this case 35°C, when at the same time the other tank gets colder reaching at the end a temperature between 15-10 °C. One particular fact is that it was found out that the heat pump did not run constantly but after a while it suddenly stopped. This happened because it was not possible for this device to work with too low temperatures as the ones reached at the end of the circled area in Fig.65 at approximately 230 minutes. However, then the HP reached the temperature value set up of 35°C, pretty above 27°C that is the melting temperature, and then the system stayed in this condition for a long time, until the end of the measurement. This allowed all the PCMs to complete their melting and to be ready for the cooling measurements. A relevant thing to point out is that at the end of the measurements the two circled areas were taken into consideration to evaluate the losses. This was made because at that time the whole tank was in a steady state (PCMboxes, water and all the other materials in the tank were in thermal balance between each other) and this means that the HP turned on for some seconds just to keep the temperature on the set value and win the losses between the tank and the environment.

In order to evaluate the latent heat that, in this case, the whole block of PCMboxes absorb from the water during the process, it was set up the following calculation.

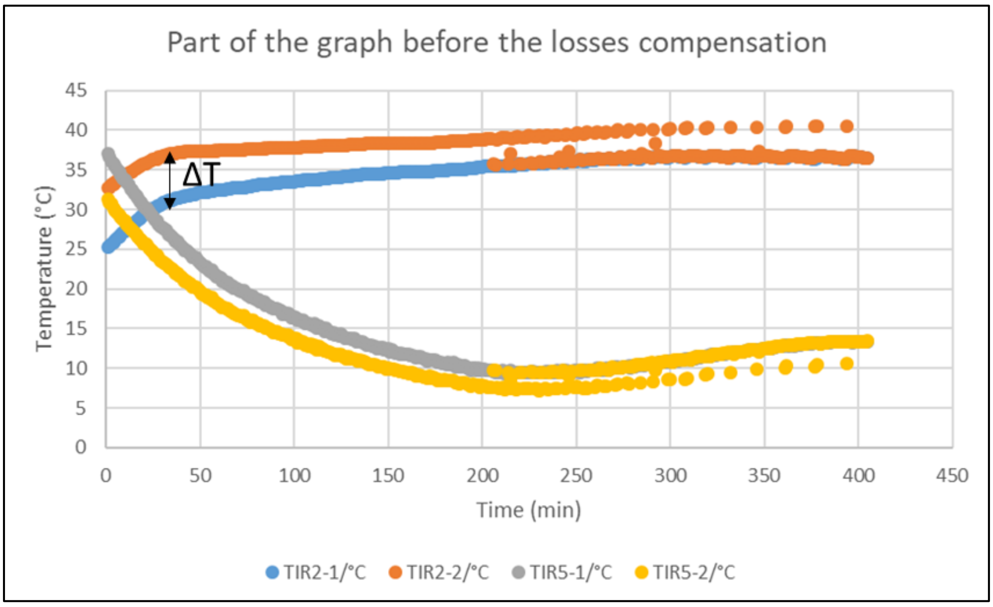

Fig. 66 - zoom in of the first part of the previous graph

Looking at the temperatures 2-1 and 2-2 related to the PCM tank side, the total energy given to the water by the heat pump can be calculated. At first it must be noticed that this evaluation does not consider the whole measurement, that lasted 1100 minutes, but only 400, because after that time the system is in a steady state condition and as already mentioned the heat pump only compensate the losses. Once again this means that the PCM is completely melted.

Then, the thermal power given by the heat pump every minute can be calculated simply by:

$$Power = \dot{m} \cdot C_{p,water} \cdot \Delta Ti$$

Therefore, the total energy given before losses compensation is equal to

$$\sum_{i} \dot{m} \cdot C_{p,water} \cdot \Delta Ti \cdot 60sec = 0.25 \cdot 4187 \cdot \Delta Ti \cdot 60sec = 71{,}9\ MJ$$

Where the index i indicates the minutes.

Then all the Energy factors that took place during the measuring were:

- Energy absorbed by the elements inside the tank = 1,05 MJ
- Losses during the whole process = 3,1 MJ
- Sensible energy of water = 16,7 MJ
- Sensible energy of PCM (liquid) = 6,6 MJ
- Sensible energy of PCM (solid) = 0,8 MJ

The energy losses of the elements in the tank consists of the energy absorbed by the plastic of the bags, the metal sheets, metal grid at the bottom of the tank and the pipe. All these elements subtract energy from the water and to calculate this energy amount the following formula was used

$$M \cdot C_{element} \cdot \Delta T$$

Where M is the mass of each element, $C_{element}$ its specific heat, and as ΔT the difference between the first and the last temperature registered in the system was considered, in this case $\Delta T = 36{,}7 - 25{,}3$. This hypothesis implies that all these elements were considered in thermal balance with the water.

Moreover, it was calculated the sensible energy of the water in the tank using the same temperature difference used for the other elements. Thus, it remains only the whole energy of the PCM either sensible or latent.

As already done for the other elements of the tank, to find out the sensible part of the energy of the PCM, it was calculated its entire mass

$$M = 180[boxes] \cdot 1{,}8 \left[\frac{kg}{box}\right] = 324[kg]$$

and multiplied by the Cp liquid or solid and by the temperature difference. Finally, only one fraction of the whole energy still remains, and it represents the heat losses between the tank and the outside ambient. To evaluate this amount, it was necessary to go back to the original data of the whole measurement at the final time of the graph. There the temperature difference from the inlet and the outlet of the HP only compensate the losses of the system with the environment, because as already explained, there were not any physical phenomena in that moment, only losses.

Table 29 – Heating process energy amounts

	Mass [kg]	$Cp\ \left[\frac{J}{kg \cdot K}\right]$	ΔT [°C]	Energy [MJ]
Steel	57,96	502	$36{,}7 - 25{,}3$	0,33
Plastic bags	33,246	1900	$36{,}7 - 25{,}3$	0,72
Water (sensible part)	350	4187	$36{,}7 - 25{,}3$	16,7
PCM (sensible part solid)	324	1420	$27 - 25{,}3$	0,78
PCM (sensible part liquid)	324	2100	$36{,}7 - 25{,}3$	6,6
Thermal losses (water)	350	4187	$15 - 12{,}9$	3,1

Finally, to obtain the latent heat of the PCM it is simply required to subtract to the energy given from the HP all these terms.

PCM latent heat $= 71{,}9 - 1{,}05 - 3{,}1 - 16{,}7 - 6{,}6 - 0{,}8 = 43{,}6\ MJ$

There is an easy way to prove if this result can be right. Taking into account the total mass of PCM, that is $324\ [kg]$ multiplying it by the theoretical latent heat (specific) measured in the laboratories $Hm = 140\ 000\ \left[\frac{J}{kg}\right]$ and one obtains the latent heat (total) = $324 \cdot 140\ 000 = 45{,}36$ MJ.

11.4.2 Cooling process

This measurement was performed immediately after the previous one because after the heating process it was sure that all the PCM was completely melted, and ready to solidify encountering a cold fluid flow.

The graph below shows the temperatures recorded for the cooling process:

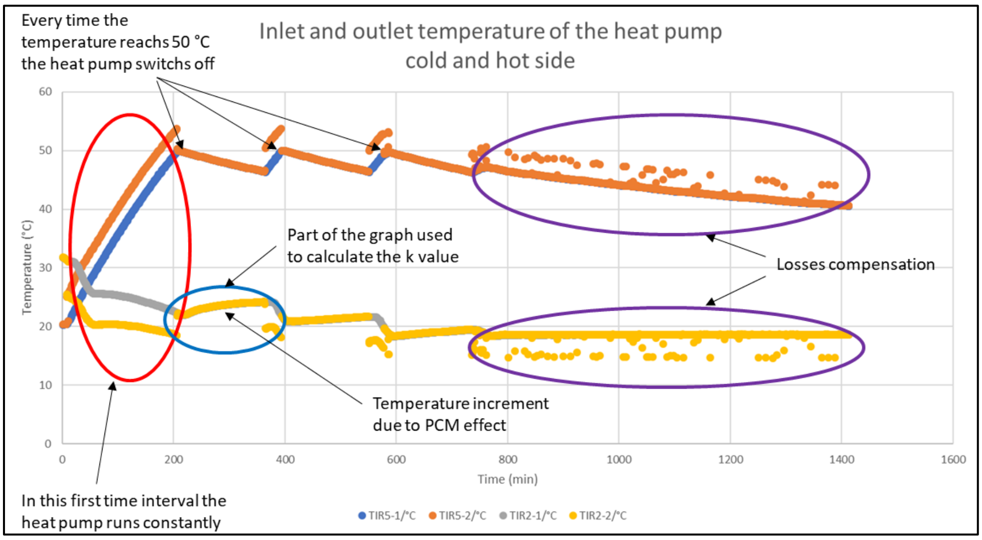

Fig. 67 - Cooling process

This time the heat pump worked without stopping until it reached 50°C in the water tank, meanwhile the PCM tank was not already at 15°C as expected to be from the imposed set up temperature value. Then the HP stopped and came back to work two more times because every time it reached 50°C it automatically stopped working. After 800 minutes, it is possible to see the same behaviour already obtained in the previous measurement. The HP did not work constantly but it switched on and off many times only to compensate the losses between the tanks and the environment until the end of the measurements.

Basically, the calculation methods are the same performed for the heating; therefore, the energy of the water given by the HP is:

$$\sum_i \dot{m} \cdot C_{p,water} \cdot \Delta Ti \cdot 60sec = 0.23 \cdot 4187 \cdot \Delta Ti \cdot 60sec = 70{,}8\ MJ$$

Where the index *i* indicates the minutes.

Table 30 - Cooling process energy amounts

	Mass [kg]	$Cp\ \left[\frac{J}{kg \cdot K}\right]$	ΔT [°C]	Energy [MJ]
Steel	57,96	502	$31{,}4 - 18{,}8$	0,36
Plastic bags	33,246	1900	$31{,}4 - 18{,}8$	0,79
Water (sensible part)	350	4187	$31{,}4 - 18{,}8$	18,4
PCM (sensible part solid)	324	1420	$27 - 18{,}8$	3,77
PCM (sensible part liquid)	324	2100	$31{,}4 - 27$	2,99
Thermal losses (water)	350	4187	$15 - 12{,}9$	3,1

As it was done for the heating process, one can estimate the PCM latent heat that in this case is given to the water:

PCM latent heat $= 70{,}8 - 1{,}2 - 18{,}4 - 3{,}77 - 2{,}99 - 3{,}1 = 41{,}3\ MJ$.

11.4.3 Calculation of the coefficient of heat transfer

To calculate the coefficient of heat transfer, the last temperature measured at the bottom of the tank is taken as the inlet temperature.

Knowing the mass flow is possible to calculate the time that the tank takes to be completely filled; thus, the temperature measured after this time at the top of the tank can be taken as the outlet temperature.

T_{inlet}= 18,8 °C, T_{outlet}=22,6 °C, $\dot{m} = 0{,}23\ [kg/s]$.

We can calculate the power absorbed by the water as:

$$Q = \dot{m} \cdot C_{p,water} \cdot (T_{outlet} - T_{inlet}) = 3660\ [W]$$

In order to calculate the coefficient of heat transfer, one needs to know the value of the exchange area and of the *mean temperature difference*:

A=exchange area= 24,48 [m^2]

$$\Delta T_{ml} = \frac{T_{inlet} - T_{outlet}}{ln\left(\frac{27 - T_{outlet}}{27 - T_{inlet}}\right)} = 6{,}1\ [K]$$

Where, ΔT_{ml} ,is the logarithmic mean temperature difference.

Now one can estimate the heat transfer coefficient using the relation below:

$$U = \frac{Q}{A \cdot \Delta T_{ml}} = 24{,}5\ \left[\frac{W}{m^2 * K}\right]$$

The obtained value of the heat transfer coefficient is in the order of magnitude of what was expected.

All the results obtained, shown in this chapter, indicate that the PCM tank designed and built represents an excellent solution.

12. Conclusions

To conclude this thesis, several studies that could be carried on in the future are suggested.

As far as the production of PCM is concerned, possibly trying to avoid paraffins, as they are toxic and flammable, and always trying to use PCM salt hydrates (inert), an attempt could be made to produce one with a phase change temperature of 34-36 °C. Keeping water at these temperatures for longer time would be more suitable for building heating systems.

Measurements on the thermal properties of PCM (solid and liquid phase specific heat and latent melting heat) could be made using more precise methods and recalibrating all thermocouples.

For the encapsulation of PCM one could try to use different shapes than the one used; an idea could be using a piece of cake shape in case one wanted to fill a cylindrical tank. The type of encapsulation is a cost that must be considered. If one can find a good type of encapsulation, which is reasonably priced, fills the tank well, and allows a good heat exchange, then this will be easily marketable.

An interesting study could be done on the complete thermofluid dynamics of the entire tank using software such as OPENFOAM or COMSOL Multiphysics. From these types of study one could obtain results that could be used in Matlab scripts for year-round numerical simulations of the entire plant.

As for the experimental system that was built, it was possible to carry out only two measurements, one for the heating process and one for the cooling process; it would certainly be more interesting to carry out more measurements on the two processes consecutively to each other and alternate them every time the system reaches the equilibrium. To carry out this experiment it would be necessary to monitor not only the water temperature but also the temperature of the PCM inside the bags; once both temperatures are equal and abundantly above (or below) the melting temperature of the PCM then the cooling (or heating) process should be started.

Such a measurement would not only provide more accurate results in terms of thermal storage capacity and heat transfer coefficient but would also provide an opportunity to see how the system responds to several consecutive heating and cooling cycles in terms of PCM stability.

Once approved the high quality of the tank full of PCMbags with the experimental apparatus, the last type of work that could be done to complete the design cycle, would be to insert it inside an existing heating system of a building for an additional test.

If the response of the system to the insertion of the tank is good, and therefore there is actually a saving in energy terms, the last step would be to market it.

The tank that was built within the CeMOS department, in case it passed all the tests and was commercialized, would be highly competitive.

Most of the tanks for this type of application on the market are made of metal and are very expensive for the same volume.

The IBC container used as a tank, instead, has a cost of about 200 euros and compared to other metal tanks, which are cylindrical, has a rectangular shape.

The rectangular shape of the tank allows to better occupy the space inside it using PCMbags which are rectangular too.

Bibliography

[1] Kinga Pielichowska, Krzysztof Pielichowski - Phase change materials for thermal energy storage;

[2] João M. P. Q. Delgado, Joana C. Martinho, Ana Vaz Sá, Ana S. Guimarães, Vitor Abrantes - Thermal Energy Storage with Phase Change Materials - A Literature Review of Applications for Buildings Materials;

[3] Mehling, Cabeza – Heat and cold storage with PCM – An up to date introduction into basics and applications.

[4] Amy S. Fleischer - Thermal Energy Storage Using Phase Change Materials - Fundamentals and Applications;

[5] I. Al-Hinti, A. Al-Ghandoor, A. Maaly, I. Abu Naqeera, Z. Al-Khateeb, O. Al-Sheikh - Experimental investigation on the use of water-phase change material storage in conventional solar water heating systems;

[6] Zhang Yinping et al 1999 Meas. Sci. Technol. 10 201 - A simple method, the T-history method, of determining the heat of fusion, specific heat and thermal conductivity of phase-change materials;